BRITISH ANTARCTIC SURVEY

SCIENTIFIC REPORTS

No. 103

THE GEOLOGY OF PART OF NORTHERN PALMER LAND

By

T. G. DAVIES, B.Sc., Ph.D.

Earth Sciences Division, British Antarctic Survey

and

Department of Geological Sciences, University of Birmingham

CAMBRIDGE: PUBLISHED BY THE BRITISH ANTARCTIC SURVEY: 1984

NATURAL ENVIRONMENT RESEARCH COUNCIL

BRITISH ANTARCTIC SURVEY SCIENTIFIC REPORTS: NO. 103

THE GEOLOGY OF PART OF NORTHERN PALMER LAND

By
T. G. DAVIES, B.Sc., Ph.D.
Earth Sciences Division, British Antarctic Survey
and
Department of Geological Sciences, University of Birmingham

(Manuscript received 4th August 1977)

ABSTRACT

THE previous exploration and geological investigations in northern Palmer Land are described and the physiography and the glacial geomorphology of this area are summarized.

Several rock groups have been distinguished in northern Palmer Land; their field relations, petrography and geochemistry are discussed and correlations have been made with other parts of the Antarctic Peninsula. The metamorphic complex comprises gneisses, amphibolites, schists and greenschists, some of which have been regionally metamorphosed to the almandine-amphibolite facies. Granitic gneisses predominate and these appear to be the products of fusion of pre-existing rocks modified by metasomatism.

A sequence of metavolcanic and metasedimentary rocks has been correlated with schists and greenschist dykes from the metamorphic complex and they seem to be of a comparable age to the (?) Carboniferous quartz-keratophyres of the Wilkins and Bowman Coasts, and the Trinity Peninsula Series.

The abundant Upper Jurassic volcanic rocks comprise volcanic breccias and tuffs with subsidiary basalt, rhyolite and dacite lavas and sedimentary rocks, which were deposited, mainly subaerially, on to an eroded surface of plutonic and metamorphic rocks. The succession of sedimentary and volcanic rocks overlying the adamellite on Mount Charity is thought to be the same age as the Upper Jurassic volcanic rocks.

There has been extensive episodic plutonic activity in northern Palmer Land, probably over a long period of time, and tonalites, granodiorites and adamellites are the predominant rock types.

In addition, several phases of basic to acid hypabyssal rocks intrude the various rock units.

CONTENTS

I. INTRODUCTION

PALMER LAND is that part of the Antarctic Peninsula south of a line joining Cape Jeremy to Kenyon Peninsula. This boundary coincides with the area where the average width of the plateau changes southward from 70 km to more than 150 km, accompanied by an increase in altitude.

The area discussed here, about 8 000 km^2, forms a rectangle, elongated east–west, lying between lat. 69°15′ and 70°00′S, and long. 63°00′ and 69°00′W (Fig. 1). Natural boundaries of this area are formed by Fleming and Bingham Glaciers to the north, George VI Sound to the west and Eureka Glacier to the south.

1. *Previous investigations*

The mainland of the Antarctic Peninsula was first discovered and partly charted by Edward Bransfield during the British expedition of 1819–20, and in the next 100 years or so the northern part of the peninsula was visited many times and was well surveyed by explorers, sealers and whalers.

However, it was not until it became practicable to use aircraft for polar travel that the topography of Palmer Land (or southern Graham Land as it was called then) began to be known. Wilkins (1929) was the first to use an aircraft in the Antarctic when he flew from Deception Island 960 km south into "southern Graham Land". On this flight, Wilkins claimed to have found channels, filled with sea ice, which broke up "Graham Land" into a series of islands. He called the southernmost channel Stefansson Strait and the land beyond it Hearst Land.

Since navigation was considered impracticable in the Weddell Sea, the aim of the British Graham Land Expedition (BGLE), 1934–37, was to establish a base somewhere in Marguerite Bay, on the west coast of the Antarctic Peninsula, and then travel by dog sledge through one of the channels to explore the Antarctic coast in that region (Rymill, 1938). Owing to problems with the ship's engine, the expedition was forced to spend its first year based in northern Graham Land. During the spring of that year (1935–36) Lincoln Ellsworth arrived off the Antarctic Peninsula to make a second attempt to cross Antarctica from the Weddell Sea to Little America (Joerg, 1936). During his flight, Ellsworth confirmed the presence of the channels and islands that Wilkins had seen and this information was passed on to the British Graham Land Expedition (Stephenson, 1940). In February 1936 the latter established a base in Marguerite Bay and managed a short survey flight to the south which showed no channels dissecting Graham Land.

Between August 1936 and February 1937, air and ground surveys found none of the channels seen by Wilkins and a later comparison of these surveys with the air photographs taken by Ellsworth proved conclusively the peninsular nature of Graham Land. During the sledge journeys of the British Graham Land Expedition geological specimens were collected in the area of the "Eternity Mountains" (Fleming, 1938).

A sledge party of the United States Antarctic Service Expedition (USASE), 1939–41, crossed the plateau from the Wordie Ice Shelf to the "Eternity Mountains" (Black, 1945) and collected geological specimens which were later described by Knowles (1945). Further valuable knowledge of this area was obtained from trimetrogon air photographic cover during the Ronne Antarctic Research Expedition (RARE), 1946–48 (Ronne, 1948). Since that time, many members of the Falkland Islands Dependencies Survey and British Antarctic Survey have crossed northern Palmer Land and completed various geological and topographical surveys, from which the 1 : 200 000 map sheets now in use were produced.

2. *Scope of the present study*

The present work is a continuation of the reconnaissance geological surveys along the western side of the Palmer Land plateau by M. E. Ayling and J. F. Pagella in 1964, C. G. Smith in 1967–68, P. J. Rowe in 1969 and A. C. Skinner in 1969–70.

The author spent two summer seasons, from October to January, in this area. In 1970, Mount Edgell, its ridges and the surrounding nunataks, and the outcrops on the south side of Fleming Glacier were mapped, and in 1971 the survey was continued in the Eternity Range and the nunataks farther east.

Plane-table surveying was carried out in order to compile a map at a scale of 1 : 100 000, on which geological data were plotted.

3. *Physiography*

The western part of this area is dominated by Mount Edgell (1 676 m) and its satellite ridges and nunataks. Eastward, the plateau rises gradually through the Relay Hills, Kinnear Mountains, Mayer Hills and Crescent Scarp to the Eternity Range (maximum height 3 226 m), which forms a backbone to the peninsula, 1 000 m above the plateau surface. Beyond, the nunatak-studded landscape descends relatively steeply to the Larsen Ice Shelf within 75 km.

A detailed account of the physiography of this area has been given by Davies (1975).

II. GENERAL STRATIGRAPHY

EIGHT rock groups have been recognized in the area mapped and these are shown in Table I in stratigraphical order with their tentative ages.

TABLE I
THE STRATIGRAPHY OF NORTHERN PALMER LAND

Tertiary	Post-Andean hypabyssal rocks
	Alkali-granite
	Andean Intrusive Suite
	Pre-Andean hypabyssal rocks
Mesozoic	Mount Charity sedimentary and volcanic rocks
	Upper Jurassic Volcanic Group
	Pre-volcanic plutonic rocks
Palaeozoic	Metavolcanic and metasedimentary rocks
	Metamorphic complex

To the east of the Eternity Range, the deformed Engel Peaks granite, which is included in the metamorphic complex, is overlain by the basal breccia of the metavolcanic and metasedimentary sequence. In the western part of Palmer Land, the Upper Jurassic Volcanic Group rests unconformably on the metamorphic rocks and the pre-volcanic plutonic rocks; these volcanic rocks are intruded by numerous minor dykes, some of which are younger than the Andean plutonic rocks. The Mount Charity sedimentary and volcanic rocks are thought to be broadly coeval with the Upper Jurassic Volcanic Group on petrographical grounds.

Although some of the igneous bodies that have been included in the Andean Intrusive Suite can either be seen to intrude the Upper Jurassic Volcanic Group or they contain xenoliths of the volcanic material, many have no contacts with older or younger rocks. Consequently, the ages of these bodies are questionable.

Since there is no direct evidence for the age of the rocks in this area, they have been grouped as Palaeozoic, Mesozoic and Tertiary by analogy with other parts of the Antarctic Peninsula (Adie, 1964) and from a study of the radiometric dates available (Grikurov and others, 1966; Halpern, 1971; Rex, 1971).

III. METAMORPHIC COMPLEX

ROCKS of the metamorphic complex are restricted in outcrop to small areas around Mount Edgell and a larger north–south-trending strip to the east of the Eternity Range. The rock types represented are basic and acid gneisses, schists, amphibolites and greenschist dykes.

A. WESTERN SIDE OF PALMER LAND

Adie (1954) described garnet-mica-schists interstratified with quartz-mica-schists from the Mica Islands, which are situated to the north of Cape Jeremy, and similar rocks were found by the author at station KG.1201 on the mainland east of the Rhyolite Islands. Here, gneisses and schists with a marked foliation dipping at approximately 26° in a direction 126° true are overlain by zeolitized Upper Jurassic volcanic rocks. A boss of tonalite belonging to the Andean Intrusive Suite intrudes the metamorphic rocks at the eastern end of station KG.1201.

1. *Gneisses*

The gneisses are coarse-grained and contain thin discontinuous bands of quartzite separated by black micaceous layers. In places, the quartzite forms more massive lenses and bands up to 2 m thick. Microscopically, the quartzite comprises ribbon-like masses of quartz crystals wtih an undulose extinction, irregular grain boundaries and containing numerous small inclusions often forming lines across the crystals, and plagioclase with a composition of approximately An_{30} which has been albitized in some cases. The black micaceous bands, which are wrapped around the broken crystals of quartz and plagioclase, are composed mainly of dark brown biotite which has been bent and kinked, almost completely pseudomorphed by pale green chlorite, and the cleavage flakes have been parted by lenticular masses of epidote-clinozoisite. Small crystals of garnet up to 0.02 mm in diameter are associated with the biotite which formed later than the garnet and has been wrapped around them. Ilmenite, partially altered to leucoxene, forms stringy masses between some of the biotite flakes, and haematite occurs as more equant grains. Pale yellow epidote is common in the micaceous bands and is present in aggregates of tiny elongated and stumpy crystals or as discontinuous veinlets in the broken quartz and plagioclase. Other accessories in the groundmass are sphene (up to 0.7 mm in diameter), small crystals of zircon and patches of calcite.

2. *Schists*

In the hand specimen, the schists are grey in colour, weather brown and are minutely folded. They contain abundant mica and a few bands of quartzite that have been folded and sheared out. Microscopically, the rock consists of bands of quartz and plagioclase separated by micaceous layers, comprising biotite which is poorly pleochroic from colourless to orange-brown, and long flakes of muscovite which have been bent and broken. An abundance of elongated masses of iron ore accompany the mica. The quartz is drawn out into ribbon-like masses of crystals with an undulose extinction and irregular grain boundaries. The plagioclase is also elongated parallel to the foliation and is of two types: either twinned andesine (approximately An_{30}; large $2V\alpha$) which is slightly sericitized or, more commonly, albite (large $2V\gamma$) which is more severely sericitized and mostly untwinned. Crystals of pink garnet up to 1 mm in length are very common in the rock and they contain numerous inclusions of quartz and iron ore. They have been shattered and the fragments have been drawn out along the foliation during a period of stress after the main metamorphism. The garnet has been replaced, mainly along the cracks, by the biotite. The cracks in the muscovite are often filled with the small flakes of biotite, again indicating the later time of formation of this mineral.

B. East of the Eternity Range

To the east of the Eternity Range, metamorphic rocks occupy a 25 km wide north–south-trending belt centred on Mount Sullivan. Several rock types are recognizable, the commonest being biotite-gneisses, augen-gneisses, amphibolites, acid gneisses, schists, minor greenschist dykes and a metamorphosed granite. The biotite-gneisses are interbedded with augen-gneisses and these units and some of the massive amphibolites are intruded by acid gneisses; the latter contain interbedded schists and are cut by greenschist dykes. The Engel Peaks granite is situated to the east of the main exposures of the metamorphic complex rocks and it is overlain on its western side by the basal breccia of the metasedimentary and metavolcanic rocks.

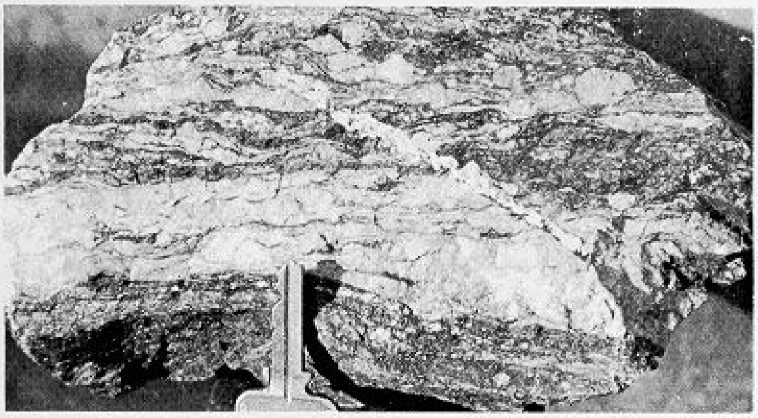

FIGURE 2

Biotite-gneiss containing feldspar-rich bands interspersed with black micaceous bands (the blade of the key is 3.5 cm long).

1. *Biotite-gneisses*

These are black gneisses containing feldspar-rich bands and lenses, usually less than 3 cm wide, interspersed with micaceous layers (Fig. 2). They occur at four stations (E.3287, 3606, 3607 and 3612) and they are usually associated with augen-gneisses; at station E.3286, bands of biotite-gneiss about 4.5 cm thick are separated by 9 m of coarse augen-gneiss (Fig. 3), the contact dipping at 21° in a direction 254° true.

Specimen E.3607.1 is a typical example of the gneisses and microscopically it contains broken porphyroclasts of plagioclase and potash feldspar, shattered garnets and schistose bands of biotite and fine recrystallized grains of quartz and feldspar. The plagioclase forms faintly twinned or untwinned equant crystals with ragged edges, and the strong Becke line and the

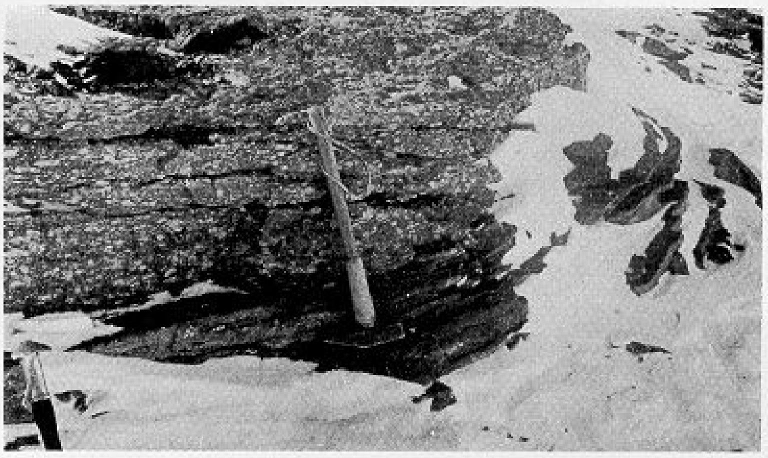

FIGURE 3

Augen-gneisses interbedded with biotite-gneisses at station E.3286 (the hammer shaft is 59 cm long).

large $2V\alpha$ suggest that it is andesine-labradorite. It has been altered to albite, sericite, muscovite and quartz blebs, and biotite fills cracks in the crystals. Fractures and deformation twins are common features in the plagioclase, indicating a period of stress after the main metamorphism. There are large crystals of microcline (up to 3.5 mm long), which are slightly sericitized and have been shattered, the numerous cracks being filled with finely granular and recrystallized feldspar and muscovite. Lobes of myrmekite protrude into the microcline from the groundmass and the quartz forms elongated aggregates with a pronounced mortar texture. The biotite, which comprises the black bands, is pleochroic from pale brown to dark brown and is associated with ragged patches and elongated crystals of iron ore aligned along the foliation. The abundance of well-rounded crystals of zircon (Fig. 4a) up to 0.1 mm in diameter in the thin section suggests a sedimentary origin for the rock.

The schistose material is wrapped around numerous garnets that have been shattered, the fragments being separated and replaced by pale green chlorite, sericite and a little biotite (Fig. 4b).

In specimen E.3612.1 the potash feldspar is a fine microcline-microperthite; the rock contains numerous small garnets and has been minutely folded (Fig. 4c). Ragged brownish green hornblende is commonly associated with biotite in specimen E.3287.1 and the broken laths of plagioclase have been replaced by veins and antiperthitic blebs of potash feldspar.

2. *Augen-gneisses*

The augen-gneisses are mostly massive and well jointed with no evidence of bedding or contacts with other rock types (E.3295, 3603, 3608, 3611 and 3614) but at stations E.3286 and 3287 they are interbedded with biotite-gneisses. The augen-gneisses are characterized by large white microcline porphyroblasts (up to 2 cm in length) with a marked preferred orientation (Fig. 5), and these feldspars are separated by discontinuous black micaceous bands.

In thin section, the porphyroblasts have either a typical cross-hatch twinning or an undulose extinction, and they have been incipiently altered to sericite and a brownish unidentifiable mineral. These xenoblastic crystals are often simply twinned and

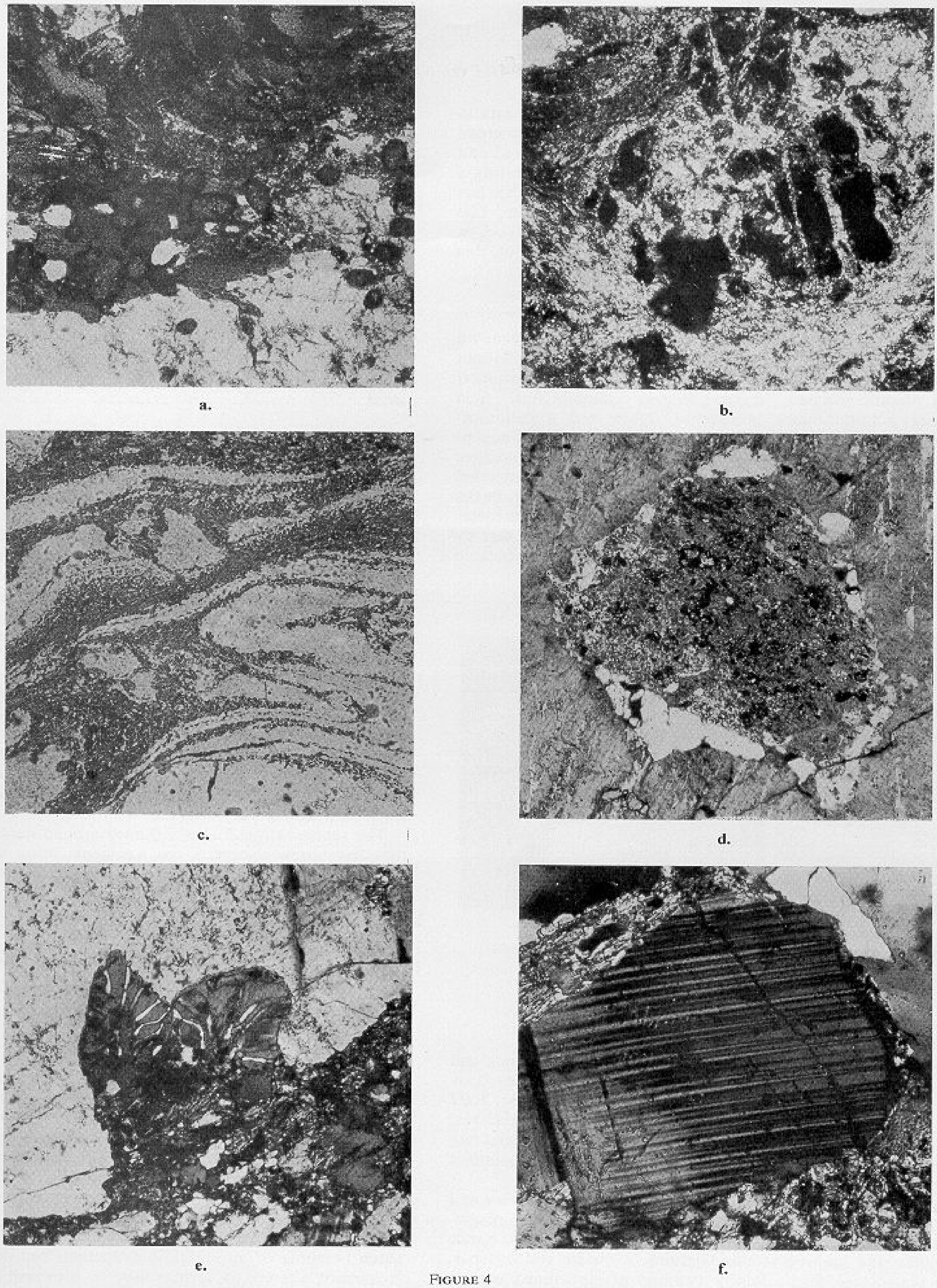

FIGURE 4

a. Rounded zircon crystals in a biotite-gneiss. (E.3607.1; X-nicols; × 53)
b. Shattered garnet crystals replaced and surrounded by chlorite, sericite and biotite. (E.3607.1; X-nicols; × 62)
c. Minute folding in a biotite-gneiss. (E.3612.1; ordinary light; × 40)
d. Albite crystal corroded and replaced by microperthite and exhibiting fine lobate boundaries and discontinuous rims of water-clear albite. (E.3295.1; X-nicols; × 58)
e. Myrmekite protruding into microperthite in an augen-gneiss. (E.3614.1; X-nicols; × 56)
f. Deformation twins in plagioclase in an augen-gneiss. (E.3614.1; X-nicols; × 170)

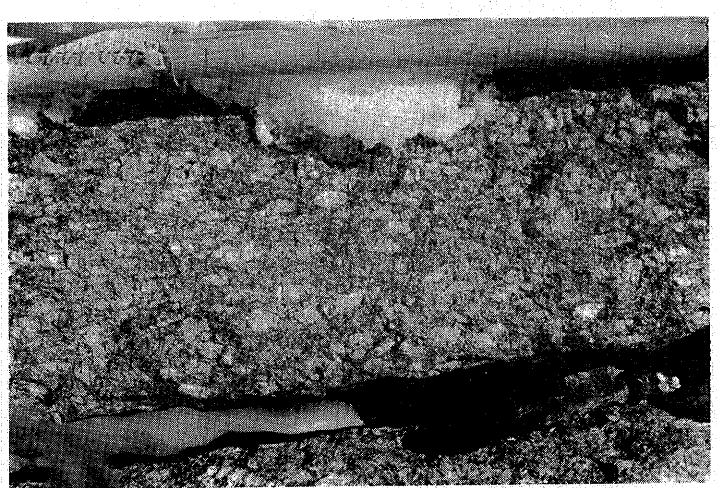

FIGURE 5
Augen-gneiss showing preferred orientation of the feldspar porphyroblasts (the hammer shaft is graduated in inches).

are usually a string microperthite but coarse patch microperthites are also represented.

The plagioclase is of two types: either, a few twinned, normally zoned crystals (about An_{32}) which have been bent and sheared, or, more commonly, highly sericitized and saussuritized, poorly twinned or untwinned albite. Many of the albite crystals have been extensively corroded and replaced by microperthite (Fig. 4d) and exhibit fine lobate boundaries and discontinuous rims of water-clear albite. The plagioclase is often antiperthitic. Myrmekite has been formed at the margins of many of the plagioclase crystals where they are in contact with microperthite and lobes of it penetrate into the latter. The mafic constituents are hornblende with a distinctive pleochroism scheme α = brown, β = greenish and γ = dark green, and greenish brown biotite which is partially pseudomorphed by chlorite. These mafic minerals occur as aggregates wrapped around the feldspars and are associated with epidote, iron ore and sphene, the latter often surrounding the iron ore. Quartz forms graphic intergrowths with microperthite but more commonly occurs as elongated aggregates with a pronounced mortar texture or granoblastic equigranular crystals with triple-point intersections.

Cracks in the microperthite are filled with finely granulated and recrystallized quartz, plagioclase, microperthite and myrmekite, indicating the operation of metamorphism after the formation of the porphyroblasts.

In specimen E.3614.1 the biotite is a deep red-brown colour and associated with it are small garnet crystals, Myrmekite is well developed in this specimen (Fig. 4e) and deformation twins (Fig. 4f) are common in the plagioclase (An_{48}).

Brown pleochroic allanite and zircon crystals are common accessory minerals in these rocks.

3. *Amphibolites*

Included under this heading are a rather varied group of rocks which crop out mainly around Mount Sullivan. They are massive, well-jointed and in the hand specimen they comprise black hornblende and biotite, often forming a weak foliation, in a white quartz–feldspar matrix.

The amphibolites have not been observed in contact with either the biotite-gneisses or the augen-gneisses but they are intruded by acid gneisses at station E.3291 and potash feldspar porphyroblasts have formed in the amphibolite up to 4 m from the contact.

Specimens E.3291.12 and 3294.1 consist of aggregates of green pleochroic hornblende crystals, associated with brown biotite, in a quartz–feldspar matrix. Plagioclase (approximately An_{43}), the commonest feldspar, forms corroded laths, patchily zoned and severely altered to sericite and calcite. The groundmass is largely formed of anhedral crystals of microperthite and granoblastic equigranular quartz.

Pale green fibrous tremolite-actinolite replaces original colourless clinopyroxene in specimen E.3282.3 and the plagioclase (andesine-labradorite) exhibits deformation twinning. Hypidioblastic crystals of muscovite (0.1–0.7 mm in length) are scattered through the rock and the groundmass comprises mainly colourless zoisite with a perfect cleavage in one direction, a large $2V\gamma$ and distinctive Berlin blue interference colours.

4. *Acid gneisses*

Acid gneisses are widespread to the north, east and south of Mount Sullivan. They are massive well-jointed rocks comprising white plagioclase, quartz, potash feldspar, green-black hornblende and biotite, often showing a preferred orientation (Fig. 6). Those to the north-east of Mount Sullivan have an abundance of epidote, giving the rock a distinctive green colour. To the south of Mount Sullivan the acid gneisses are pink in colour and the biotite flakes show a strong parallelism. They are mostly massive and well jointed but they are foliated on the eastern side of station E.3290. At station E.3291 the gneiss intrudes a massive amphibolite, the contact being vertical and

FIGURE 6
Acid gneiss showing preferred orientation of biotite (E.3290.1; the key is 5.9 cm long).

striking 025° true. The gneiss has been contaminated at the margin and large white feldspar porphyroblasts have grown in the amphibolite within 12 m of the contact.

In thin section the greenish gneisses have a porphyroblastic texture with large laths of plagioclase (albite) up to 3.5 mm in length which may be twinned; they have been severely altered to sericite and saussurite. There are a few remnants of twinned andesine (approximately An_{32}) which have been altered to sericite and saussurite in their cores, and patchily altered to potash feldspar in some cases. All of the plagioclase has been extensively corroded by microperthite and quartz to give lobate or serrated sutured boundaries. In some cases the microperthite has the cross-hatch twinning of microcline, has been incipiently altered to sericite and forms large xenoblastic crystals which are interstitial or poikiloblastic towards the plagioclase. Quartz forms irregularly shaped patches consisting of large and small crystals with an undulose extinction, often exhibiting sutured margins. These crystals sometimes enclose remnants of plagioclase and microcline. Quartz also forms interstitial aggregates of smaller crystals and many are unstrained. A prominent constituent of the gneisses is the distinctive biotite, pleochroic from pale brown to greenish brown, often 3.5 mm in length, and altered in the cores to pale yellow pleochroic epidote and at the margins to pale green chlorite. The foliation in these rocks is produced by elongated aggregates of this biotite. The biotite contains numerous small inclusions of apatite and associated with the biotite are euhedral crystals of sphene up to 0.7 mm in length and small crystals of garnet.

5. *Schists*

Two bodies of schist, one 2 m wide and the other 100 m across, occur on the western side of station E.3283; both dip steeply and trend between 066° and 081° true. They are interbedded with acid gneisses and they seem to contain inclusions of the gneisses close to the contacts, indicating that they are younger than the gneisses.

In the hand specimen, the schists are coarse-grained, grey-green in colour with discontinuous black micaceous bands and euhedral porphyroblasts of white potash feldspar which may be over 1 cm in length (Fig. 7). Microscopically, the potash feldspar appears to be microcline-microperthite, dusty with fine inclusions, incipiently sericitized and exhibiting a faint cross-hatch twinning. It is poikiloblastic towards the small plagioclase crystals and it has a slightly irregular boundary with the small crystals of the groundmass.

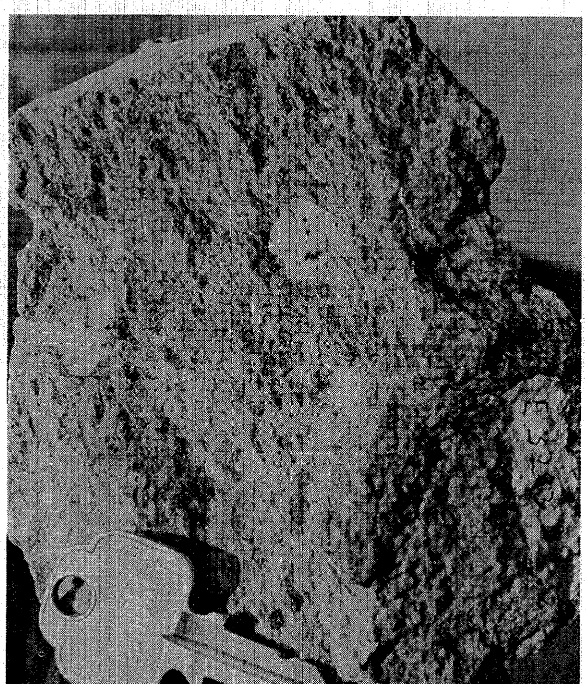

FIGURE 7
Porphyroblasts of potash feldspar in a schist (E.3283.3; the key is 5.9 cm long).

Apart from the microcline porphyroblasts, the rock has the porphyritic texture typical of a dyke or lava and comprises phenocrysts of quartz and plagioclase set in a fine-grained groundmass. The plagioclase (An_4) forms twinned crystals or glomeroporphyritic aggregates which have been altered to calcite, sericite and saussurite and have been peripherally corroded to give finely serrated boundaries. The crystals have retained their original lath shapes but they have been broken, the cracks being filled with fine angular fragments of plagioclase, quartz and small flakes of sericite and biotite.

The quartz phenocrysts are rounded embayed crystals whose boundaries have been modified by partial recrystallization to give a serrated appearance.

The elongated or equant mafic minerals have been completely pseudomorphed by pale yellow epidote, green biotite, small grains of sphene and leucoxene. The matrix of the rock comprises mainly recrystallized quartz and feldspar with much sericite and biotite which are wrapped around the phenocrysts. The biotite is pleochroic from straw to green-brown and forms elongated aggregates of small crystals 0.1 mm or less in length; associated with the biotite are radiating crystals of yellow epidote and a number of broken euhedral crystals of sphene (0.4–1 mm in length). Haematite, calcite and small crystals of zircon are common accessories in the groundmass.

6. *Minor greenschist*

Minor greenschist dykes are conspicuous in the acid gneisses and they are easily distinguished from the younger basic dykes by their schistosity. At station E.3291, a schistose dyke 1.4 m wide and dipping at 60° in a direction 086° true intrudes massive acid gneisses similar to those at station E.3290. Microscopically, this rock consists mainly of ragged fibrous hornblende (large $2V\alpha$; $\gamma{:}c = 29°$) with a pleochroism scheme α = pale bluish green, β = pale green and γ = pale brown. The hornblende has been bent and fractured, the fragments being separated and altered to biotite. Clear plagioclase (An_{51}) forms small irregular crystals which are often twinned and have a slight undulose extinction. They contain numerous very small inclusions in addition to small crystals of hornblende.

Quartz, iron ore and sphene are the main accessory minerals and small crystals of the latter often surround the elongated masses of iron ore.

In specimen E.3296.2, clusters of elongated crystals of epidote up to 0.4 mm in length are abundant.

7. *Engel Peaks granite*

This granite at Engel Peaks forms a pluton elongated north–south and approximately 2 km wide, and is situated in the extreme north-eastern part of the area. The granite pluton is separate from the main outcrops of the metamorphic complex but, since it is overlain by the basal breccia of the metavolcanic sequence, it is included within the metamorphic complex.

In the hand specimen it is coarse-grained, pink in colour and comprises plagioclase, potash feldspar, quartz and black mafic minerals. Specimen E.3271.1 has been examined in thin section and has an unusual texture (Fig. 8), the major components—quartz, potash feldspar and plagioclase—having a ragged appearance.

The plagioclase (up to 7 mm in length) exhibits deformation

FIGURE 8
The texture of the Engel Peaks granite showing dactylitic intergrowths of quartz and feldspar. (E.3271.7; X-nicols; × 44)

twinning and it has been replaced to a variable extent by patches of turbid potash feldspar, and all gradations between antiperthite and coarse patch-perthite are represented.

The remainder of the rock consists of xenomorphic crystals of fine microperthite which form dactylitic intergrowths with strained quartz. The microperthite is poikilitic towards the plagioclase and often the twinning in the plagioclase component of the microperthite is parallel to that in the plagioclase.

The only mafic mineral present is ilmenite which forms irregular masses that have been partially altered to leucoxene. Small crystals of sphene are common and muscovite occurs in sheaves of crystals with a decussate texture but this is relatively rare.

C. GEOCHEMISTRY

Twenty-six specimens of the major rock types in the metamorphic complex to the east of the Eternity Range have been analysed (Table II). The purposes of this study are:

i. To compare these rocks with metamorphic rocks from other parts of the Antarctic Peninsula.
ii. To study various rock types within the metamorphic complex and to attempt to determine their origins and histories.
iii. To provide chemical criteria to discriminate between the igneous rocks of the metamorphic complex and the younger plutonic rocks.

The analyses of the metamorphic rocks of northern Palmer Land have been plotted on triangular variation diagrams with coordinates (Fe″+Fe‴)–Alk–Mg and K–Na–Ca (Fig. 9), and in Fig. 10 these are compared with the analyses of Hoskins (1963) and Fraser (1965) from Marguerite Bay, and those of Marsh (1968) and Stubbs (1968) from the Oscar II, Foyn and Bowman Coasts, on the east coast of Graham Land.

It is evident from Fig. 10 that, while the metamorphic rocks from Marguerite Bay and the east coast of Graham Land are broadly comparable, those from northern Palmer Land are much richer in alkalis, especially potassium. Although some of

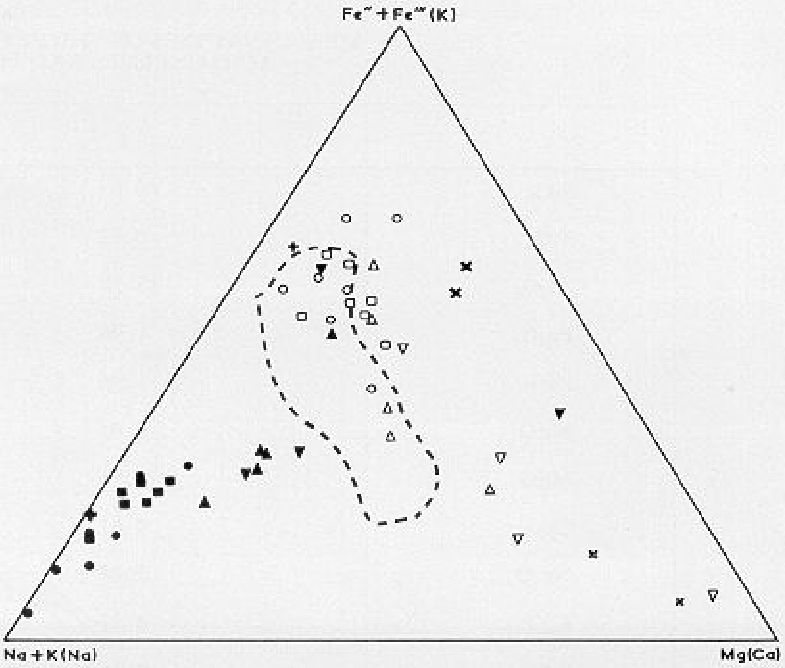

FIGURE 9
Triangular variation diagram plotted on the coordinates (Fe″+Fe‴)–Alk–Mg (▲■●+▼X) and Ca–Na–K (△□○+▽x) for rocks from the metamorphic complex. The dashed line delineates the field of magmatic rocks (Raju and Rao, 1972).

▲ and △	Biotite-gneisses.	+ and +	Engel Peaks granite.
■ and □	Augen-gneisses.	▼ and ▽	Amphibolites.
● and ○	Acid gneisses.	X and x	Greenschist dykes.

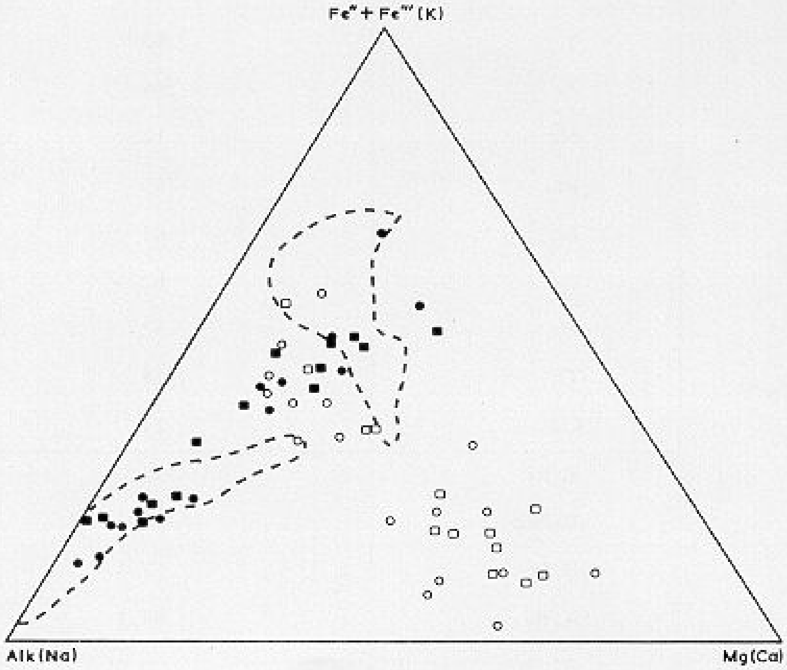

FIGURE 10
Triangular variation diagram plotted on the coordinates (Fe″+Fe‴)–Alk–Mg (■ and ●) and Ca–Na–K (□ and ○) for metamorphic rocks from the Oscar II, Foyn and Bowman Coasts (● and ○; Marsh, 1968; Stubbs, 1968) and Marguerite Bay (■ and □; Hoskins, 1963; Fraser, 1965). The dashed lines delineate the main concentration of rocks from northern Palmer Land (Fig. 9).

TABLE III
MEAN ANALYSES OF THE BIOTITE-GNEISSES, AUGEN-GNEISSES, ACID GNEISSES AND THE ENGEL PEAKS GRANITE

	1	2	3	4
SiO_2	66.69	70.76	70.64	74.13
TiO_2	0.62	0.37	0.27	0.44
Al_2O_3	15.58	14.62	16.10	12.82
Fe_2O_3	1.98	1.22	1.08	2.51
FeO	1.96	1.45	1.09	0.30
MnO	0.05	0.05	0.04	0.03
MgO	2.75	0.60	0.58	0.07
CaO	2.61	1.47	1.71	0.55
Na_2O	2.84	3.23	3.18	3.51
K_2O	4.17	5.41	5.83	6.28
P_2O_5	0.16	0.09	0.12	0.07
H_2O+	0.27	0.21	0.21	0.20
H_2O-	0.21	0.17	0.21	0.12
Cr	43	13	6	–
Ni	30	7	6	5
Rb	183	230	280	242
Sr	451	157	333	28
Y	62	84	88	111
Zr	298	236	165	427
Nb	12	13	13	19
Ba	791	788	783	933
La	41	62	45	64
Ce	62	98	64	95
Pb	52	41	60	70
Th	24	31	30	30
Ga	24	18	20	10
K/Rb	191	193	171	215
Ba/Rb	4.3	3.4	3.9	3.9
K/Sr	77.4	282	144	1 862
K/Ba	44.1	56.3	61.3	55.9
Rb/Sr	0.41	1.46	0.84	8.64
Ca/Sr	41.7	83.4	36.3	140.5
Ba/Sr	1.75	5.00	2.35	33.3

1. Average of four biotite-gneisses (E.3606.1, 3607.1, 3612.1, 3612.2).
2. Average of seven augen-gneisses (E. 3286.2, 3259.1, 3296.1, 3603.1, 3608.1, 3611.1, 3614.1).
3. Average of seven acid gneisses (E. 3279.6, 3285.1, 3286.4, 3290.1, 3291.1, 3609.1, 3613.1).
4. Engel Peaks granite (E.3271.1).

these differences may be attributable to the errors due to the different methods of analysis and/or a bias in sampling (Stubbs has not analysed porphyroblastic and augen-gneisses), it is clear that the calcium-, magnesium- and iron-rich rocks, which are abundant in the metamorphic complexes of Graham Land, are rare in northern Palmer Land.

The acid gneisses, augen-gneisses, metasomatized amphibolite and all but one of the biotite-gneisses have similar compositions (Fig. 9; Table III). There is a marked similarity in the oxide percentages, trace-element abundances and most of the element ratios. The main differences between the various gneiss groups are that the biotite-gneisses have lower silica and potassium, and higher magnesium, calcium and iron than the acid gneisses and augen-gneisses, and most of the acid gneisses have a higher alkali content than the augen-gneisses (Fig. 11). The remaining amphibolites and the greenschist dykes plot away from the other rocks on the triangular variation diagrams and do not seem to be genetically related to them; the greenschist dykes can probably be correlated with the basic metavolcanic rocks described on p. 14 and their geochemistry will be discussed in relation to the other basic volcanic and hypabyssal rocks on p. 38–40.

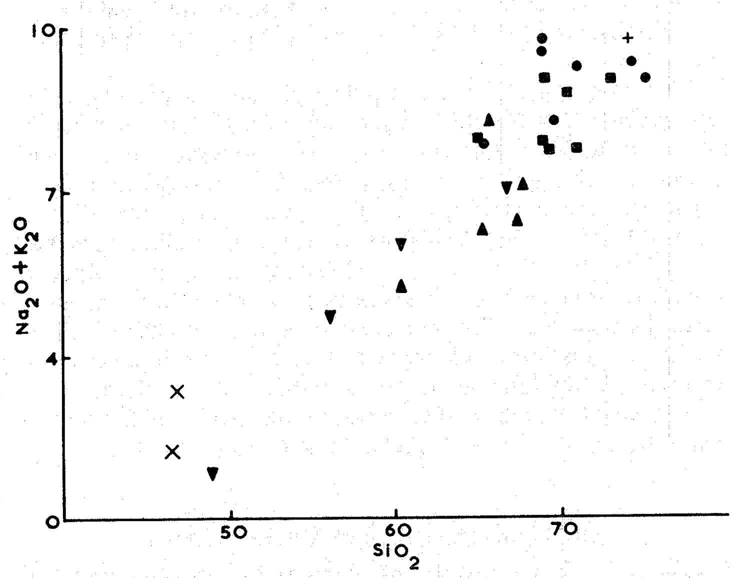

FIGURE 11
A plot of total alkalis against silica for rocks from the metamorphic complex. The symbols are the same as in Fig. 9.

Because the augen-gneisses and acid gneisses have a granitic composition, their chemistry can be compared with the results of phase-equilibrium experiments in systems resembling granitic rocks. Tuttle and Bowen (1958) and Luth and others (1964) examined the system $NaAlSi_3O_8$–$KAlSi_3O_8$–SiO_2–H_2O at water pressures of between 0.5 and 10 kbar, and they found that minimum crystallization takes place with acid plagioclase, potassium feldspar and quartz crystallizing together at temperatures from 760° to 625°C; this minimum becomes a ternary eutectic at between 3 and 4 kbar, and its composition moves towards the $NaAlSi_3O_8$ apex with increasing water-vapour pressure. Tuttle and Bowen (1958) compared the normative Q,

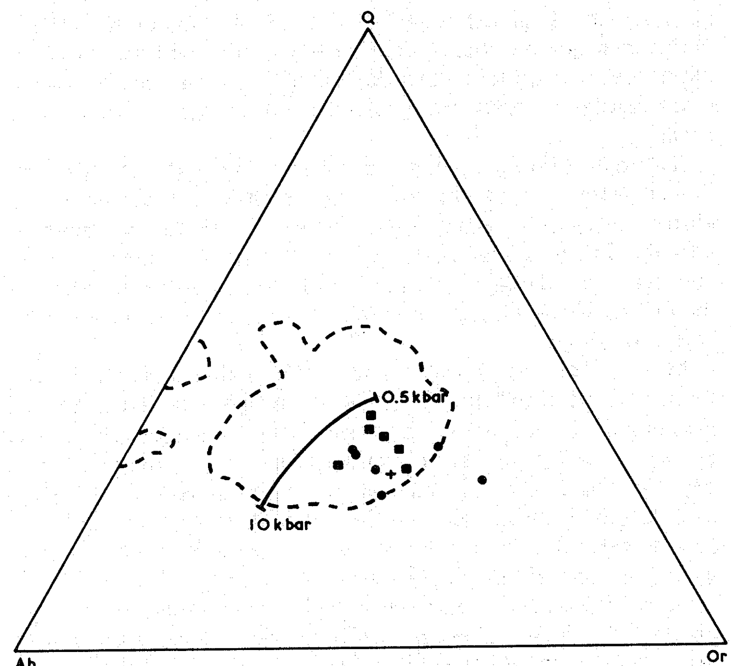

FIGURE 12
A plot of normative quartz, albite and orthoclase for the Engel Peaks granite, and the augen-gneisses and acid gneisses which contain normative Q+Ab+Or > 79%.

■ Augen-gneisses.
● Acid gneisses.
\+ Engel Peaks granite.

The solid line indicates the trend of the ternary minima and eutectics at water pressures of between 0.5 and 10 kbar (Tuttle and Bowen, 1958; Luth and others, 1964). The dashed line encloses 86% of all the granites considered by Winkler (1974, fig. 18-11).

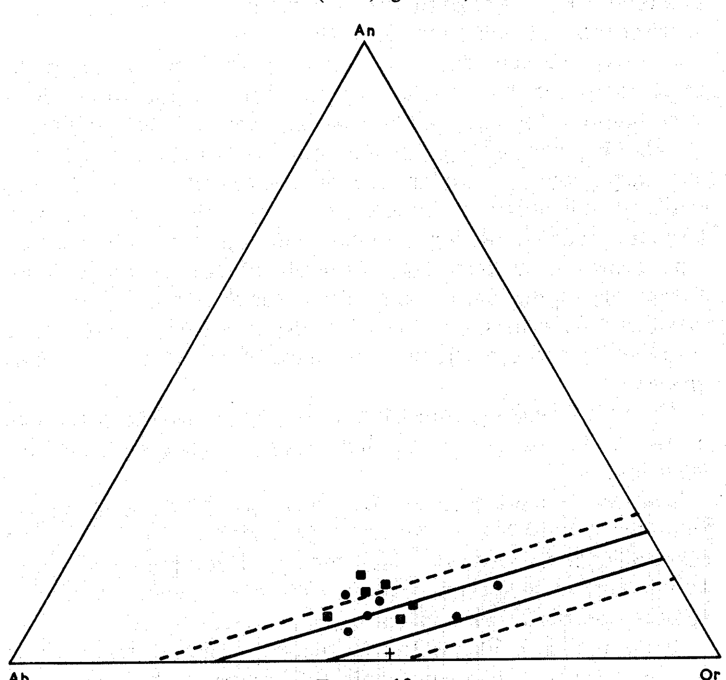

FIGURE 13
A plot of normative anorthite, albite and orthoclase for the Engel Peaks granite, the augen-gneisses and acid gneisses which contain normative Q+Ab+Or > 79%.
The symbols are the same as in Fig. 12. The low-temperature trough in this system is enclosed by the continuous parallel lines, while the dashed lines enclose the outer limits of compositions indicative of crystallization of liquids in the thermal trough allowing for analytical error (Kleeman, 1965, fig 4A).

Or and Ab of all the analysed rocks in Washington's (1917) tables in which normative Q+Or+Ab $\geqslant$ 80% with their experimental results and they concluded that "there can be little doubt that magmatic liquids are involved in the genesis of the granitic rocks".

Kleeman (1965) studied the system Or–Ab–An–SiO_2 at 5 kbar water-vapour pressure and he showed that there is a closer correlation between the "average" granite composition and the low-temperature trough in this system than there is between the "average" granite composition and the minima in the Or–Ab–SiO_2 system, especially at water-vapour pressures of 2 kbar or more.

Most of the acid gneisses and augen-gneisses from northern Palmer Land which have been analysed have at least 79% of normative Q+Ab+Or and these have been plotted on a Q–Ab–Or diagram (Fig. 12) and an Or–Ab–An diagram (Fig. 13). On the Q–Ab–Or diagram the augen-gneisses plot fairly close together and trend from the low-temperature end of Tuttle and Bowen's minimum towards the Or apex; all of the points lie within the field of "average" granites (Winkler, 1974, fig. 18-11). Three of the augen-gneisses fall in the low-temperature trough on the Or–Ab–An diagram, while the other three are grouped just outside of it and, similarly, on the K–Na–Ca diagram (Fig. 9) four out of six augen-gneisses fall in the field of magmatic granites (Raju and Rao, 1972). It seems, therefore, that many of these gneisses have a magmatic origin. As there is no evidence to suggest that they are the products of the differentiation of more basic rocks, they, like the intrusive granites studied by Bowes (1967), are probably the products of partial melting at low water-vapour pressure, and the orthoclase-enrichment trend is due to a metasomatic replacement of plagioclase by microcline. The relatively rare crystals of microcline in some of the biotite-gneisses were probably formed at this time.

Most of the acid gneisses plot within the field of magmatic granites on the K–Na–Ca diagram (Fig. 9) and in the low-temperature trough on the Or–Ab–An diagram (Fig. 13). On the Q–Ab–Or diagram (Fig. 12) they plot below the augen-gneisses but they have a similar orthoclase-enrichment trend. The evidence indicates a magmatic origin and they were probably formed by partial melting at higher water-vapour pressures than those existing during the formation of the augen-gneisses. Potash metasomatism again accounts for the orthoclase-enrichment, and the presence of potash-feldspar porphyroblasts in the amphibolite and the schists is evidence of the efficiency of this process.

The Engel Peaks granite plots close to the acid gneisses in all of the diagrams and a similar origin is suggested for this intrusion.

Two of the acid gneisses (E.3290.1 and 3291.10) stand out from the rest with their much lower K/Rb and lower Ba/Rb ratios (Table II), both of which indicate fractionation (Taylor, 1965). These two specimens were taken from adjacent nunataks and they probably belong to the same igneous body.

There is little evidence to indicate the original nature of the biotite-gneisses. The most significant differences between these biotite-gneisses and the augen-gneisses and acid gneisses are the much higher chromium and nickel values of the former (Table III). In Table IV the chromium and nickel values of the biotite-gneisses are compared with the average of six Andean non-hybrid granodiorites and sedimentary rocks from the Danco Coast (West, 1974). All of the rocks in this table contain between 60 and 68% SiO_2, and it is clear that the chromium and nickel values resemble more closely those of the sedimentary rocks. It was suggested, on petrographic grounds, that one of the biotite-gneisses (E.3607.1) was derived from sedimentary rocks.

TABLE IV

A COMPARISON OF THE CHROMIUM AND NICKEL ABUNDANCES OF THE BIOTITE-GNEISSES WITH THOSE OF AN AVERAGE GRANODIORITE FROM NORTHERN PALMER LAND AND SEDIMENTARY ROCKS FROM THE DANCO COAST

	1	2	3	4
Cr	43	66	60	7
Ni	30	31	25	8

1. Average of four biotite-gneisses (E.3606.1, 3607.1, 3612.1, 3612.2).
2. Average of four siltstones from the Danco Coast (West, 1974, table III, column 6).
3. Feldspathic sandstone from the Danco Coast (West, 1974, table III, column 1).
4. Average of six non-hybrid Andean granodiorites from norther Palmer Land (E.3245.3, 3246.1, 3620.3, KG.1200.6, 1207.3 and 1221.1).

The amphibolites are a heterogeneous group of rocks. Specimen E.3282.3, in its major and trace elements, especially the high magnesium, iron, calcium, chromium and nickel, resembles a basic igneous rock. Specimens E.3291.11 and 12 show the chemical effects of the metasomatic formation of potash feldspar porphyroblasts in the amphibolite, specimen E.3291.11 having come from close to the contact with the intruding acid gneisses and specimen E.3291.12 12 m away from the contact. The metasomatism has introduced silica, sodium, potassium and associated trace elements, and has depleted the amphibolite in iron, magnesium and calcium.

The geochemistry of the metamorphic rocks will be compared with that of the younger plutonic rocks on p. 31–35.

D. METAMORPHISM AND METASOMATISM

The lack of characteristic metamorphic minerals makes it difficult to determine the metamorphic grade reached in these rocks. However, the mineralogy of the schists and gneisses from the western side of Palmer Land and the biotite-gneisses east of the Eternity Range, i.e. the presence of large crystals of garnet associated with plagioclase (andesine-labradorite), indicates regional metamorphism to the almandine-amphibolite facies (Turner and Verhoogen, 1960, p. 544). This was followed by a marked shearing stress when the garnet crystals were shattered and partially replaced by either biotite or chlorite; the transformation of garnet to biotite rather than chlorite is thought to occur when the temperature is higher, at an earlier stage in the retrograde metamorphism (Harker, 1950, p. 350), according to the formula:

$$\underset{\text{garnet}}{R_3Al_2(SiO_4)_3} + \underset{\text{potash feldspar}}{2KAlSi_3O_8} + 2H_2O \longrightarrow \underset{\text{biotite}}{H_2KR_3Al(SiO_4)_3 . H_2KAl_3(SiO_4)_3} + 3SiO_2 .$$

Associated with the break-down of the garnet is the alteration of the plagioclase to albite.

There are deformed porphyroblasts of potash feldspar in some of the biotite-gneisses and these were probably introduced during the intrusion of the augen-gneisses. Both the biotite-gneisses and the augen-gneisses have a strong foliation marked by abundant biotite and recrystallized quartz and feldspar, and this is wrapped around the broken garnet crystals, the plagioclase and the microcline; this foliation distinguishes these rocks from the younger metamorphic rocks.

The intrusion of the acid gneisses was also accompanied by potash metasomatism in the host amphibolites. Some of these acid gneisses have a weak foliation marked by the preferred orientation of biotite.

The presence of potash-feldspar porphyroblasts in the schists is more difficult to explain as these rocks are quartz-plagioclase-porphyries and they seem to be younger than the surrounding acid gneisses. These schists may be equivalent to the dacitic rocks belonging to the metavolcanic and metasedimentary group and, if this is the case, a relatively young period of potash metasomatism is present. This metasomatism is unlikely to have been associated with the undeformed plutonic rocks because the granodiorites in this area are relatively depleted in potash and, consequently, it is possible that some of the acid gneisses are younger than the metavolcanic and metasedimentary rocks.

This limited evidence suggests that at least three phases of metamorphism and metasomatism have affected these metamorphic rocks. The biotite-gneisses were subjected to almandine-amphibolite metamorphism and, after the intrusion of the augen-gneisses, the garnet crystals in the biotite-gneisses were broken up and a strong foliation was imparted on both rock types. A younger metamorphism has imposed a weak foliation on some of the acid gneisses and this event may be the one which affected the metavolcanic and metasedimentary rocks. Potash metasomatism accompanied the intrusion of the augen-gneisses and the acid gneisses, and the presence of potash-feldspar porphyroblasts in the schists suggests a third younger period of metasomatism.

E. Age of the Metamorphic Complex

From the field evidence, it is only possible to give relative ages to the metamorphic rocks. The biotite-gneisses have been intruded by the augen-gneisses and in places they have a *lit-par-lit* relationship. No contacts were observed between either the biotite-gneisses or the augen-gneisses and the amphibolites, but the latter are intruded by acid gneisses. In turn, these are intruded by the minor greenschist dykes but it is uncertain whether they are younger or older than the schists which are interbedded with and are younger than the acid gneisses. The Engel Peaks granite is situated some distance away from the main metamorphic complex but in its composition it is closely similar to the acid gneisses; this granite forms a basement to the metavolcanic and the metasedimentary rocks.

No radiometric ages have been obtained for the metamorphic rocks of northern Palmer Land. The schists exposed in the Mica Islands have been included by Adie (1954) in the "Basement Complex", which he tentatively suggested "as being early Palaeozoic but more probably Archaean". However, radiometric age determinations on rocks of the "Basement Complex" of Marguerite Bay carried out by Halpern (1971) and Grikurov and others (1966, p. 1401) have yielded ages much younger than Precambrian. The Rb-Sr determinations carried out by Halpern (1971) on *ortho*gneisses gave a total-rock age of 200 ± 10 Ma (Triassic) but K-Ar age of only 108 ± 5 Ma (Cretaceous) for biotite from one of the gneisses. The latter is similar to the K-Ar age determinations of Grikurov and others (1966) and it implies a loss of radiogenic argon and strontium from the biotite during the "Andean" orogeny (Upper Cretaceous–Lower Tertiary).

From radiometric evidence, Marsh (1968) suggested that the amphibolite facies of regional metamorphism of the metamorphic rocks on the eastern side of Graham Land ended in the Permian. This age is within the range which has been suggested for the Trinity Peninsula Series.

In view of the limited radiometric evidence and the problems of correlating the various rock groups from different parts of the Antarctic Peninsula, it is not possible to suggest absolute ages for any of the events in the metamorphic complex of northern Palmer Land.

IV. METAVOLCANIC AND METASEDIMENTARY ROCKS

This is a distinctive sequence of rocks exposed to the east and west of the metamorphic complex, east of the Eternity Range. Lavas, altered tuffs and metasedimentary rocks are represented and, although original textures are much in evidence, the development of small flakes of biotite with a marked preferred orientation indicates regional metamorphism up to the greenschist facies. The lavas are generally massive and well jointed, while the pyroclastic rocks and metasediments are cleaved and jointed.

A. Field Relations

The base of the succession is a breccia, which rests on the deformed Engel Peaks granite (E.3271.1), and the contact dips at approximately 80° in a direction 352° true. The exposure at station E.3271 is very fragmented and, although the actual contact is not visible, there is a definite transition westward from boulders of solid granite to a consolidated breccia containing angular fragments which are variable in size but mostly less than 8 cm in diameter within 1.5 m of the contact. About 90 m from the contact there is a 3 m wide argillaceous band and above this is a conglomerate, which is similar to the breccia except for slight rounding of the clasts and the presence of inclusions of the argillaceous rock. At the extreme western end of the outcrop, the conglomerate is overlain by a few centimetres of green slate containing fragments of granite and these are succeeded by black slates; the contact between the green slates and the conglomerate dips at 70° in a direction 255° true.

This sequence of rocks is also exposed in various nunataks to the north, west and south of Engel Peaks but no marker horizons were recognized and so the scattered outcrops cannot be correlated with certainty. However, the attitude of the bedding is very consistent with steep dips to the west and strikes varying between 156° and 168° true. The exposures of lava (E.3268 and 3276) are generally small and the massive well-jointed rocks have been frost-shattered, but at station E.3267 there are massive volcanic tuffs and at station E.3270 coarse-grained metasedimentary rocks are interbedded with layers (less than 1 m thick) of white fine-grained rocks which are sometimes banded.

West of the metamorphic complex the metasedimentary and metavolcanic succession is represented by cleaved quartz-keratophyre tuffs and lavas dipping at 70° to 240° true on the north-eastern side of Mount Charity (E.3616), sheared dacites on the south-eastern side of Mount Faith (E.3601), and inter-bedded sandstones and shales at station E.3615. At station E.3616 the quartz-keratophyres are intruded by granitic rocks which are thought to be equivalent to the pre-volcanic adamellite exposed farther south, and these works are overlain by the Mount Charity sedimentary and volcanic succession.

B. Petrography

1. *Basic lavas*

These lavas are greenish black in colour and are sometimes amygdaloidal. Specimen E.3276.1 has quartz-filled amygdales (2–14 mm in length), which have been deformed to an elliptical shape, and small quartz veinlets. There are also patches of pale green epidote which seem to be filling amygdales. In thin section the rock is equigranular and the quartz-filled amygdales have an irregular outline and a rim of small recrystallized quartz grains about 0.1 mm in diameter with straight boundaries and triple-point intersections. The interiors of the amygdales contain irregular crystals up to 0.4 mm in diameter with an undulose extinction and fine lobate sutured boundaries; these seem to have formed by partial recrystallization during the period of stress that caused the elongation of the amygdales. The epidote-filled amygdales contain equant crystals up to 0.4 mm in diameter which are pleochroic from pale yellow to greenish yellow. A later generation of epidote is represented by small crystals less than 0.1 mm in diameter. These form patches and discontinuous veinlets with quartz and they cut the epidote-filled amygdales. The groundmass consists of twinned plagioclase (An_6) microlites 0.07–0.35 mm in length, abundant ilmenite, leucoxene, sphene, epidote and small flakes of green biotite.

Specimen E.3268.1 is finer-grained than the one described above and it contains amygdales of epidote set in a groundmass of small plagioclase microlites and ragged green tremolite-actinolite ($\gamma{:}c = 18°$); ilmenite, which is partially altered to leucoxene, and chlorite are also prominent in the groundmass. There are a few large elongated crystals up to 1.2 mm in length which have been completely replaced by a combination of pale green amphibole, chlorite, epidote, green biotite and ilmenite.

The chemistry of these lavas (Table V) differs appreciably from that of the Upper Jurassic lavas, mainly in the lower alumina and higher iron of the former. These basic lavas are, however, similar to the greenschist dykes of the metamorphic complex. Their chemistry will be discussed more fully on p. 38–40.

2. *Sheared andesites*

In the hand specimen the sheared andesites are black or grey in colour and they may have a speckled appearance due to the

Table V

CHEMICAL ANALYSES OF METABASALTS FROM THE ENGEL PEAKS AREA

	1	2
SiO_2	48.40	53.46
TiO_2	0.57	1.99
Al_2O_3	12.54	11.15
Fe_2O_3	7.46	12.63
FeO	4.19	4.12
MnO	0.17	0.25
MgO	11.22	3.36
CaO	9.55	5.49
Na_2O	1.96	4.88
K_2O	0.71	1.49
P_2O_5	0.06	0.36
H_2O+	1.30	0.60
H_2O-	0.22	0.28
Total	98.35	100.06
ELEMENT PERCENTAGES LESS TOTAL WATER		
Si^{4+}	23.37	10.91
Ti^{4+}	0.35	0.52
Al^{3+}	6.85	2.57
Fe^{3+}	5.39	34.37
Fe^{2+}	3.36	11.57
Mn^{2+}	0.14	0.08
Mg^{2+}	6.99	0.88
Ca^{2+}	7.05	1.71
Na^{+}	1.50	1.58
K^{+}	0.61	0.54
P^{5+}	0.03	0.07
O^{2-}	44.36	35.19

	1	2
C.I.P.W. NORMS		
Q	2.03	3.53
Z	–	0.02
or	4.32	3.84
ab	17.09	18.01
an	24.03	1.80
di	19.12	7.07
hy	20.79	0.37
mt	11.15	45.81
cm	0.21	–
il	1.12	1.65
hm	–	17.53
ap	0.15	0.37
Position (1/3 Si+K)−(Ca+Mg)	−5.47	+3.60
TRACE ELEMENTS		
Cr	904	9
Ni	334	1
Ga	14	25
Rb	28	42
Sr	152	32
Y	14	43
Zr	31	195
Nb	1	11
Ba	205	258
La	12	42
Ce	8	64
Pb	3	20
Th	–	8
ELEMENT RATIOS		
K/Rb	218	129
Ba/Rb	7.3	6.1
COORDINATES OF TRIANGULAR DIAGRAM		
Fe	49.0	93.9
Alk	11.8	4.3
Mg	39.2	1.8

1. E.3268.1 South of Engel Peaks.
2. E.3276.1 South-east of Engel Peaks.

presence of white plagioclase crystals. Microscopically, they have a porphyroclastic texture with large broken plagioclase crystals (An_{36}) and a few rock fragments set in a fine-grained matrix. The plagioclase crystals, which are antiperthitic, have been bent and sheared, and some crystals have been welded together.

The matrix consists largely of greenish brown biotite, chlorite and small flakes of sericite concentrated into schistose bands which are wrapped around the broken porphyroclasts. Crystals of ilmenite often occur as inclusions in the feldspar and they are generally broken and surrounded by leucoxene and sphene. There is much fine-grained and partially recrystallized quartz and plagioclase in the matrix.

3. *Sheared dacites*

These are pink-coloured porphyritic tuff or lava containing phenocrysts of embayed quartz and plagioclase (An_{32}) set in a granulated and sericitized groundmass. The plagioclase crystals have been replaced to various degrees by potash feldspar and some contain quartz blebs. The fine-grained matrix seems to consist of small recrystallized grains of feldspar, crystals of haematite and shear planes smeared with sericite which are wrapped around the phenocrysts.

4. *Quartz-keratophyres*

The quartz-keratophyres are pale grey cleaved porphyritic rocks with phenocrysts of subhedral embayed quartz and plagioclase, which often has chequer twinning. Plagioclase (An_{33}) is present as clots of small crystals (Fig. 14a), which may be elongated along the foliation, or as albitic plagioclase with a chequered structure; small inclusions of the andesine are contained in the latter (Fig. 14b). Potash feldspar has replaced the plagioclase to various degrees; it extends inwards from the crystal margins along cracks and cleavages, and with quartz it also forms veins which extend beyond the margins of the crystals.

Battey (1955) has explained similar chequered albites in keratophyres as having formed by "porphyroblastic growth proceeding from numerous centres and approaching axial parallelism by successive recrystallizations" and similar potash-feldspar intergrowths with the chequered albite as replacement rather than exsolution features.

Most of the quartz-keratophyre tuffs and lavas have sheared groundmasses of recrystallized quartz, haematite and sericite wrapped around the porphyritic crystals, but the relatively undeformed specimens contain devitrified glass fragments.

5. *Metasedimentary rocks*

The coarse-grained types are grey semi-schists which possess a marked stratification suggesting a sedimentary origin. In thin section these rocks are composed of porphyroclasts of plagioclase set in a fine-grained matrix containing abundant brown biotite with a preferred orientation. The porphyroclasts may be single crystals or aggregates and two types of plagioclase are represented: andesine and optically positive albitic plagioclase. The foliated matrix is wrapped around the porphyroclasts, leaving pressure shadows containing relatively coarse recrystallized quartz and sometimes calcite.

Specimen E.3270.7 consists of lenses and layers of polygonized quartz with occasional irregular crystals of albitic

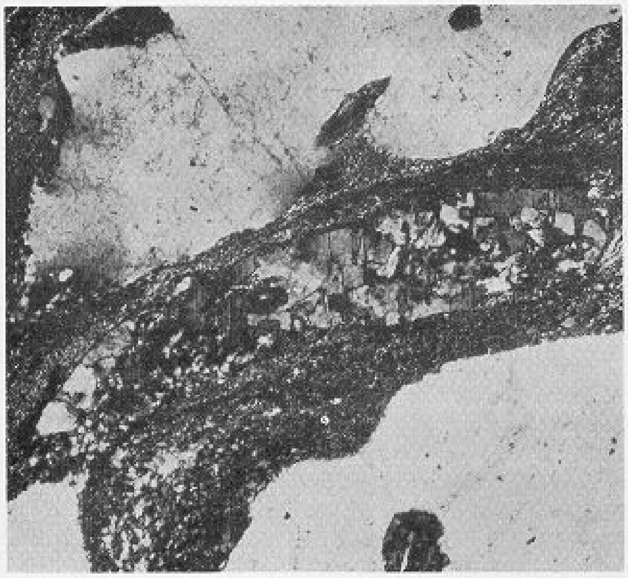

a.

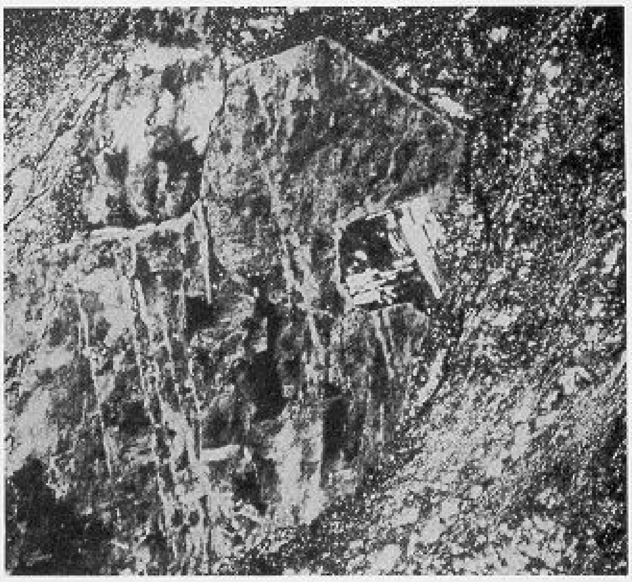

b.

FIGURE 14

a. A lenticular clot comprising small crystals of andesine. (E.3616.1; X-nicols; × 50)
b. An inclusion of andesine in chequered albite. (E. 3616.1; X-nicols; × 57)

plagioclase. The quartzose layers are separated by a finer-grained matrix of biotite, iron ore, quartz and feldspar.

Fine-grained siltstones or ashes crop out mainly at station E.3270, where they are intercalated with the coarser rocks described above; they form relatively thin beds which may be either white and massive or finely banded. Specimen E.3270.4 has interpenetrating black and white bands (Fig. 15). In thin section, the light-coloured bands consist of fine layers and lenses of crystals, mainly recrystallized quartz with straight boundaries and triple-point intersections, patches of calcite, small flakes of green biotite with a marked preferred orientation and a few larger grains of corroded microcline. The banding is transected by small quartz veinlets in which the crystals are elongated along the veins.

The dark bands in the rock have an abundance of epidote and sericite but they lack the biotite and tend to be more inequigranular. These bands contain relatively large irregularly shaped crystals of quartz and plagioclase up to 0.25 mm in length set in a finer-grained matrix containing much sericite.

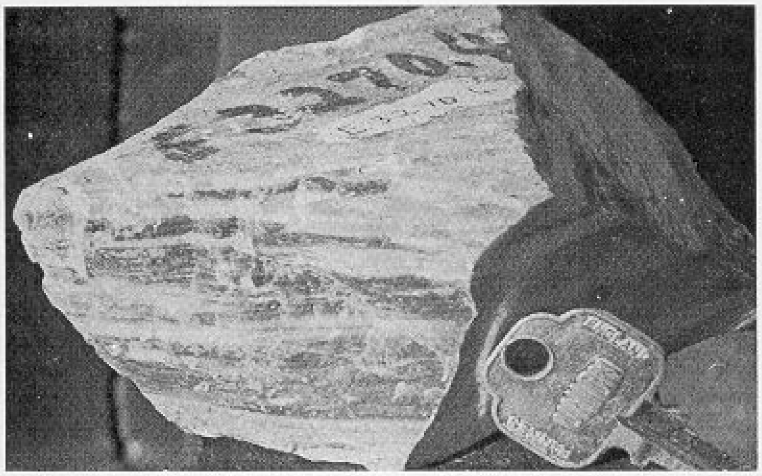

FIGURE 15

Interpenetrating black and white bands in a metamorphosed siltstone. (E.3270.4; the head of the key is 2.6 cm wide)

The fine-grained white rocks seem to be composed of similar constituents to those in the light-coloured bands in specimen E.3270.4.

At station E.3615, green sandstone beds, a few centimetres thick, are interbedded with highly cleaved shales. The sandstones are equigranular with clasts of quartz and feldspar up to 0.2 mm in diameter. Quartz is the most abundant mineral; it has slight undulose extinction, contains abundant inclusions and has been recrystallized in places. Both types of plagioclase described above are present. There is an abundance of sericite around the crystals and some of this has recrystallized to form muscovite flakes up to 0.6 mm in length. Patches of calcite and chlorite are common in the groundmass, some of the latter being replacement products of detrital biotite. Also in the groundmass are vermicular structures up to 2 mm long consisting of a colourless isotropic mineral and they are conformable with the bedding, although their character suggests that they are post-depositional but earlier than the formation of muscovite. Heavy minerals are concentrated into zones parallel to the bedding, zircon, sphene and iron ore being most abundant. There are several shear zones in these rocks comprising granulated and recrystallized quartz and haematite staining.

6. *Greenstones*

This is a term used for very altered green-coloured rocks which may have been dykes, sediments or basic volcanic rocks.

Specimen E.3270.2 is a grey-green tuffaceous rock composed mainly of ragged plagioclase (andesine and albitic plagioclase) and pale green pleochroic tremolite-actinolite ($\gamma{:}c = 17°$). Yellow epidote occurs as single stumpy anhedral or subhedral crystals or as clusters of such crystals associated with chlorite or calcite. Euhedral magnetite and small clots of biotite are common in this rock.

Specimens E.3274.1 and 2 are similar to the one described above but they contain patches of spongy epidote with sutured margins, and subordinate quartz and chlorite; these may be amygdales.

C. Regional Correlation

The lack of fossil evidence or radiometric dates makes the correlation of the metasedimentary and metavolcanic rocks with other sequences in the Antarctic Peninsula very difficult. However, deformed sequences of sedimentary and volcanic rocks have been described from several areas.

Elliot (1965, 1966) described a sequence of unfossiliferous deformed sandstones, siltstones and shales containing a small proportion of pebbly shale and greenschist which becomes progressively more sheared, folded and metamorphosed (to greenschist facies) southward; these rocks have been included in the Trinity Peninsula Series, for which Adie (1957) suggested a late Palaeozoic (probably Carboniferous) age. A Permo-Carboniferous age has been ascribed to the Trinity Peninsula Series and similar rocks in Alexander Island by Grikurov (1971). The deformation of these rocks is thought to have occurred in the Upper Trias–Lower Jurassic (Miller, 1960).

At Cape Legoupil, rocks both lithologically and structurally similar to the Trinity Peninsula Series contain fossils of a Triassic age (Thomson, 1975*b*) and this suggests that either the Trinity Peninsula Series conditions of deposition extended into the Trias, or the Cape Legoupil rocks are a younger succession (Thomson, 1975*c*).

Unfossiliferous cataclastic sediments from the extreme north-eastern part of Palmer Land have been correlated with the Trinity Peninsula Series, and the associated keratophyres and related volcanic rocks (some of which are similar to the meta-volcanic rocks described by the author) are thought to be of a similar age (Fraser and Grimley, 1972).

All the ages suggested for the deformed rocks mentioned above have been Trias or older, but in the Lassiter Coast and southern Black Coast a sequence of intensely folded black siltstones, sandstones and shales and minor tan quartzitic and arkosic sandstones (Williams, 1970), called the Latady Formation, has been dated as late Jurassic by fossil marine invertebrates and plant fragments (Rowley, 1973). Intensely folded acid and intermediate lava flows and ash-flow tuffs apparently overlie the Latady Formation at Mount Poster and similar volcanic rocks have also been found farther north (Rowley, 1973).

The discovery of these late Jurassic deformed sedimentary and volcanic rocks makes the correlation of unfossiliferous deformed rocks, which are quite common on the eastern side of Palmer Land, difficult. Although Williams and Rowley (1972) have cited petrographical differences between rocks of the Trinity Peninsula Series and the Latady Formation, the only suggestion that the two successions may exist in the same area has been made by Kamenev (1973), who equated the more metamorphosed "fillites and metavolcanics" on the Lassiter Coast with the "Trinity series of English geologists".

In a discussion on the age of the metasedimentary and metavolcanic rocks of northern Palmer Land, probably the most critical exposure is at the northern end of Mount Charity, where sheared quartz-keratophyres are intruded by granitic rocks which are overlain by the undeformed Mount Charity sedimentary and volcanic rocks. On petrographical grounds, these rocks are considered to be approximately equivalent to the Upper Jurassic volcanic rocks. As an appreciable time and tectonic gap must exist between the formation of the quartz-keratophyres and the Mount Charity sequence, it is reasonable to correlate the latter with the keratophyres of the Bowman and Wilkins Coasts (Fraser and Grimley, 1972) and the Trinity Peninsula Series. It is also probable that the other scattered exposures of metasedimentary and metavolcanic rocks to the east of the Eternity Range are of a comparable age.

V. PRE-VOLCANIC PLUTONIC ROCKS

Plutonic rocks older than the Upper Jurassic Volcanic Group occur at two stations (E.3248 and 3618) in northern Palmer Land.

No radiometric ages are at present available for these rocks but both Adie (1954) and Goldring (1962) have described granitic intrusions that are older than the Upper Jurassic volcanic rocks and these have been tentatively assigned an early Palaeozoic age. Radiometric determinations carried out by Grikurov and others (1966) on these rocks are inconclusive because they have been affected by the later Andean intrusions. Marsh (1968) also described a suite of calc-alkaline plutonic rocks from the Oscar II and Foyn Coasts; many of these have been radiometrically dated as Jurassic. These rocks are thought to be intermediate in age between the two groups of pyroclastic rocks which occur in this area. The pre-volcanic plutonic rocks will be referred to again and their geochemistry will be discussed together with that of the Andean plutonic rocks on p. 31–35.

A. Field Relations

At station E.3248, sedimentary rocks and volcanic tuffs belonging to the Upper Jurassic Volcanic Group overlie a granodiorite pluton and the contact dips at 35° to the north. The basal conglomerate of the Mount Charity sedimentary and volcanic succession, believed to be broadly coeval with the Upper Jurassic Volcanic Group on petrographical evidence, overlies an adamellite on the north-eastern ridge of Mount Charity (E.3618).

B. Petrography

1. *Granodiorite*

In the hand specimen, the granodiorite (E.3248.2) is weathered, coarse-grained and has a spotted appearance due to the abundance of mafic minerals in the white plagioclase; yellow-green epidote veins and pods are common. Microscopically, it consists mainly of twinned plagioclase (An_{38}) laths up to

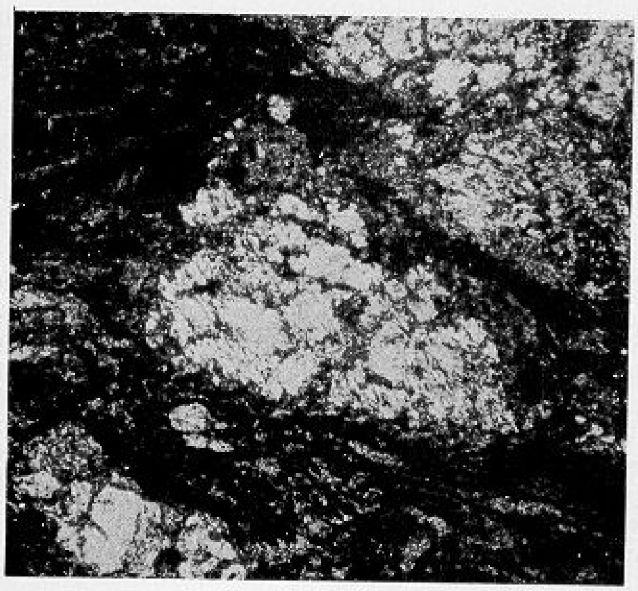

a.

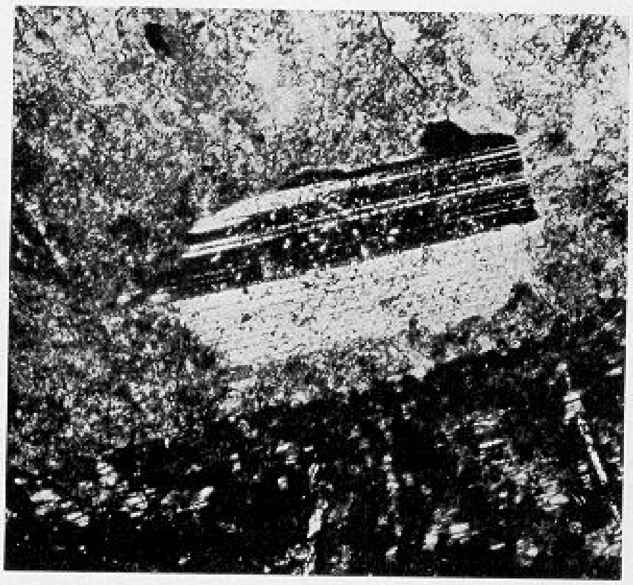

b.

FIGURE 16

a. Streaky aggregates of biotite, chlorite and epidote surrounding plagioclase in the pre-volcanic granodiorite. (E.3248.2; X-nicols; × 61)
b. Microperthite poikilitically enclosing and replacing plagioclase. (E.3618.2; X-nicols; × 60)

3.5 mm long which have been altered to sericite and epidote; some of them have been severely altered and replaced by quartz blebs. Myrmekite has developed at the margins of the plagioclase laths and in small crystals in the groundmass. The quartz forms in groups of crystals with an undulose extinction and they have corroded the plagioclase.

The effect of the contact metamorphism associated with the adjacent Andean intrusive rocks is apparent from the streaky aggregates of green-brown biotite, chlorite and epidote (Fig. 16a). Associated with these minerals are zircon, iron ore, sphene (which often surrounds the latter) and apatite. In places the epidote forms as veinlets or pods of yellow crystals which may be elongated and up to 0.35 mm in length.

2. *Adamellite*

Specimen E.3618.2 is a coarse-grained equigranular red rock; in thin section it is composed of large laths of plagioclase (0.3–3.6 mm in length; An_{29}), which have been replaced by large flakes of sericite (0.01–0.1 mm long), and patches of calcite. The plagioclase has been partially replaced by large xenomorphic crystals of microperthite (Fig. 16b); this is mostly coarse string microperthite but patch types also occur. Intergranular albite has formed between adjacent grains of microperthite. No myrmekite seems to be present; this is surprising since it is fairly abundant in the microperthite-rich acid gneisses of the metamorphic complex and in some of the Andean adamellites.

There are two generations of quartz in the thin section: hypidiomorphic to rounded crystals (0.35–0.7 mm) are enclosed and marginally replaced by microperthite; a second generation comprising large masses of xenomorphic quartz which contains irregularly shaped inclusions and tongues of plagioclase, microperthite and quartz. The biotite has an unusual pleochroism scheme α = pale yellowish brown and $\beta = \gamma$ = dark green; this colour is attributed to the very low TiO_2 content and relatively high $Fe_2O_3/(Fe_2O_3+FeO)$ ratio (Hayama, 1959). The biotite is kinked in places and has been partially replaced by haematite and patches of sericite. Haematite also forms small veinlets and patches in the rock.

Specimen E.3622.4, a sheared adamellite with a mineralogy similar to that of the above, was collected from the col between Mount Faith and Mount Charity.

VI. UPPER JURASSIC VOLCANIC GROUP

THE Upper Jurassic volcanic rocks are by far the most widespread group in the area between the Eternity Range and George VI Sound. Green-coloured volcanic breccias and coarse tuffs are commonest and the former are generally massive and unstratified. However, a dacitic lava crops out in the Rhyolite Islands (KG.1202), and at station KG.1212 there is a sequence of lava flows interbedded with tuffs and dipping on average at 6° to the east-south-east. The complete volcanic succession is not seen but the maximum continuous exposure is at station KG.1208 where approximately 2 000 m of tuffs and breccias are represented. No fossils were found in these rocks and as yet no radiometric ages are available. However, these rocks can be compared with volcanic rocks described from other parts of the Antarctic Peninsula (Goldring, 1962; Hooper, 1962; Curtis, 1966; Elliot, 1966; Dewar, 1970) and some of these contain fossils of Upper Jurassic age (Thomson, 1972). The various sequences of the Upper Jurassic volcanic rocks and their stratigraphical significance have been summarized and discussed by Taylor and others (1979). They have concluded that "although volcanic sequences can accumulate rapidly, the widespread distribution of the 'Upper Jurassic Volcanic Group' in the Antarctic Peninsula and the localized thick successions suggest that these rocks may not be confined to the narrow time limit of the Upper Jurassic." This is confirmed by the various radiometric determinations from rocks of the "Upper Jurassic Volcanic Group" which give ages of 165 Ma (Middle Jurassic) for unaltered andesites (Adie, 1971*b*), and 156 (Upper Jurassic) and 186 Ma (late Triassic) for basalts (Rex, 1971).

A. Field Relations

The various pyroclastic rocks and lavas are interbedded and are seen in contact with a number of the older and younger rock groups. At the head of Fleming Glacier, a pluton of granodiorite belonging to the pre-volcanic plutonic rocks is overlain by sedimentary rocks and tuffs containing fragments of the granodiorite, and on the northern side of the Rhyolite Islands (KG.1202) a dacite lava (KG.1202.1) rests on gneisses, the contact dipping at 40° to the west. This gives way westward to a lapilli-tuff (with fragments less than 2.5 mm in diameter), which grades upwards into volcanic breccia containing fragments over 23 cm in diameter. Similar coarse, unstratified volcanic breccias are overlain by south-westerly dipping crystal tuffs at stations KG.1200 and 1208, and at the former the breccia is intruded by Andean granodiorite. Volcanic rocks are also intruded by Andean rocks on the north side of Mount Edgell.

At a small exposure to the west of Mount Edgell (KG.1212), bedded lavas and tuffs, each 2.4–2.8 m thick, dip gently eastward and overlie the breccia exposed at station KG.1217. The basal bed is a vitric tuff overlain by crystal tuffs, which are succeeded by two lavas (KG.1212.5 and 7) separated by a rubbly weathered layer. The top lava (KG.1212.9) is succeeded by a tuff (KG.1212.8) and this in turn is overlain unconformably by the highest basalt (KG.1212.9).

B. Petrography

1. *Volcanic breccias*

The lithic fragments comprising the volcanic breccias are varied and include crystal tuffs, porphyritic lava fragments, often exhibiting a marked trachytic texture, and granitic fragments of quartz, potash feldspar and sericite. A preponderance of lava fragments, some with trachytic textures while others contain chlorite-filled amygdales, characterize the breccias from the Rhyolite Islands.

The interclast areas of these breccias are crystal tuffs with some vitric fragments and comprising embayed quartz crystals and subhedral plagioclase laths set in a fine-grained matrix of sericite, chlorite, epidote, calcite, quartz and feldspar. Alteration of the matrices of these rocks is extensive and several distinctive minerals have been recognized. Pumpellyite and small green crystals of secondary biotite and hornblende were identified in specimen KG.1216.1 (Fig. 17a); in specimen KG.1200.2 the plagioclase has been partially or wholly replaced by heulandite (Fig. 17b), and specimen KG.1200.4 contains sheaves of prehnite.

The dark colour of some of these breccias is due to the abundance of ilmenite and leucoxene.

2. *Crystal tuffs*

Crystal tuffs are the most widespread group of volcanic rocks after the coarse breccias. They are usually well bedded, compact and they either rest on top of breccias, as at station KG.1200, or crop out in the lava–tuff sequence of station KG.1212.

The crystal tuffs are porphyritic (E.3248.5, KG.1200.1 and 8) with large, often twinned altered plagioclase (andesine), up to 4 mm in length, set in a fine-grained matrix of acicular plagioclase microlites, sericite, quartz and/or potash feldspar. Iron ore and apatite are common accessory minerals.

Specimen KG.1212.1 has a dacitic composition and consists of embayed quartz and corroded plagioclase in a fine-grained altered matrix.

As with the volcanic breccias, the crystal tuffs have been extremely altered and a characteristic of specimen KG.1200.1 is that the plagioclase has been replaced by chlorite, either almost completely (Fig. 17c) or along discrete compositional zones (Fig. 17d).

3. *Lithic tuffs*

Lithic tuffs occur at two stations, KG.1212 and 1223. At station KG.1212, the tuff forms a thin rubbly layer separating the lavas KG.1212.5 and 7. It is a greyish green rock and individual clasts are easily distinguished. These include vitric tuffs, probably obtained from the similar tuff at the base of the succession, fine-grained microcrystalline fragments probably from the porphyritic rhyolite, which is also in the same lava–tuff succession, devitrified lavas similar to the dacites cropping out farther west, and some clasts with a trachytic texture of plagioclase microlites altered to calcite, chlorite and iron ore.

The groundmass comprises small lithic fragments, broken embayed quartz and plagioclase, and much calcite, chlorite and sericite. In addition, prehnite replaces plagioclase and part of the groundmass, and there is a fibrous radiating zeolite which has the optical properties of thomsonite.

At station KG.1223 the lithic tuff is separated from the other volcanic rocks by a steeply dipping fault. It is difficult to distinguish the clasts from the matrix in both the hand specimen and thin section. The clasts are porphyritic with plagioclase phenocrysts, often highly epidotized and kaolinized, set in a matrix of plagioclase microlites. Some of them are highly altered with much iron ore and chlorite in the groundmass. The interclast area is a crystal tuff comprising plagioclase which has been extensively albitized, epidotized and chloritized.

4. *Vitric tuff*

The vitric tuff lies at the bottom of the lava–tuff succession at station KG.1212 and appears to overlie the breccia at station KG.1217. In the hand specimen, the rock is compact with a conchoidal fracture and is a dark olive-green colour with black patches and irregular black veins containing pyrite. Microscopically, the rock consists of small devitrified glass shards, crystal fragments and rare lithic fragments in a very fine-grained matrix, which is largely unidentifiable but contains specks of iron ore, sericite and chlorite. Most of the shards are spicules but more exotic curved forms are also present and some have been replaced by chlorite. There are several shards containing chlorite-filled amygdales but the volcanic glass has devitrified to a mosaic of small crystals of quartz, feldspar and chlorite. Other seemingly isolated patches of chlorite are probably amygdales where the glass has been broken and scattered. A fibrous zeolite is present in some of the amygdales.

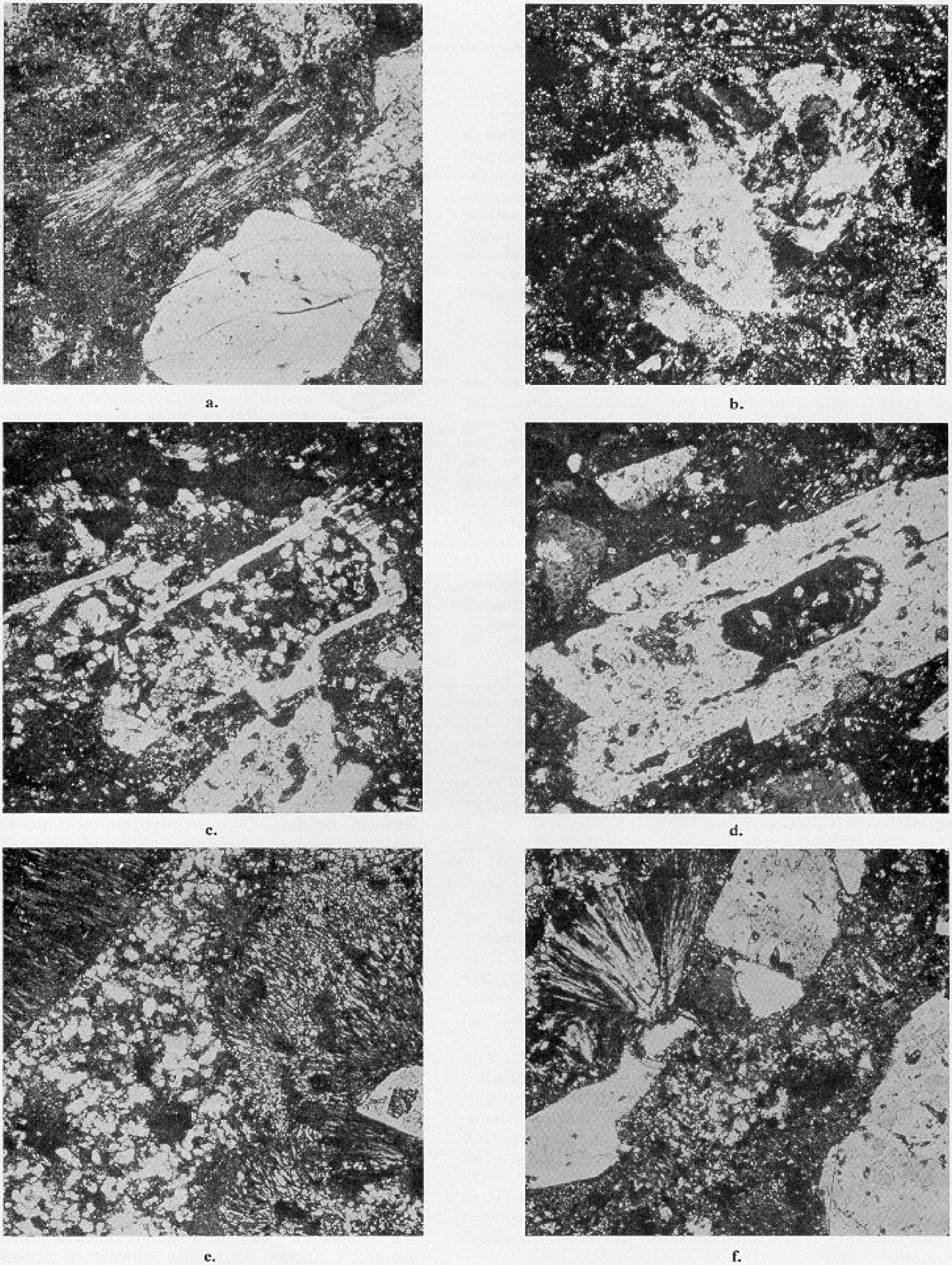

FIGURE 17

a. Sheaves of pumpellyite in an agglomerate. (KG.1216.1; X-nicols; × 47)
b. Plagioclase partially replaced by heulandite. (KG.1200.2; X-nicols; × 55)
c. The sericitized margin left after replacement of plagioclase by chlorite, quartz, sericite, epidote and leucoxene. (KG.1200.1; X-nicols; × 48)
d. Plagioclase partially replaced by chlorite. (KG.1200.1; X-nicols; × 48)
e. Radiating zeolites replacing porphyritic volcanic tuff. (KG.1218.10; X-nicols; × 60)
f. Potash feldspar replacing plagioclase in a zeolitized volcanic tuff. (KG.1218.6; X-nicols; × 59)

5. *Zeolitized volcanic rocks*

Specimens KG.1218.7 and 10 are both porphyritic rocks with broken and deformed antiperthitic plagioclase (An_{42}) phenocrysts set in a quartz, feldspar, epidote and leucoxene groundmass. Most of the rock has been replaced by masses of radiating zeolite (Fig. 17e). These are usually vein-like with cuspate boundaries but irregular masses are also represented; all are cut by veins of quartz or finely divided epidote. The zeolite has a positive optical sign, and both length-fast and length-slow fibres are represented, suggesting that it may be thomsonite. The zeolites in specimen KG.1218.7 are brown in colour.

A lithic crystal tuff (KG.1218.6) crops out above specimen KG.1218.7 and here the zeolites are less common, only occurring as individual radiating crystals in the matrix. The lithic fragments are altered fine-grained lavas with plagioclase microlites and the porphyritic crystals are of quartz and feldspar. The latter vary in their proportion of potash feldspar from perthite to antiperthite. The albite twins in the andesine (approximately An_{33}) have been obliterated by the potash feldspar (Fig. 17f), indicating its secondary replacement origin.

A few chloritized bomb fragments and shards were recognized, and epidote and chlorite are common in the groundmass and in the veins.

6. *Lavas*

a. *Basalts*. The two basalt specimens were collected from the lava–tuff succession at station KG.1212. The lowest in the sequence (KG.1212.5) is a fine-grained porphyritic basalt with white plagioclase phenocrysts. Microscopically, two generations of plagioclase can be recognized and both have been altered to sericite, calcite and epidote. The large phenocrysts (0.7–3 mm in length) have a composition of An_{61} and the smaller microlites up to 0.4 mm in length have a composition of about An_{50}. There are a few twinned crystals of colourless clinopyroxene (large $2V\gamma$) which have been altered marginally and along the cracks to chlorite. Moreover, the aggregates of chlorite crystals in the rock probably represent the complete break-down of clinopyroxene. Interstitial quartz and iron ore (0.01–0.1 mm in diameter) are the major accessory minerals.

The numerous amygdales in the rock are filled with a combination of either prehnite, quartz and chlorite, quartz and calcite, or chlorite and epidote. Secondary calcite and epidote are also common in the groundmass.

The highest lava in the succession (KG.1212.9) is a basalt similar to specimen KG.1212.5. The phenocrysts of plagioclase (0.5–8 mm in length) have a slightly more sodic composition (An_{54}) but they are severely altered to epidote, sericite and calcite; the groundmass microlites are andesine-labradorite. The colourless pyroxene ($\gamma{:}c = 34°$) is also altered to calcite and chlorite.

b. *Andesites*. One andesite specimen was recovered as a block in a breccia on the western side of station KG.1200. In the hand specimen, it is grey-green, amygdaloidal and porphyritic, containing plagioclase phenocrysts up to 4 mm long; smaller phenocrysts of hornblende are also present. The twinned plagioclase phenocrysts have a composition of about An_{40} and they have been severely altered to calcite, epidote and albite. The epidote forms patches while the calcite occupies cleavage partings, certain concentric zones probably related to compositional zoning, or it is vein-like; the albite forms in irregular veins. A green pleochroic hornblende forms a few phenocrysts up to 0.7 mm in length but it is very widespread as small groundmass crystals associated with oligoclase laths and iron ore.

The amygdales contain elongated subhedral crystals of green hornblende which are surrounded by calcite. Patches comprising small interlocking and radiating crystals of prehnite are common and, although these patches are elongated, they terminate abruptly and do not have a vein-like appearance.

Lying on top of the lowest basalt at station KG.1212 and separated from it by a weathered layer is an altered lava. It is porphyritic but it only contains a few scattered plagioclase phenocrysts which have been almost completely altered, mainly to calcite, but also to chlorite, epidote and a dark reddish brown mineral, probably biotite. The matrix of plagioclase microlites and quartz contains much sericite, long flakes of muscovite and patches of calcite.

c. *Dacites*. A small area of dacitic lava crops out in the Rhyolite Islands (KG.1202). Specimen KG.1202.1 contains phenocrysts of plagioclase (An_{31}) and quartz. The former are elongated (2–3 mm in length), peripherally corroded and sericitized, and they frequently occur in glomeroporphyritic clusters. Cracks in the crystals are filled with chlorite and a few crystals have been almost completely altered to chlorite, small grains of epidote, dark brown pleochroic biotite and leucoxene. The idiomorphic quartz is cracked and the crystals have been strongly embayed, indicating strong resorption in the magma prior to extrusion (Spry, 1969). The groundmass is a mass of ragged, equant interpenetrating crystals of quartz, feldspar and patches of chlorite, formed by the devitrification of the glass. Secondary quartz forms overgrowths around and in optical continuity with the embayed quartz. Leucoxene and haematite are the accessory minerals.

The rare amygdales are filled with pale green chlorite which is surrounded by a zone of small acicular, randomly orientated crystals of yellow epidote (up to 0.4 mm in length). The surrounding rock up to 4 mm from the margins of the amygdales is severely altered to epidote and the crystals become progressively smaller and less numerous towards the outer edge of the zone.

A similar dacite crops out below tuffs at station KG.1208. It contains embayed quartz and plagioclase phenocrysts and a devitrified groundmass, which contains a green pleochroic fibrous amphibole as well as chlorite. These minerals also replace feldspar and occur in clusters or form elongated masses along cracks.

Dacite specimens KG.1201.6 and 1218.2 have crystallized directly from the magma, because the groundmass consists of plagioclase microlites surrounded by quartz. Secondary overgrowths occur on the phenocrysts of quartz and plagioclase and there are phenocrysts of both andesine (An_{31}) and albite-oligoclase. The presence of more than one markedly different variety of plagioclase is a common feature of volcanic associations in orogenic regions and it has been explained by Turner and Verhoogen (1960, p. 276) by a "thorough mixing of partially crystallized magmas of common parentage, but at different stages of differentiation and possibly modified to different degrees by assimulative reaction with adjoining rocks." Original ferromagnesian minerals are represented by elongated pseudomorphs comprising pale green pleochroic chlorite, pale yellow epidote, calcite and small patches of leucoxene, and the amygdales are thought to be represented by patches of large interlocking crystals of quartz with an undulating extinction.

The groundmass contains fibrous radiating zeolites and veinlets of epidote.

d. *Porphyritic rhyolite.* Specimen KG.1212.4 is porphyritic with phenocrysts and glomeroporphyritic aggregates of albite (An_9). These have serrated edges due to corrosion and many of the crystals exhibit bent and broken twin lamellae and slight undulose extinction. The cryptocrystalline matrix is mainly quartz with some feldspar and chlorite, and it contains many amygdales and veins. The former are composed of radiating epidote, chlorite, leucoxene and euhedral pyrite, while the latter are of quartz or epidote.

7. *Sedimentary rocks*

Associated with the volcanic rocks at two localities (E.3248.4 and KG.1213.1) are poorly sorted sedimentary deposits comprising quartz clasts in a fine-grained matrix (Fig. 18); these clasts are angular and many are polycrystalline. The matrix

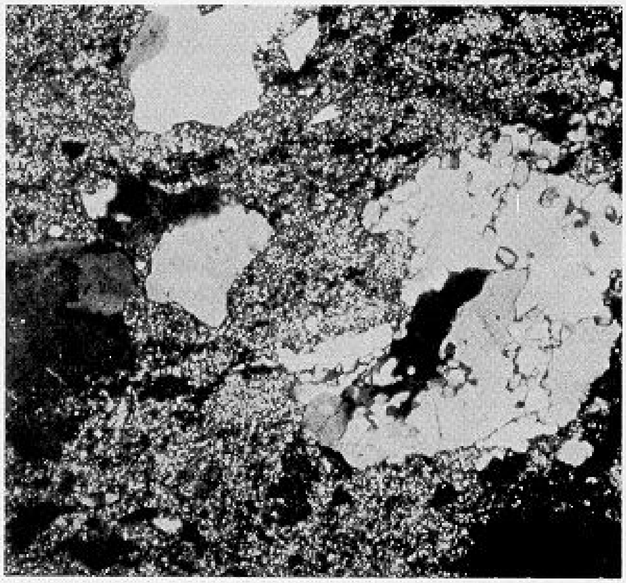

FIGURE 18
Quartz clasts in a sedimentary rock. (KG.1213.1; X-nicols; ×33)

seems to consist mainly of sericite, chlorite, quartz, small crystals of iron ore and streaks of haematite; larger crystals of ilmenite are also present. Some of the clasts are of quartz and finer-grained material, or fine-grained material alone, the latter being indistinguishable from the matrix except for its lack of iron ore. Clots of secondary brown biotite are common in the groundmass and as pseudomorphs; epidote replaces some clasts and veins of chlorite transect the rock.

These rocks are very different from the plagioclase-rich volcanic rocks with which they are associated and their origin is problematical; it is difficult to explain the extremely angular fragments, the high proportion of matrix to clasts and the lack of feldspar. It is probable that these rocks formed from the weathering products of pre-volcanic igneous or metamorphic rocks and that the conditions during their formation were conducive to the complete break-down of feldspar, this being represented by the iron ore-free patches mentioned above.

C. ALTERATION

Numerous secondary minerals have been formed by one more of the following processes: hydrothermal alteration, lo grade regional (burial) metamorphism or contact met morphism. The following mineral assemblages were recogniz in the area around Mount Edgell:

Pumpellyite, epidote, albite, amphibole, biotite.
Prehnite, epidote, albite, calcite, chlorite, zeoli sphene, amphibole.
Heulandite, epidote, albite, calcite, chlorite.
Fibrous zeolites, epidote, chlorite, calcite.

Similar assemblages of minerals have been grouped into met morphic facies and sub-facies in other parts of the world, t zeolites being included under the broad term "zeolites facie (Coombs, 1971), prehnite–pumpellyite assemblages bei assigned to the prehnite–pumpellyite metagreywacke faci (Coombs, 1960). Although Seki (1966) subdivided zeoli assemblages into four facies characterized by mordenite–quart heulandite–quartz, laumontite–quartz and wairakite–quart Coombs' broader definition, which included all miner assemblages characterized in rocks of appropriate compositic by zeolites other than the analcime of silica-deficient enviro ments, is more suitable as the composition of the zeolites in th area is not accurately known; this classification is independe of the mode of formation of the zeolites, as hydrotherm diagenetic or metamorphic.

The prehnite–pumpellyite metagreywacke facies was su divided into two sub-facies (Coombs, 1960): a lower-gra quartz–prehnite zone in which a combination of the following found: quartz, albite, prehnite, pumpellyite, chlorite, calci sphene, orthoclase and muscovite; and a higher-grade zone wi some combination of quartz, albite, chlorite, sphene, actinoli muscovite, calcite, stilpnomelane, pumpellyite and epido Hashimoto (1966) restricted the term prehnite–pumpelly facies to the lower-grade sub-facies of Coombs and, with the di appearance of prehnite, the rocks pass into the pu pellyite–actinolite facies.

In keeping with other areas of the world (Coombs, 1971), t zone of fibrous zeolites to the west of Mount Edgell and in t Rhyolite Islands and the adjacent mainland passes eastward a north-eastward into a zone where the volcanic rocks conta mainly prehnite or pumpellyite; zeolites do, however, co-exi with prehnite in some specimens. Although heulandite occurs one specimen, laumontite has not been identified in these rock It is possible that the composition of these rocks may ha inhibited its formation because of the reaction

$$\text{laumontite} + \text{chlorite} \rightarrow \text{pumpellyite} + \text{clay mineral} + H_2O$$

taking place before it became stable (Coombs, 1971).

Prehnite does not occur with pumpellyite in any of the roc examined from northern Palmer Land. However, the pu pellyite is the strongly pleochroic variety, which Bishop (197 suggested is typical of the prehnite–pumpellyite facies and low grade of the pumpellyite–actinolite facies in a metagreywac terrain. The association of zeolites with prehnite in som exposures also suggests that the prehnite–pumpellyite facies represented. Although amphibole exists with the pumpellyite, i close association with biotite which replaces the pumpellyite a its occurrence in rocks containing prehnite suggests that formed due to later contact metamorphism.

Zen (1961) has proved that the characteristic minerals of the low-grade metamorphic facies can be formed isothermally and isobarically by changing the chemical potential of carbon dioxide and water, but in many areas of the world the facies occur in zones with a continuous passage from the zeolite facies through the prehnite–pumpellyite facies into the greenschist facies, and it is likely that all the variables of pressure, temperature and chemical potentials of carbon dioxide and water play an important part (Coombs and others, 1970); the composition and lithology of the rocks being altered are also significant factors.

Previously, many of the low-grade metamorphic mineral assemblages have been related mainly to the depth of burial at temperature–pressure values appropriate to the regional geothermal gradient. However, the great variation in the estimated depth of formation of these mineral assemblages in different parts of the world clearly shows that burial is not the only determining factor (Packham and Crook, 1960; Zen, 1974).

Experimental work associated with geological knowledge offers some indication of the conditions of formation of the characteristic minerals of the various facies. With regard to the zeolites, Coombs and others (1959) suggested that, in quartz-free systems, zeolites are not stable above 320°C, although they have been synthesized at temperatures as high as 450°C. Liou (1971) examined the reaction

$$5 \text{ prehnite} + 2 \text{ zoisite} \rightarrow 2 \text{ grossular} + 3 \text{ quartz} + 4H_2O$$

and took it as forming the upper end of the prehnite–pumpellyite association. This reaction takes place at 403°C at 3 kbar and 393°C at 5 kbar where $P_{H_2O} = P_{total}$. However, in normal environments where P_{H_2O} is less than P_{total} and where more complicated reactions take place, the temperature would be lower and around 280–380°C at 3 kbar for the prehnite–pumpellyite facies. Such reactions may be

$$\text{prehnite} + \text{chlorite} + H_2O \rightarrow \text{pumpellyite} + \text{actinolite} + \text{quartz},$$

which represents the upper limit of the prehnite–pumpellyite facies and

$$\text{pumpellyite} + \text{chlorite} + \text{quartz} \rightarrow \text{epidote} + \text{actinolite} + H_2O,$$

the upper limit of the pumpellyite–actinolite facies, both having been studied by Nitsch (1971). The former is stable at 2 kbar to 345°±20°C and at 7 kbar to 260°±20°C, while the latter has values at 7 kbar of 260°±20°C to 370°±20°C and only occurs at pressures greater than 2.5 kbar. These results give slightly lower values than those of Liou.

Bishop (1972) has summarized the experimental results of Liou (1971), Coombs (1971) and Nitsch (1971) in a P–T facies diagram shown in Fig. 19 and the approximate positions of the rocks of northern Palmer Land are indicated.

The numerous igneous intrusions in the Mount Edgell area must have appreciably altered the surrounding volcanic rocks, although the products of the contact metamorphism are not easily distinguishable from those of the low-grade regional metamorphism described above or hydrothermal alteration. Minerals such as albite, epidote, chlorite, sphene and amphibole could have been produced by any of these processes but, where the biotite crystals and hornblende are associated, contact metamorphism of at least albite-epidote-hornfels facies and possibly

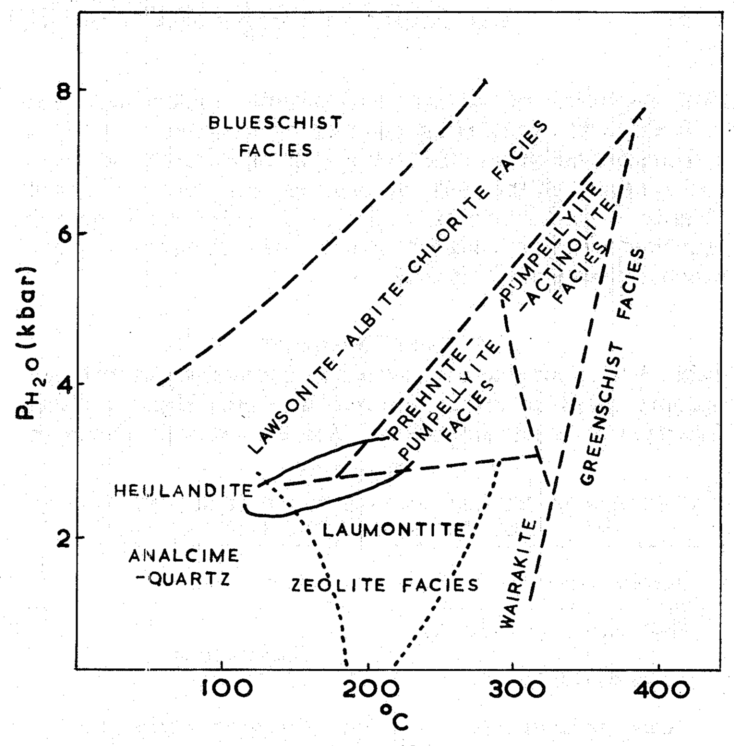

FIGURE 19

P–T facies diagram for low μ_{co_2} environments, after Bishop (1972, fig. 10). The solid line defines the approximate position of the Upper Jurassic volcanic rocks of northern Palmer Land.

up to hornblende-hornfels facies (Turner and Verhoogen, 1960) was effective.

D. Geochemistry

Four lava specimens have been analysed, three from station KG.1212, to the west of Mount Edgell, and one from the Rhyolite Islands. When plotted on an AFM diagram, these rocks fall in the field of calc-alkaline rocks (Irvine and Baragar, 1971) and their high alumina content confirms this classification.

The analyses of these lavas, including various oxide and element ratios (Table VI) have been compared with those of Jakes and White (1972, table 3) and, while it is clear that the basalts resemble island-arc rocks, the acid lavas have ambiguous characteristics. The normative constituents of these acid rocks have been plotted on a quartz–orthoclase–albite ternary diagram (Fig. 38) and, when compared with the experimental results of Tuttle and Bowen (1958), they plot well into the quartz field, indicating that they could not have formed directly by differentiation from more basic rocks but may have formed by fusion of pre-existing rocks or by the mixing of magmas and/or assimilation, as suggested by the presence of two different types of plagioclase in the dacites; no evidence was found in the thin sections of these specimens to suggest an addition of secondary silica, which could also account for these rocks plotting in the quartz field.

The chemistry of these lavas will be discussed again in relation to the hypabyssal rocks on p. 38–41.

Table VI

CHEMICAL ANALYSES OF LAVAS FROM THE UPPER JURASSIC VOLCANIC GROUP

	1	2	3	4
SiO_2	52.26	52.50	73.68	74.19
TiO_2	0.88	0.90	0.12	0.09
Al_2O_3	17.07	17.24	16.40	14.35
Fe_2O_3	4.08	4.59	0.90	1.07
FeO	4.27	3.71	0.18	1.06
MnO	0.13	0.14	0.08	0.06
MgO	4.91	4.94	0.37	0.24
CaO	7.38	7.04	1.63	0.49
Na_2O	3.08	3.15	3.21	3.78
K_2O	1.24	1.44	2.56	3.53
P_2O_5	0.29	0.28	0.06	–
H_2O+	1.84	1.55	0.67	0.26
H_2O-	0.22	0.32	0.28	0.26
Total	97.65	97.80	100.14	99.38
Element percentages less total water				
Si^{4+}	25.56	25.59	34.73	35.08
Ti^{4+}	0 55	0.56	0.07	0.05
Al^{3+}	9.45	9.51	8.75	7.68
Fe^{3+}	2.99	3.35	0.63	0.76
Fe^{2+}	3.47	3.01	0.14	0.83
Mn^{2+}	0.11	0.11	0.06	0.05
Mg^{2+}	3.10	3.11	0.23	0.15
Ca^{2+}	5.52	5.24	1.17	0.35
Na^{+}	2.39	2.44	2.40	2.84
K^{+}	1.08	1.25	2.14	2.96
P^{5+}	0.13	0.13	0.04	–
O^{2-}	45.66	45.72	49.64	49.24
C.I.P.W. norms				
Q	7.24	7.35	41.55	37.07
C	–	–	5.49	3.36
Z	0.04	0.04	0.02	0.04
or	7.66	8.86	15.24	21.12
ab	27.23	27.75	27.36	32.32
an	30.39	29.83	7.98	2.70
di	5.00	3.97	–	–
hy	13.79	12.80	0.93	1.64
mt	6.18	6.93	0.50	1.57
il	1.75	1.78	0.23	0.17
hm	–	–	0.56	–
ap	0.72	0.69	0.14	–
Position $(\frac{1}{3}Si + K)-(Ca + Mg)$	+0.92	+1.35	+12.20	+13.98
Trace elements				
Cr	13	10	–	1
Ni	22	17	3	2
Ga	2	28	16	21
Rb	26	33	58	111
Sr	799	780	201	160
Y	23	11	7	26
Zr	167	171	90	180
Nb	12	7	8	14
Ba	585	627	747	906
La	56	26	24	37
Ce	44	50	40	63
Pb	39	16	14	68
Th	28	6	4	13
Element ratios				
K/Rb	415	379	369	267
Ba/Rb	22.5	19.0	12.9	8.2
Coordinates of triangular diagrams				
Fe	49.6	48.3	14.0	21.1
Alk	26.6	28.0	82.0	77.0
Mg	23.8	23.6	4.1	1.9
Q†	*	*	47.4	39.5
Ab	*	*	17.4	22.0
Or	*	*	35.2	38.5

* Not determined.
† Calculated from mesonorms.

1. KG.1212.5 West of Mount Edgell.
2. KG.1212.9 West of Mount Edgell.
3. KG.1212.7 West of Mount Edgell.
4. KG.1202.1 Rhyolite Islands.

[face page 23

VII. MOUNT CHARITY SEDIMENTARY AND VOLCANIC ROCKS

The discovery of relatively undeformed sedimentary and volcanic rocks overlying the plutonic rocks of Mount Charity is a significant addition to the stratigraphy of Palmer Land. These rocks occur on the northern and eastern ridges of Mount Charity at an altitude of 2 100–2 700 m and are tentatively estimated, from a consideration of their attitude and areal extent, to be about 650 m thick.

A. Field Relations

Table VII shows the stratigraphical successions of the sedimentary rocks on the eastern and northern ridges of Mount Charity. On the eastern ridge of Mount Charity the adamellite

TABLE VII

STRATIGRAPHICAL SUCCESSIONS IN THE SEDIMENTARY AND VOLCANIC ROCKS ON MOUNT CHARITY

Northern ridge		*Eastern ridge*
Well-bedded volcanic rocks		
		Conglomerate
Conglomerate		
Coarse red sandstones	1.3 m	Coarse green sandstones 3 m
Conglomerate		
		Conglomerate
Red sandstone	1 m	
Yellow sandstone	5 m	
Haematitized sandstone	3 m	
Weathered basic intrusion		
Adamellite		Adamellite

(E.3618.3) forming most of the mountain gives way down the ridge to patchy exposures of a coarse conglomerate, the contact being snow-covered. Farther down the ridge the conglomerate passes into a sequence of sandstones (Fig. 20) (E.3619.1). These are coarse-grained, green in colour and are generally poorly consolidated. Individual layers vary from coarse sandstone to pebble-conglomerate size (Pettijohn, 1957, p. 19) and are extremely irregular in attitude, but they tend to dip at 35–50° to the north. A few vertical joints striking at 164° true were the only deformation observed in the conglomerate.

On the north ridge (E.3623), the relationship between the sedimentary rocks and the adamellite is obscured by deep weathering, partial snow cover and the presence of a weathered basic dyke near the contact. Proceeding southward up the ridge, the fresh adamellite passes up into a weathered zone containing a basic dyke, beyond which is the base of the sedimentary sequence, a red haematitized sandstone. At the southern end of station E.3623 the conglomerate contains a sequence of coarse red sandstones similar in lithology to those at station E.3618. The layers of coarser material in the sandstones dip at 15° in a direction 185° true. About 60 cm above the sandstone sequence there is a tabular body of microdiorite under 1 m thick; this seems to be a dyke dipping at 15° in a direction 110° true. Although the few metres of rock above the dyke are conglomerate, an exposure higher up the ridge consists of well-bedded rocks which dip at 10° to the south-south-east; these have been mapped by K. D. Holmes as a sequence of tuffs and lavas lying conformably on the conglomerates.

B. Petrography

1. *Polymict conglomerates*

The polymict conglomerates are unstratified, poorly sorted and they contain large clasts 70 cm or more in diameter (Fig. 21). The largest clasts are of adamellite and these are more angular than the smaller ones, many of which are fine-grained, sometimes porphyritic, green or greenish black basic volcanic rocks.

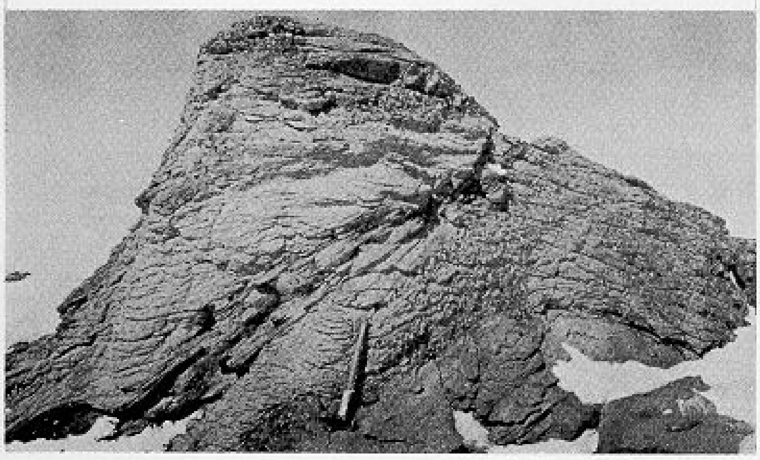

FIGURE 20
Coarse sandstone on the eastern ridge of Mount Charity (the hammer shaft is 59 cm long).

FIGURE 21
A poorly sorted polymict conglomerate on the eastern ridge of Mount Charity (the hammer shaft is graduated in inches).

2. *Sandstones*

The sandstones at the base of the sedimentary succession at station E.3623 are very weathered and seem to represent the break-down of the adamellite virtually *in situ*. Specimen E.3623.6, from the lowest part of the succession, is heavily veined by haematite which occurs in patches and veinlets, and forms a coating around the clasts of plagioclase, quartz and rock fragments.

The coarse-grained green and red sandstones at stations E.3619 and 3623 (Figs 22 and 23) can be classified on the basis of their modal analyses (Table VIII) as arkoses (Pettijohn and others, 1972, p. 158) and the main constituents are similar in both cases. There is over 30% of feldspar of four types: twinned plagioclase (An_{30}), albite-oligoclase, microperthite and microcline with cross-hatch twinning. The quartz grains (up to 0.7 mm long) in both of the specimens are sub-rounded to sub-angular and have an undulose extinction. Some of the clasts in specimen E.3623.2 are formed of two or more large crystals of quartz which have been derived from a vein or pegmatite.

The rock fragments are composed of a mosaic of quartz with flakes of sericite and they probably originated from the meta-volcanic and metasedimentary sequence. Some of the clasts have a marked preferred orientation of the mica and seem to be slates.

The plates of brown biotite (0.2–0.35 mm in length) have been almost completely replaced by pale green chlorite, calcite and haematite, the latter either coating the grains or being aligned along the cleavages, and they have been deformed between the other grains during diagenesis.

Muscovite, zircon and leucoxene are the main accessory minerals.

Whilst calcite is an important cement in both of the specimens, the distinctive red colour of specimen E.3623.2 is due to haematite which coats the grains and forms anhedral masses. Chlorite and sericite are also cementing media especially in specimen E.3619.1, in which the haematite and calcite are

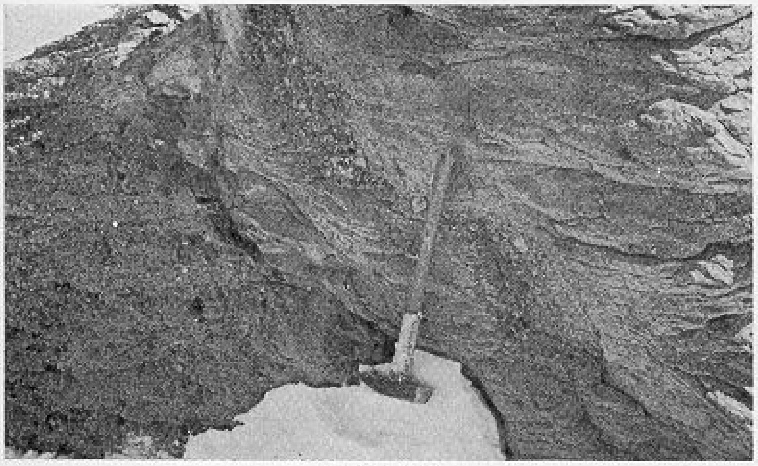

FIGURE 22
Coarse green sandstones with fine conglomerate bands on the eastern ridge of Mount Charity (the hammer shaft is 59 cm long).

TABLE VIII
MODAL ANALYSES OF TWO SANDSTONES FROM THE MOUNT CHARITY SEDIMENTARY SEQUENCE

	E.3619.2	E.3623.2
Quartz	39.8	32.5
Feldspar	35.3	31.8
Rock fragments	15.0	9.9
Mica	0.5	1.1
Cement	7.3	22.0
Matrix	0.6	1.1
Haematite	0.4	1.3
Ilmenite	0.3	–
Chlorite, sphene, leucoxene, zircon	0.8	0.3
Q = Quartz	44.0	43.1
F = Feldspar	39.1	42.3
M = Rock fragments+mica	16.9	14.6

E.3619.2 Sandstone. (Arkose; Pettijohn and others (1972).)
E.3623.2 Sandstone. (Arkose; Pettijohn and others (1972).)

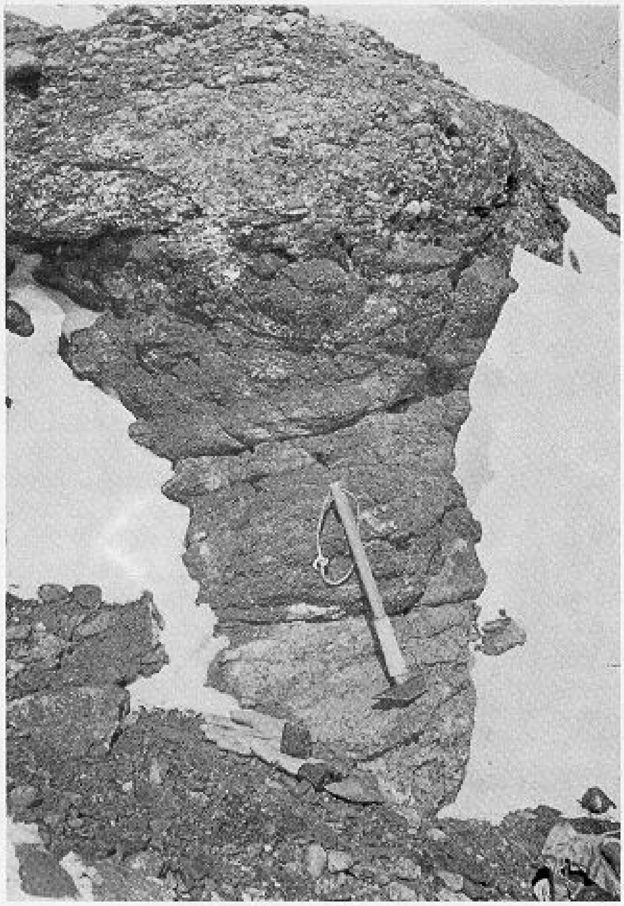

FIGURE 23
Coarse red sandstones in the conglomerates on the northern ridge of Mount Charity (the hammer shaft is 59 cm long).

TABLE IX

MODAL ANALYSES OF ROCKS FROM THE ANDEAN INTRUSIVE SUITE

	1	2	3	4	5	6	7	8	9
Quartz	0.35	11.35	9.25	19.1	17.4	28.5	34.2	35.4	38.9
Potash feldspar	–	–	4.75	6.2	19.5	16.7	6.9	35.6	23.0
Plagioclase	69.3	65.95	56.5	59.7	47.8	48.6	44.7	24.3	36.1
Clinopyroxene	tr	–	7.75	–	–	–	–	–	–
Hypersthene	9.5	–	–	–	–	–	–	–	–
Hornblende	–	12.7	8.85	–	7.9	0.8	2.3	–	–
Tremolite-actinolite	11.05	–	–	–	–	–	–	–	–
Biotite	3.5	3.95	5.5	8.1	2.5	0.6	2.3	4.4	–
Muscovite	–	–	–	1.9	–	–	–	–	–
Chlorite	1.6	3.2	6.25	2.9	2.8	2.9	6.9	tr	1.4
Iron ore	4.0	2.1	0.8	0.1	1.2	1.5	0.6	0.3	0.2
Sphene	–	tr	tr	–	tr	tr	tr	tr	–
Apatite	0.65	–	0.25	0.2	–	–	–	–	–
Epidote	0.05	0.75	0.01	1.8	0.9	0.4	2.1	tr	0.4
Plagioclase composition	An_{58}	An_{49-37}	An_{62-39}	An_{33-26}	An_{51-28}	*	An_{50-30}	An_{34-16}	An_{32-11}

tr Trace.
* Indeterminate.

1. KG.1207.4 Norite.
2. KG.1201.1 Tonalite.
3. KG.1206.7 Tonalite.
4. E.3620.3 Granodiorite.
5. KG.1200.6 Granodiorite.
6. KG.1221.1 Granodiorite.
7. KG.1201.3 Hybrid granodiorite.
8. KG.1207.2 Adamellite.
9. KG.1201.2 Adamellite dyke intruding tonalite to give the hybrid granodiorite (KG.1201.3).

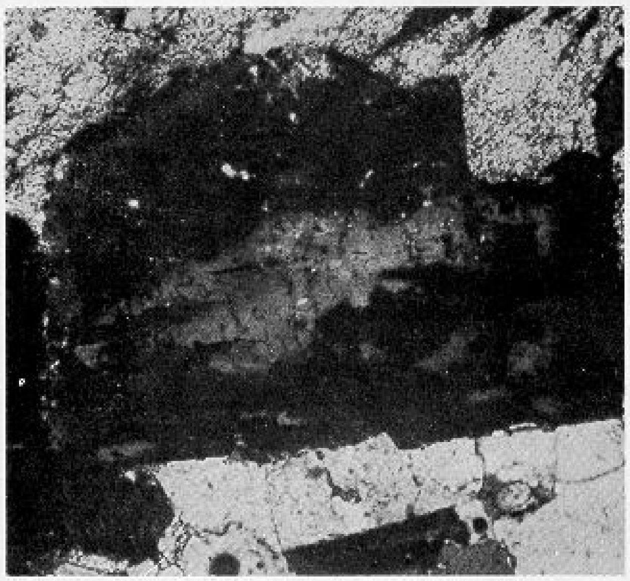

a.

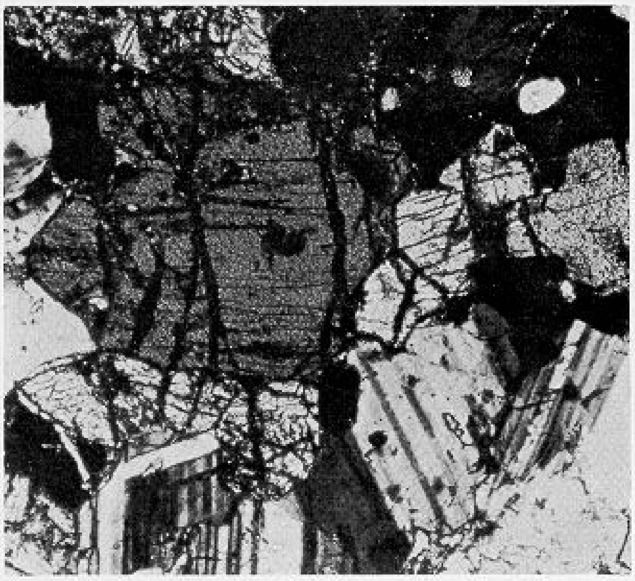

b.

FIGURE 24

a. Patchy zoning in plagioclase. (E.3293.1; X-nicols; × 66)
b. Hypersthene in a norite. (KB.1207.4; X-nicols; × 60)

less abundant. Most of the sericite is probably derived from the break-down of the feldspar but some of it may be authigenic, having been formed by the reaction of potassium-bearing waters (generally sea-water) on montmorillonite and to a lesser extent kaolinite (Pettijohn, 1957, p. 667). Similarly, the chlorite may have been formed from kaolinite and perhaps montmorillonite by the addition of magnesium.

3. *Volcanic rocks*

The base of the volcanic sequence is a very altered grey porphyritic tuff or lava containing phenocrysts of plagioclase, almost completely replaced by calcite, and elongated pseudomorphs of chlorite with subsidiary calcite (up to 1.5 mm in length) which probably replaced pyroxene. Ilmenite crystals, partially altered to leucoxene, and amygdales containing radiating quartz crystals are also a feature of this rock. The groundmass comprises plagioclase microlites with much chlorite, calcite and leucoxene.

Two other specimens were collected from the volcanic succession, one about 40–60 m above the conglomerates (E.2217.36) and the other towards the top of the sequence (E.2217.35). Specimen E.2217.36 is a green tuff containing purple lava fragments. In thin section it consists of plagioclase phenocrysts in an altered groundmass of chloritized or devitrified pumiceous fragments, shards, calcite, chlorite and ilmenite, which is patchily altered to leucoxene. The twinned feldspar laths are up to 4 mm long and are mostly strongly zoned with cores about An_{60}; oscillatory zoning is commonest but normally zoned and unzoned varieties are also represented. The plagioclase has been altered to one or more of the following minerals: veins of albite, calcite, sericite, chlorite, ilmenite and quartz. Elongated pseudomorphs of chlorite, calcite and ilmenite are present and these have probably replaced pyroxene.

Specimen E.2217.35 looks like a dark grey porphyritic lava in the hand specimen but in thin section it is seen to contain numerous pumiceous fragments and shards, some being devitrified while others are chloritized. This rock is similar to specimen E.2217.36 in its major constituents of plagioclase phenocrysts and pseudomorphs of chlorite and calcite, but it also has vesicles or vugs filled with pale green chlorite surrounded by calcite.

C. Discussion

As feldspars decompose fairly readily, arkoses are believed to be the product of either high relief and rapid erosion or a rigorous climate where decomposition is inhibited (Pettijohn and others, 1972, p. 186). However, there are differing opinions as to which of these two factors is the more important. Work on modern arkoses in Mexico (Krynine, 1935) and in the River Amazon (Gibbs, 1967) shows that high relief with rapid erosion is the major factor in their formation, whereas Strakhov (1969) considered that the climatic element is more important.

The age of the Mount Charity sedimentary rocks is uncertain so that the climatic conditions prevailing at the time of their formation can only be surmised but, if these rocks are Lower Tertiary in age, it is possible that a rigorous climate existed during their deposition. Adie (1964, p. 155) stated that the climate in northern Graham Land was cool enough in the late Oligocene to Lower Miocene to support penguins, and that the marine molluscan fauna in sedimentary rocks of this age indicates cold marine conditions and the flora indicates a cool-temperate climate. Moreover, evidence of subglacial volcanism in Marie Byrd Land suggests that there has been an ice sheet in western Antarctica since the Eocene (LeMasurier, 1971).

However, it is evident from the close association between the arkoses of Mount Charity and the coarse, poorly sorted polymict conglomerate containing a high proportion of adamellite boulders and pebbles that this area has suffered a major uplift and rapid erosion (Pettijohn, 1957, p. 257) which is probably the major factor in the formation of these arkoses.

The lack of a radiometric age for the underlying adamellite or any fossil evidence within the sedimentary rocks makes it difficult to estimate their age and their palaeogeographical setting. When these sedimentary rocks were first mapped, their unconformable position on an intrusion which was thought to belong to the Andean Intrusive Suite (Adie, 1955) suggested an early Tertiary age. But, a more detailed study of the plutonic rocks of the Antarctic Peninsula has shown that they were intruded over a much greater time range than Upper Cretaceous to Lower Tertiary, and Rex (1971) has identified at least four phases of igneous activity between the Lower Jurassic and the early Tertiary.

Rocks similar to those found at Mount Charity have been described from other parts of the Antarctic Peninsula and Alexander Island, and these will be discussed below.

Fraser and Grimley (1972) described conglomerates and associated arkoses having a strong green or purple coloration in north-eastern Palmer Land. These rocks are strongly deformed and highly cleaved, and their position in the stratigraphical succession, with volcanic rocks below and above, is thought to be due to thrusting; however, thrusting has only modified an unconformity below the arkoses. The volcanic rocks are thought to be Carboniferous in age and the arkoses have been assigned to the Jurassic.

On Adelaide Island, Dewar (1970) found faulted conglomerates with clasts of diorite, tonalite and granodiorite from the "ancient plutonic rocks of the Antarctic Peninsula" and also some metamorphic rocks. These conglomerates are thought to have been faulted down from the well-stratified Mount Bouvier summit succession, where quench-brecciated eruptive rocks pass up through tuffites into conglomerates with volcanic detritus and plutonic clasts. Dewar concluded that the sedimentary rocks within the volcanic sequence on Adelaide Island were coastal sediments and this has been verified by the discovery of marine bivalves and ammonites in tuffs of the Mount Bouvier massif (Thomson, 1972); these are thought to be Upper Jurassic in age.

Bell (1973) has described Cenozoic volcanic rocks unconformably overlying crushed and sheared arkosic sediment on Beethoven Peninsula, south-western Alexander Island. Similar arkosic sediments exposed in central Alexander Island had been tentatively correlated with the (?) Carboniferous Trinity Peninsula Series of north-east Graham Land (Grikurov and others, 1966). The Cenozoic volcanic rocks are relatively unconsolidated and include coarsely bedded vitrophyric olivine-tuffs and palagonite-tuffs associated with olivine-basalt lava flows and dykes.

In south-eastern Alexander Island there is a Cretaceous sequence of current-bedded and channelled sandstones (arkoses) with minor silt and clay interbeds and locally developed thick polymict pebble-conglomerates (Horne, 1968). These are thought to be deltaic sediments derived from a geanticlinal area in the present position of Palmer Land. Both Bell (1974*a*) and

Horne (1968) have presented evidence of intermittent andesitic and dacitic volcanic activity within or adjacent to the sedimentary basin, and this continued from Upper Oxfordian–Kimmeridgian to Albian, according to Bell (1974*a*).

Although there is a distinct similarity in colour between the Mount Charity arkoses and those in north-eastern Palmer Land, those of the latter area are highly deformed and cleaved. This difference in deformation, if the two units were coeval, could be explained by the fact that the Mount Charity rocks rest on a relatively rigid plutonic basement. However, this lack of deformation in the Mount Charity rocks favours a comparison with the polymict conglomerates and arkoses of south-eastern Alexander Island, and this is endorsed by a comparison of the volcanic rocks. The tuffs on Mount Charity are much more akin to the andesitic Upper Jurassic volcanic tuffs of western Palmer Land than to the Cenozoic olivine-basalts and tuffs of south-western Alexander Island, and this "Upper Jurassic" period of volcanicity has been proved to extend up into the Albian in south-eastern Alexander Island.

The correlation made above strongly suggests that the Mount Charity sequence is Upper Jurassic to Lower Cretaceous in age. The palaeogeographical reconstruction is, however, more difficult. It is clear that the arkoses were deposited in an aqueous environment and that the upper tuffs are subaerial. This sequence may have been at the margin of either the marine basin or basins associated with the rocks of south-eastern Alexander Island, Carse Point on the eastern side of George VI Sound (Thomson, 1975*a*) and Adelaide Island, or it may have been associated with a more restricted marine basin represented by faulted mudstones with subsidiary arkoses found at Crabeater Point, north-eastern Palmer Land, and which contain marine fossils of a probable Cretaceous age (Thomson, 1967).

VIII. ANDEAN INTRUSIVE SUITE

Plutonic rocks have a widespread distribution over this area. Acid, basic and intermediate types are represented and some of them are thought to be hybrids. At a few stations (E.3244, 3246 and KG.1220) these rocks are seen to intrude the Upper Jurassic volcanic rocks and at other exposures where the contacts between the two groups are not visible, the plutonic rocks contain xenoliths of volcanic rocks. These rocks are therefore broadly comparable with other intrusives in the Antarctic Peninsula which have been referred to as the Andean Intrusive Suite (Adie, 1955; Goldring, 1962; Hooper, 1962; Curtis, 1966). However, there are many plutonic rocks in northern Palmer Land which are not in contact with any other rock groups and, although their ages are unknown, they are included with these Andean plutonic rocks.

Radiometric methods have isolated six intrusive episodes in the Antarctic Peninsula (Adie, 1971*a*) and four of these are post-Upper Jurassic in age. In view of the number of intrusive episodes recognized so far, and the length of time that plutonic activity has been taking place, much radiometric dating needs to be carried out in northern Palmer Land to elucidate the plutonic history.

At some localities, within the plutonic rocks, it is possible to determine an order of intrusion. At station KG.1207, norite is intruded by adamellite and the latter contains xenoliths of granodiorite. This relationship agrees with observations in other parts of the Antarctic Peninsula where basic plutonic rocks are intruded by acid types (Adie, 1955, p. 16; Goldring, 1962, p. 26; Curtis, 1966, p. 21).

Modal analyses of nine specimens are given in Table IX to provide a framework for the classification of these rocks.

A. Field Relations and Petrography

1. *Gabbros*

a. *Field relations*. Basic plutonic rocks are rare in this part of northern Palmer Land. A norite crops out at station KG.1207, on the south-western side of Mount Edgell, and two exposures of gabbro have been mapped to the east of the Eternity Range. An area of gabbro was found on the north-trending ridge of Mount Sullivan (KG.3293), where it seems to be intruding gneisses of the metamorphic complex, and farther east at station KG.3269, where a nunatak of gabbro is surrounded by exposures of metasedimentary and metavolcanic rocks.

b. *Petrography*. At station E.3293 the gabbro is a black rock composed mainly of hornblende and plagioclase. The hornblende is pleochroic from yellow–pale brown to dark greenish brown and it forms large euhedral poikilitic crystals containing inclusions of plagioclase and iron ore; patches of colourless clinopyroxene in the hornblende indicate that the latter formed by replacement of the former. Many of the plagioclase crystals exhibit oscillatory and normal zoning from approximately An_{54} to An_{36} but some crystals have deformation twins and a form of patchy zoning (Fig. 24a); this patchy zoning is common in many of the plutonic rocks of northern Palmer Land. It does not exhibit the sharp compositional differences and the poikilitic inclusions in the sodic patches which Vance (1965) described. The mottled appearance can probably be attributed to an homogenization of the plagioclase due to deformation or a lowering of temperature. Further evidence of deformation is indicated by the presence of kinked biotite flakes. Iron ore is a common constituent of the groundmass and sphene and quartz are the main accessory minerals.

A greater degree of deformation is shown in specimen E.3269.1 with deformation twinning and patchy zoning being more prominent in the plagioclase (An_{54}) and patches of recrystallized granoblastic grains of plagioclase exhibiting triple-point intersections. Replacement of colourless clinopyroxene ($\gamma{:}c = 38°$) by greenish brown hornblende is at a less advanced stage than in specimen E.3293.1. Brown biotite is abundant in the rock; it forms inclusions in hornblende and clinopyroxene and has a penetrative and corrosive relationship to plagioclase.

2. *Norite*

a. *Field relations*. Norite crops out extensively at station KG.1207, a prominent south-westerly trending ridge of Mount

Edgell. At its western end, the norite is intruded by a steeply dipping body of adamellite which contains xenoliths of granodiorite.

b. *Petrography*. This rock is coarse-grained, dark grey in colour and weathers to brown. Almost 70% of the rock is plagioclase (An_{58}), dusty in appearance due to incipient alteration, and exhibiting albite, Carlsbad and pericline twinning. It occurs in laths up to 2.5 mm in length and more than one generation is represented because almost completely resorbed fragments of slightly more basic plagioclase occur in some of the laths. Patchy zoning, the occurrence of secondary blebs and veinlets of quartz and potash feldspar are also characteristic of the plagioclase. Interstitial to the plagioclase is hypersthene (large $2V\alpha$), which is weakly pleochroic from neutral to pale pink; these equant or elongated crystals are slightly rounded (Fig. 24b). Alteration of the hypersthene takes two forms: either to a fine micaceous yellow aggregate which forms along cracks and completely pseudomorphs the mineral in places, or to pleochroic pale green, fibrous tremolite-actinolite (moderate $2V\alpha$; $\gamma{:}c = 19°$). Associated with the latter are patches of iron ore and deep red-brown biotite, which has been partially replaced by chlorite. A few small remnants of clinopyroxene can be distinguished amongst the secondary amphibole.

Associated with the tremolite-actinolite and the biotite are small colourless, equant or elongated, rounded crystals with first-order grey interference colours and a biaxially positive interference figure. In all its characters, except for the interference figure, it resembles apatite and in many thin sections where the crystals are too small to obtain an interference figure it is indistinguishable from the latter. As this mineral and/or apatite are common accessory minerals in the plutonic rocks of the Antarctic Peninsula, they need to be extracted and a detailed study made to provide a positive identification.

3. *Diorite*

a. *Field relations*. Diorite has only been recorded from station E.4238, a small nunatak north-east of Crescent Scarp. The grey porphyritic diorite is cut by numerous red felsite dykes, each less than 1 m thick.

b. *Petrography*. Specimen E.4238.1 of the diorite contains large euhedral and subhedral greenish brown phenocrysts of hornblende in a fine-grained groundmass of plagioclase laths; the latter have a composition of approximately An_{49} but some crystals exhibit strong normal zoning. The hornblende phenocrysts are up to 4 mm long and they poikilitically enclose corroded crystals of the plagioclase and previously formed hornblende. Subhedral to angular crystals of iron ore are common in the thin section and small patches of chlorite replace hornblende and occur in the groundmass.

4. *Tonalites*

a. *Field relations*. Except for a small exposure on the northern side of Mount Hope (E.3299), tonalites are confined to the nunataks around Mount Edgell (E.3241, KG.1201, 1206, 1219 and 1222) and they account for an appreciable volume of the exposed plutonic rocks. At stations E.3241, KG.1201 and 1222 the bosses are cut by felsite dykes, and at the former the tonalite contains small xenoliths of a volcanic tuff. At station KG.1206 the well-jointed tonalite, containing xenoliths (2.5–7.5 cm in length) of a fine-grained dioritic rock and exhibiting weak igneous layering, seems to intrude steeply dipping volcanic rocks at its western end. Small fine-grained xenoliths of a more basic tonalite were recorded at station KG.1219.

b. *Petrography*. All the tonalites are coarse-grained massive rocks, relatively homogeneous in appearance and consist largely of hornblende and biotite set in a white or grey groundmass of plagioclase. Staining of these rocks by malachite and brown iron oxide is common and shear planes containing green epidote are often abundant.

Although all the tonalites have similarities, they can be subdivided into two groups based on their mafic minerals. Specimens E.3299.1, KG.1201.1 and 1219.4 have large subhedral, often twinned, poikilitic crystals of hornblende with a pleochroism scheme α = pale yellow-brown, β = green and γ = dark green, which contain small embayed inclusions of plagioclase and clinopyroxene. The plagioclase laths are normally zoned from approximately An_{49} to An_{37}, have been altered to sericite and saussurite, and have been deformed in places to give deformation twinning and patchy zoning. Subhedral or anhedral crystals of iron ore and ragged flakes of biotite, which have been replaced by chlorite, and flattened lenses of epidote-clinozoisite are common. In specimen E.3299.1 the biotite flakes are particularly large, less altered and they have squeezed between crystals of plagioclase and quartz, suggesting that they formed at a late stage or were partially re-mobilized; inclusions of biotite within biotite indicate that two generations are present. Minor quartz and potash feldspar are interstitial.

In the second group of tonalites (E.3241.1, 3, KG.1206.7 and 1222.2) the mafic minerals are very altered. Original clinopyroxene (moderate $2V\gamma$ and $\alpha{:}c = 41°$) is more abundant in these rocks but it has been extensively altered to one or more of the following minerals: dark green hornblende, tremolite-actinolite, uralite, iron ore, biotite or chlorite. The result is that the mafic minerals are very ragged and they often occur in clots of small crystals. The other constituents of these tonalites, i.e. biotite, plagioclase, potash feldspar, quartz and the accessories haematite, sphene, epidote and apatite, are similar in both groups.

Specimen E.3241.3 has appreciably more potash feldspar than the other tonalites and this string micro-perthite forms graphic intergrowths with quartz and corrodes previously formed minerals.

5. *Granodiorites*

a. *Field relations*. Three types of granodiorite have been distinguished and these are homogeneous, porphyritic and xenolithic types. There are four intrusions of homogeneous granodiorite: on the eastern ridge of Mount Charity (E.3620.3), on the southern side of Bingham Glacier (E.3278.2), on the northern part of Mount Edgell (KG.1221.1) and at station KG.1200, to the south of Mount Edgell; in the last two areas the country rock is volcanic tuff and breccia. As the undeformed granodiorite of station E.3278 is surrounded by metamorphic rocks, it intrudes the latter.

The porphyritic granodiorites intrude volcanic rocks at stations E.3245.3 and KG.1220.

The xenolithic granodiorites are clearly hybrid rocks. Fig. 25 shows the relationship at station KG.1201, where the tonalite described previously (KG.1201.1) is intruded by a pink adamellite (KG.1201.2). Blocks of the tonalite have been wedged loose by the adamellite and partial assimilation has caused con-

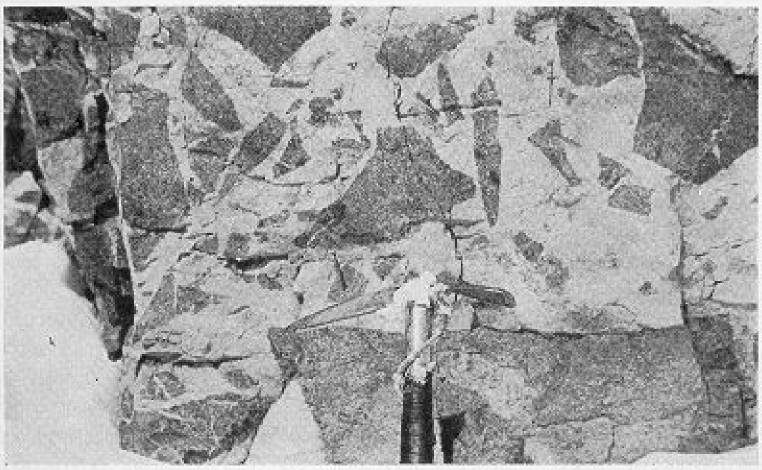

FIGURE 25
Tonalite intruded by adamellite at station KG.1201.

tamination of the engulfing material; the contaminated material is grey in colour but the adamellite is pink. Although this is a small-scale example, a similar process has taken place at stations KG.1205 and 1210 which are much bigger nunataks and here xenoliths, which have been assimilated to different degrees, float in a grey heterogeneous, often layered, mass of granodiorite.

b. *Petrography*. All the homogeneous granodiorites are so coarse-grained that their major constituents—white plagioclase, pink potash feldspar, quartz, hornblende and biotite—can be distinguished with the naked eye. Microscopically, the high proportion of plagioclase (47–59%) is characteristic of all the specimens.

In specimen E.3260.3 the plagioclase is normally zoned from An_{33} to An_{26} but oscillatory zoning is present in some crystals. Alteration of the plagioclase varies from the incipient formation of clay minerals and sericite to almost complete replacement by sericite. Xenomorphic quartz and microperthite are largely interstitial but there are some large crystals of the latter which poikilitically enclose small plagioclase crystals. Quartz occasionally forms large polycrystalline masses, the crystals having sutured boundaries and an undulose extinction. Rim myrmekite has developed in two adjacent crystals of plagioclase. It is located between the oscillatorily zoned plagioclase crystals and microperthite and, while the plagioclase component of the myrmekite is in optical continuity with the former, its boundary with the microperthite is very ragged. Phillips (1974), in his review of the literature on myrmekite, suggested that a formation by exsolution has the most appeal. The large brown biotite crystals forming streaky interstitial clots are reminiscent of the biotite in the pre-volcanic granodiorite (E.3248.2); it is extensively altered to chlorite, epidote and iron ore. Plates of muscovite accompany the biotite and apatite is the main accessory mineral.

Elongated crystals of green hornblende, which have been altered to epidote and chlorite, are abundant in specimen KG.1221.1 in addition to altered plates of biotite. The plagioclase in this specimen is often normally zoned (An_{51-28}) but occasionally the cores have patchy zoning; many of the laths also contain antiperthitic blebs and have been strongly corroded and infiltrated by microperthite (Fig. 26a) and quartz. Mafic minerals are less abundant in specimen KG.1221.1 and the hornblende has been altered to a felted mass of chlorite, sphene, epidote and iron ore; the plagioclase has been altered as evidenced by obliteration of twin planes and its replacement by quartz blebs.

Specimen E.3278.2 has a similar texture to the tonalite (E.3299.1) from the Eternity Range and this includes the large, relatively unaltered dark brown biotite present. As in the tonalite, the biotite is younger than and tends to corrode the plagioclase but its relationship to the hornblende is uncertain. This rock also possesses the large polycrystalline masses of quartz.

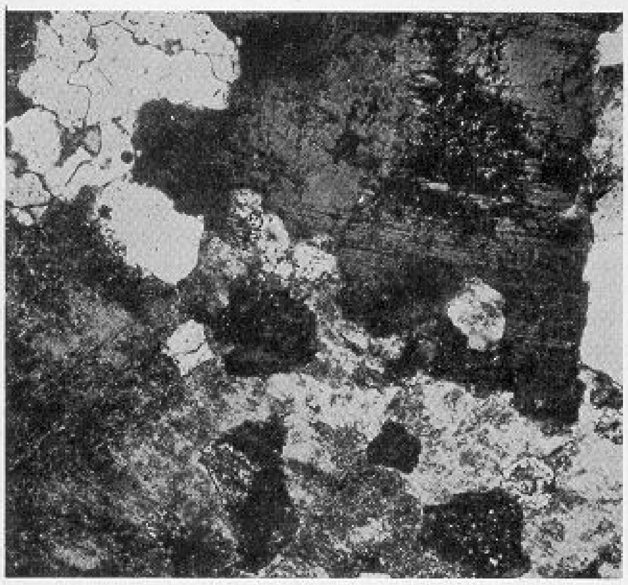

a.

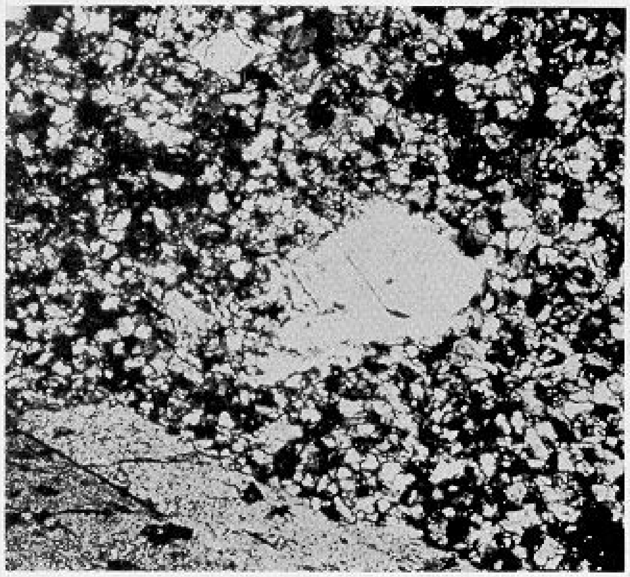

b.

FIGURE 26
a. Microperthite replacing plagioclase in a granodiorite. (KG.1221.1; X-nicols; × 59)
b. A quartz porphyroblast in a porphyritic granodiorite. (KG.1220.1; X-nicols; × 52)

Porphyritic granodiorites, KG.1203.1 and 1220.1, although separated by 15 km have similar textures and consist of large (up to 1 cm) subhedral to rounded cracked phenocrysts of quartz, together with large subhedral corroded plagioclase laths set in a fine-grained quartzo-feldspathic groundmass. In specimen KG.1220.1 the plagioclase (An_{32}) is severely saussuritized and it contains inclusions of iron ore. The original subhedral crystals of ilmenite have been altered to leucoxene, and veins and patches of yellow epidote are in evidence everywhere. Anhedral patches of quartz, which finger outwards into the groundmass (Fig. 26b), are thought to be porphyroblasts. Clots of small green biotite crystals, similar to those described from the volcanic rocks, are alteration products in the matrix. In specimen KG.1203.1 this alteration is more intense with small flakes of blue-green amphibole and a host of iron ore grains forming in addition to the biotite. As in the volcanic rocks, this form of alteration is considered to be due to contact metamorphism by later intrusions.

The porphyritic granodiorite at station E.3245 lacks the quartz phenocrysts, and plagioclase, forming single crystals and glomeroporphyritic aggregates, is the dominant mineral; it shows normal (An_{50-14}) and oscillatory zoning and sometimes has patchy zoning in the cores. Colourless augite ($\alpha{:}c = 48°$), partially altered to fibrous pale green tremolite-actinolite, is associated with the plagioclase in the glomeroporphyritic clusters. Subhedral plates of biotite and euhedral hornblende form the remainder of the porphyritic part of this rock. The matrix, which is finer-grained than in the specimens described above, has similarities to the devitrified groundmass of the dacitic lavas, indicating a possible shallow depth of intrusion and relatively rapid cooling.

The hybrid granodiorite at station KG.1201 is the best known, as the two source rocks, tonalite and adamellite, have been sampled. The modal analysis (Table IX) of the hybrid granodiorite shows that the percentages of the various constituents fall between those of the tonalite and the intruding adamellite. The tonalite has been described above. The adamellite (KG.1202.2) has a granitic texture with the subhedral plagioclase laths being peripherally replaced by anhedral potash feldspar and quartz; the former has the typical cross-hatch twinning of microcline. The plagioclase is sericitized and is normally zoned (An_{32-11}). Chlorite, which has replaced biotite, and iron ore are the only mafic minerals present.

The plagioclase in the hybrid rock is extremely sericitized but the few relatively unaltered specimens are normally zoned with a similar composition to the tonalite (An_{50-30}) but some of the crystals have patchy zoning. Although there are isolated corroded crystals of hornblende similar to those in the tonalite, hornblende usually forms small crystals in clots and is associated with altered biotite and iron ore; the brown biotite has been pseudomorphed by chlorite, epidote and iron ore. The quartz, which often forms polycrystalline aggregates, and potash feldspar are anhedral, the latter forming large crystals which are poikilitic towards the plagioclase. Sphene is an abundant accessory mineral associated with hornblende.

At station KG.1205 the hybrid material is less altered than specimen KG.1201.3. The plagioclase is only weakly sericitized and it is normally and oscillatorily zoned; some crystals have patchy zoning in their cores. However, the mafic minerals, though less altered, still form clots of small crystals, mostly hornblende but also brown biotite and iron ore. The quartz and potash feldspar form poikilitic crystals sprinkled with corroded plagioclase, hornblende and biotite. The larger hornblende crystals contain ragged cores of pyroxene, indicating that the hornblende has formed by the replacement of the latter; in some instances the pyroxene is pink hypersthene similar to that in the norite which crops out 5 km farther north. Therefore, this hybrid rock may have been formed by the contamination of an acid magma by norite.

The hybrid rocks at station KG.1210 lack the mafic minerals of the other hybrid rocks; the small original biotites have been pseudomorphed by chlorite, yellow epidote and sphene, and ilmenite has been almost completely replaced by leucoxene. These rocks are largely composed of sericitized and saussuritized laths of albite-oligoclase, which have been corroded by quartz and potash feldspar (patch microperthite). Quartz is abundant and large crystals up to 7 mm across have formed; at their edges, graphic intergrowths with albite and microperthite have been produced. The fact that a single quartz crystal forms intergrowths with both albite and microperthite, and its observed penetration along inter-crystal boundaries, suggests that it is replacing the other minerals.

6. *Adamellites*

a. *Field relations*. The adamellite at station E.3247 is found in a nunatak adjacent to the alkaline granite, specimen E.3247.2, but its contact with the latter is not seen. Specimen KG.1207.2 belongs to the boss of adamellite which intrudes the norite.

b. *Petrography*. The pink colour of the adamellites is spotted by black mafic minerals, white plagioclase and colourless quartz. These rocks have complex textures due to the formation of microperthite, graphic and myrmekitic intergrowths, and the resorption and replacement of earlier formed crystals.

The plagioclase laths (albite-oligoclase) of specimen E.3247.1 show weak normal and oscillatory zoning, and have been extensively sericitized in their cores. The potash feldspar is a fine string or patch microperthite forming anhedral grains which corrode the plagioclase; a reaction rim of clear albite forms around the corroded plagioclase. Quartz also corrodes plagioclase and in places it seems to corrode microperthite, but elsewhere blebs of quartz in the microperthite suggest graphic intergrowths. Ragged pseudomorphs of chlorite, epidote, iron ore and sphene, after biotite, are the only mafic minerals present.

Specimen KG.1207.2 is very inequigranular with large remnant plagioclases and the development of several large poikilitic crystals of twinned microperthite and quartz. As there are inclusions of quartz in microperthite and vice versa, there is probably more than one generation of each represented but some of the former may have formed during simultaneous crystallization to give graphic intergrowths. The relatively fresh biotite seems to have been squeezed along boundaries between quartz, plagioclase and potash feldspar, indicating that it formed later than these minerals.

B. Geochemistry

Three pre-volcanic plutonic rocks and 27 other plutonic rocks have been analysed for the major elements and 13 trace elements (Table X) using X-ray fluorescence methods. These analyses have been plotted on triangular variation diagrams with the coordinates (Fe″ + Fe‴)–Alk–Mg (Fig. 27) and K–Na–Ca (Fig. 28). On the former they show a typical calc-alkaline trend

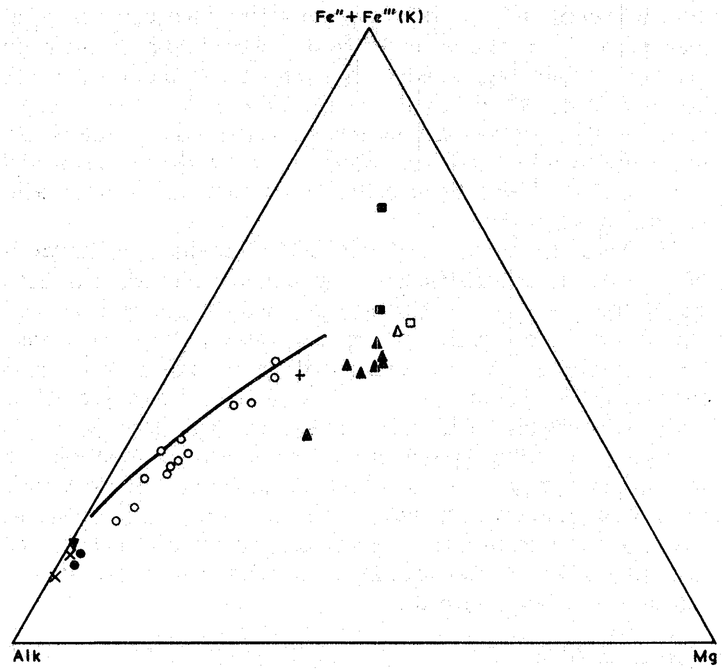

FIGURE 27

Triangular variation diagram plotted on the coordinates (Fe''+Fe''')–Alk–Mg for the plutonic rocks. The trend for the Andean Intrusive Suite (Adie, 1955) is shown.

□	Norite.	●	Adamellite.
■	Gabbro.	▼	Alkali-granite.
△	Diorite.	+	Pre-volcanic granodiorite.
▲	Tonalite.	X	Pre-volcanic adamellite.
○	Granodiorite.		

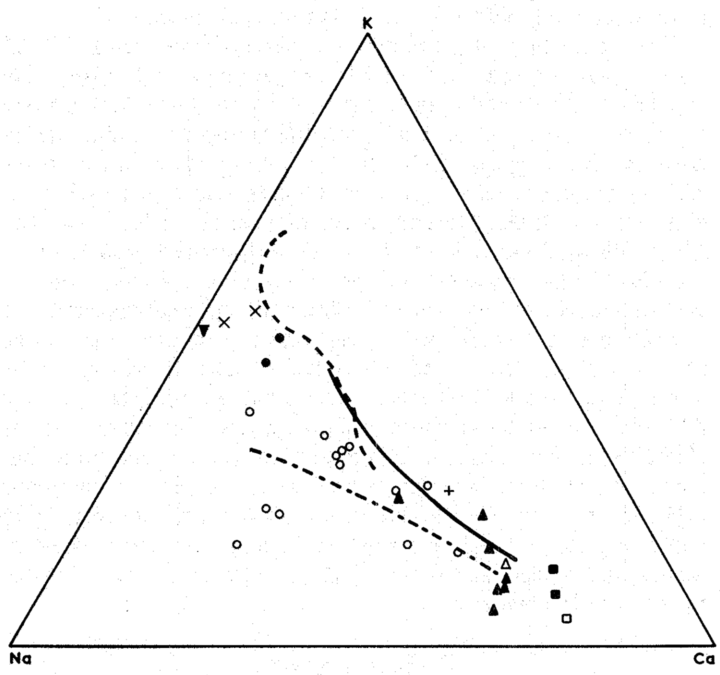

FIGURE 28

Triangular variation diagram plotted on the coordinates K–Na–Ca for the plutonic rocks. The symbols are the same as in Fig. 27.

The solid line is the trend of the Andean Intrusive Suite (Adie, 1955).

The dot-dash line is the trend of the plutonic rocks from Anvers Island (Hooper, 1966).

The pecked line defines the field of the potash-rich metamorphic complex rocks.

which is broadly comparable to the trends obtained by other workers for plutonic rocks from the Antarctic Peninsula (Adie, 1955; Marsh, 1968; West, 1974). On the K–Na–Ca diagram (Fig. 28) there is an alkali-enrichment trend but three of the analyses plot away from this trend towards the sodium apex of the triangle; two of these are hybrid granodiorites and the other one is a porphyritic granodiorite.

Various processes have been proposed to account for the origin of the plutonic rocks in the Antarctic Peninsula. Adie (1955) and Marsh (1968) suggested that fractional crystallization was the main process, West (1974) considered that in the Danco Coast the gabbros and granophyres were primary rocks but that the intermediate rocks were the products of magma contamination, and Hooper (1962) described primary gabbros and tonalites which had been extensively altered by regional metasomatism to form hybrid rocks.

The chemical data have also been presented on linear variation diagrams (Fig. 29), in which element percentages and element ratios have been plotted against the modified Larsen factor ($\frac{1}{3}$ Si+K)–(Ca+Mg) (Nockolds and Allen, 1953), thus allowing a comparison of the rock groups with each other and with other rocks from the Antarctic Peninsula.

1. *Norite, gabbros and diorite*

Basic plutonic rocks are relatively rare in northern Palmer Land, and except for the norite, are limited to small exposures.

One of the gabbros (E.3293.1) is chemically distinct from the other basic plutonic rocks in its significantly lower alumina and strontium contents, and higher ferrous iron and titania; these features indicate a possible genetic relationship to the greenschist dykes (Table II) and the metavolcanic rocks (Table V), which crop out in the same area. The norite, diorite and the other gabbro are more similar in their chemistry and, although the K/Rb and Ba/Rb ratios fall from the more basic norite to the other gabbro and the diorite (Fig. 29), the wide separation of the exposures and the differences in mineralogy, make a relationship by differentiation unlikely. The diorite and gabbro (E.3269.1) have higher contents of potassium and the associated trace elements, rubidium, strontium and barium, than the averages for basaltic rocks (Turekian and Wedepohl, 1961) and higher than the values for the numerous gabbros on the Danco Coast (West, 1974). However, there is no indication in the thin sections that a metasomatic addition of potash has taken place.

2. *Tonalites*

The large volume of tonalites present in northern Palmer Land, compared with the basic rocks, makes it unlikely that they have formed by the differentiation of a gabbro magma. The variation diagrams (Fig. 29) also suggest that the tonalites are chemically unrelated to the more basic rocks; potassium, barium and rubidium values for the tonalites are much the same as for the gabbros, whereas the tonalites with their much higher modified Larsen factors (Nockolds and Allen, 1953) would be expected to have higher values for these elements if the two groups were related by a differentiation process.

There is no progressive decrease of the K/Rb ratio with increasing modified Larsen factor within the tonalites (Fig. 29) and, although the Ba/Rb ratios decrease sharply, there is a considerable scatter on many of the variation diagrams. Therefore, it is unlikely that differentiation has been active within the tonalite group.

Table X

CHEMICAL ANALYSES OF PLUTONIC ROCKS FROM NORTHERN PALMER LAND

	1	2	3	4	5	6	7	8	9	10	11	12	13	14	15	16	17	18	19	20	21	22	23	24	25	26	27	28	29	30
SiO_2	48.68	49.98	48.99	51.70	57.17	55.57	56.64	57.57	58.47	59.23	56.62	60.39	59.88	64.96	68.63	61.42	65.79	66.75	65.00	70.92	70.38	60.93	64.43	72.40	72.24	74.14	73.86	72.98	73.81	75.50
TiO_2	1.23	2.04	0.84	1.15	0.79	0.87	1.16	0.78	0.80	0.87	0.90	0.72	0.61	0.41	0.48	0.64	0.56	0.41	0.59	0.29	0.37	0.60	0.84	0.32	0.30	0.06	0.15	0.18	0.21	0.18
Al_2O_3	17.31	11.96	18.79	16.53	18.23	17.37	13.82	15.57	16.26	17.11	16.03	15.47	18.93	17.82	16.17	18.18	17.35	17.33	16.69	15.39	14.93	17.66	15.07	14.77	14.75	14.54	13.76	15.12	14.85	11.42
Fe_2O_3	4.71	4.65	3.97	5.65	3.41	2.72	4.06	2.90	2.97	3.40	2.77	3.01	2.74	0.62	1.61	2.42	2.55	1.79	2.86	2.24	2.07	3.18	2.77	1.48	0.92	0.96	0.68	0.18	0.97	0.90
FeO	5.60	13.12	5.58	3.65	3.73	4.46	5.18	4.02	4.05	2.67	4.66	3.08	3.07	3.32	0.88	2.98	1.25	1.53	1.26	1.02	1.49	2.30	2.52	1.20	1.23	0.30	0.88	1.34	0.42	0.99
MnO	0.23	0.26	0.21	0.15	0.12	0.13	0.19	0.14	0.15	0.12	0.14	0.13	0.14	0.05	0.09	0.12	0.11	0.10	0.11	0.04	0.11	0.11	0.08	0.05	0.04	0.05	0.04	0.04	0.03	0.21
MgO	5.80	5.40	6.89	6.35	5.66	5.58	6.62	5.44	5.66	5.28	5.24	3.29	2.20	1.16	0.78	2.11	1.32	1.23	1.56	1.17	0.81	2.49	2.31	0.71	0.76	0.06	0.21	0.37	0.38	0.10
CaO	9.80	9.34	10.87	8.44	7.61	7.28	7.12	7.24	7.40	5.27	6.73	5.31	6.65	3.38	1.66	5.18	3.22	3.64	3.56	3.16	2.40	5.77	4.86	2.59	2.25	0.39	0.74	1.38	1.36	0.12
Na_2O	2.28	2.28	2.65	3.02	3.19	2.88	2.61	2.75	2.98	3.97	2.59	2.67	3.32	4.19	5.38	4.01	4.48	4.08	4.21	3.77	5.00	3.40	3.45	4.73	5.57	4.59	3.90	4.36	3.88	4.75
K_2O	1.51	0.95	0.52	1.51	0.57	1.68	1.10	0.88	0.91	2.67	2.23	2.32	1.60	3.02	3.84	2.71	3.50	3.30	3.18	2.59	1.93	2.87	1.48	1.79	1.41	4.92	4.96	4.38	4.70	4.58
P_2O_5	0.74	0.59	0.30	0.36	0.19	0.24	0.23	0.11	0.12	0.26	0.17	0.13	0.27	0.17	0.10	0.18	0.14	0.14	0.19	0.03	0.09	0.15	0.15	0.05	0.05	0.01	0.03	0.05	0.05	–
H_2O+	0.45	0.70	0.16	1.01	1.60	0.44	0.86	0.55	0.25	0.93	0.78	1.09	0.33	0.21	0.43	0.55	0.11	0.35	0.43	0.37	0.36	0.22	0.99	0.74	0.50	0.15	0.08	0.01	0.16	0.06
H_2O-	0.16	0.10	0.40	0.22	0.16	0.36	0.24	0.24	0.28	0.32	0.23	0.20	0.24	0.18	0.20	0.30	0.20	0.18	0.10	0.26	0.16	0.22	0.38	0.16	0.20	0.20	0.16	0.26	0.12	0.22
Total	98.40	100.37	100.17	99.74	102.43	99.58	99.83	98.19	100.30	102.10	100.09	97.81	99.98	99.49	100.25	100.80	99.58	100.83	99.74	101.25	100.10	99.91	99.03	100.99	100.23	100.36	99.62	100.86	100.94	99.03
ELEMENT PERCENTAGES LESS TOTAL WATER																														
Si^{4+}	23.25	23.00	22.99	24.54	26.55	26.30	26.82	27.63	27.40	27.45	26.99	29.25	28.16	30.64	32.21	28.73	30.67	31.11	30.63	32.95	33.04	28.63	30.75	33.82	33.94	34.65	34.80	33.99	34.28	35.74
Ti^{4+}	0.75	1.23	0.51	0.70	0.47	0.53	0.70	0.48	0.48	0.53	0.55	0.45	0.37	0.25	0.29	0.38	0.33	0.25	0.36	0.17	0.22	0.38	0.51	0.19	0.18	0.04	0.09	0.11	0.13	0.11
Al^{3+}	9.36	6.36	9.98	8.88	9.58	9.31	7.41	8.46	8.62	8.98	8.65	8.48	10.08	9.52	8.59	9.63	9.16	9.14	8.90	8.09	7.93	9.39	8.14	7.81	7.84	7.69	7.34	7.97	7.81	6.12
Fe^{3+}	3.36	3.27	2.79	4.01	2.37	1.93	2.88	2.08	2.08	2.36	1.98	2.18	1.93	0.44	1.13	1.69	1.78	1.25	2.02	1.56	1.45	2.24	1.98	1.03	0.65	0.67	0.48	0.13	0.67	0.64
Fe^{2+}	4.45	10.24	4.35	2.88	2.88	3.51	4.08	3.21	3.16	2.06	3.69	2.48	2.40	2.60	0.69	2.32	0.97	1.19	0.99	0.79	1.16	1.80	2.00	0.93	0.96	0.23	0.69	1.04	0.32	0.78
Mn^{2+}	0.18	0.20	0.16	0.12	0.09	0.10	0.15	0.11	0.12	0.09	0.11	0.10	0.11	0.04	0.07	0.09	0.08	0.08	0.09	0.03	0.09	0.09	0.06	0.04	0.03	0.04	0.03	0.03	0.02	0.16
Mg^{2+}	3.57	3.27	4.17	3.89	3.39	3.41	4.04	3.37	3.42	3.16	3.22	2.06	1.33	0.71	0.47	1.27	0.79	0.74	0.95	0.70	0.49	1.51	1.42	0.43	0.46	0.04	0.13	0.22	0.23	0.06
Ca^{2+}	7.15	6.70	7.80	6.12	5.40	5.27	5.15	5.31	5.30	3.73	4.90	3.93	4.78	2.44	1.19	3.70	2.30	2.59	2.56	2.24	1.72	4.14	3.55	1.85	1.62	0.28	0.53	0.98	0.97	0.09
Na^{+}	1.73	1.70	1.97	2.27	2.35	2.16	1.96	2.09	2.22	2.92	1.96	2.05	2.48	3.14	4.01	2.98	3.31	3.02	3.15	2.78	3.73	2.54	2.61	3.51	4.15	3.40	2.92	3.22	2.86	3.57
K^{+}	1.38	0.79	0.43	1.27	0.47	1.41	0.92	0.75	0.76	2.20	1.89	2.00	1.34	2.53	3.20	2.25	2.90	2.73	2.66	2.14	1.61	2.39	1.25	1.48	1.18	4.08	4.15	3.62	3.88	3.85
P^{5+}	0.33	0.26	0.13	0.16	0.08	0.11	0.10	0.05	0.05	0.11	0.08	0.06	0.12	0.07	0.04	0.08	0.06	0.06	0.08	0.01	0.04	0.07	0.07	0.02	0.02	–	0.01	0.02	0.02	–
O^{2-}	44.58	42.98	44.70	45.16	46.36	45.97	45.78	46.45	46.39	46.42	45.98	46.96	46.91	47.63	48.11	46.88	47.64	47.84	47.62	48.53	48.51	46.83	47.65	48.89	48.98	48.87	48.82	48.67	48.82	48.88
Position (1/3 Si+K) −(Ca+Mg)	−1.67	−1.52	−3.87	−0.56	+0.52	+1.47	+0.64	+1.23	+1.15	+4.48	+2.69	+5.54	+4.57	+9.50	+12.21	+6.83	+10.04	+9.78	+9.27	+10.22	+10.35	+6.24	+6.39	+10.47	+10.34	+15.31	+14.95	+13.78	+14.19	+15.40
C.I.P.W. NORMS																														
Q	2.30	2.68	–	4.28	11.36	8.10	13.18	15.08	13.49	7.38	10.56	20.11	16.41	18.18	18.06	12.90	17.62	20.50	18.89	30.36	27.54	14.85	25.62	31.20	28.18	27.60	30.13	26.30	29.57	31.71
C	–	–	–	–	–	–	–	–	–	–	–	–	0.17	1.77	0.25	–	0.54	0.63	0.18	0.65	0.40	–	–	0.40	0.03	0.92	0.67	0.73	0.94	–
Z	0.02	0.02	–	0.03	–	0.03	0.04	0.03	0.04	0.05	0.03	0.04	0.03	0.04	0.07	0.04	0.06	0.04	0.05	0.02	0.04	0.04	0.04	0.03	0.03	0.02	0.03	0.02	0.03	1.31
or	9.10	5.63	3.08	9.05	3.34	10.04	6.58	5.34	5.38	15.58	13.42	14.19	9.50	18.03	22.78	16.00	20.64	19.46	18.92	15.23	11.44	17.03	8.92	10.56	8.37	29.13	29.59	25.81	27.62	27.22
ab	19.68	19.36	22.49	25.91	26.80	24.65	22.35	23.87	25.25	33.17	22.32	23.38	28.23	35.73	45.63	33.91	37.76	34.38	35.86	31.69	42.45	28.89	29.77	39.96	47.33	38.81	33.24	36.73	32.59	33.25
an	33.19	19.66	37.96	27.46	33.50	29.84	23.02	28.26	28.34	20.72	26.00	24.19	31.72	16.21	7.95	23.59	15.33	17.42	16.88	15.52	11.54	24.55	21.69	12.68	11.05	1.98	3.56	6.69	6.68	–
ac	–	–	–	–	–	–	–	–	–	–	–	–	–	–	–	–	–	–	–	–	–	–	–	–	–	–	–	–	–	2.61
ns	–	–	–	–	–	–	–	–	–	–	–	–	–	–	–	–	–	–	–	–	–	–	–	–	–	–	–	–	–	0.95
di	9.53	19.34	11.59	18.18	2.36	4.33	9.11	6.44	6.37	3.99	5.75	2.04	–	–	–	1.01	–	–	–	–	–	2.76	1.69	–	–	–	–	–	–	0.93
hy	15.05	21.25	14.60	11.71	15.80	16.78	16.99	14.89	15.02	11.96	15.67	9.81	8.14	7.95	1.95	7.40	3.27	3.89	3.91	2.89	2.65	5.69	6.19	2.31	2.98	0.15	1.41	3.00	0.94	1.68
ol	–	–	2.19	–	–	–	–	–	–	–	–	–	–	–	–	–	–	–	–	–	–	–	–	–	–	–	–	–	–	–
mt	6.97	6.77	5.77	8.31	4.91	3.99	5.96	4.31	4.31	4.87	4.09	4.52	3.99	0.91	1.74	3.51	2.75	2.58	2.73	2.56	3.01	4.63	4.10	2.14	1.34	0.96	0.99	0.26	0.84	–
il	2.38	3.89	1.60	2.21	1.49	1.67	2.23	1.52	1.52	1.67	1.74	1.42	1.16	0.78	0.91	1.21	1.06	0.78	1.13	0.55	0.71	1.20	1.63	0.61	0.57	0.11	0.29	0.34	0.40	0.34
hm	–	–	–	–	–	–	–	–	–	–	–	–	–	–	0.41	–	0.64	–	1.00	0.46	–	–	–	–	–	0.30	–	–	0.39	–
ap	1.79	1.40	0.71	0.86	0.45	0.57	0.55	0.27	0.28	0.61	0.41	0.32	0.64	0.41	0.24	0.43	0.33	0.33	0.45	0.07	0.21	0.36	0.36	0.12	0.12	0.02	0.07	0.12	0.12	–
TRACE ELEMENTS (ppm)																														
Cr	19	14	25	17	42	25	33	29	22	19	27	36	14	6	1	17	5	7	6	9	–	23	31	3	2	1	–	1	2	–
Ni	2	–	26	37	36	25	15	25	29	19	15	32	8	5	5	15	7	9	5	8	2	16	34	1	2	3	4	3	4	4
Ga	24	25	25	25	23	24	21	21	25	26	23	18	23	32	21	20	18	17	21	12	15	19	18	11	11	15	20	16	12	23
Rb	47	19	9	36	16	58	37	25	46	77	82	78	66	140	104	78	103	124	89	99	56	81	58	53	37	235	192	138	152	244
Sr	858	298	711	995	535	575	417	408	686	753	527	559	663	776	378	511	385	507	504	128	228	514	409	193	139	29	56	238	165	5
Y	27	33	13	15	13	20	25	20	22	28	27	19	17	10	20	23	26	15	18	20	25	21	16	24	25	25	22	4	13	64
Zr	60	93	8	102	54	111	201	121	154	253	146	176	120	183	343	193	265	173	245	90	184	173	162	147	156	119	146	111	140	648
Nb	6	5	2	7	4	3	3	6	13	16	7	7	8	8	13	8	7	6	9	4	7	4	7	5	5	21	18	13	9	33
Ba	643	509	270	581	277	564	347	303	579	670	462	840	623	829	1 085	773	984	863	900	499	522	615	420	524	608	480	260	591	730	164
La	28	46	15	33	38	25	12	19	34	39	31	25	28	44	40	35	48	42	33	17	28	32	22	23	14	41	43	32	31	42
Ce	50	69	18	40	18	40	28	24	41	56	42	34	45	71	65	55	63	61	55	24	38	53	29	32	29	83	65	46	40	79
Pb	7	13	17	14	15	22	16	26	14	22	18	57	13	31	26	36	32	22	56	15	41	25	16	22	16	22	39	22	21	68
Th	5	–	–	4	3	3	–	4	7	16	7	13	5	15	12	15	20	23	13	8	3	14	5	7	5	24	27	27	33	31
ELEMENT RATIOS																														
K/Rb	272	416	478	353	294	243	249	300	165	286	230	256	203	181	308	288	282	215	299	216	286	392	216	279	319	174	216	301	255	158
Ba/Rb	13.7	26.8	30.0	16.1	17.3	9.7	9.4	12.1	12.6	8.7	5.6	5.6	9.4	5.9	10.4	9.9	9.6	7.0	10.1	5.0	9.3	7.6	7.2	9.9	16.4	2.0	1.4	4.3	4.8	0.59
COORDINATES OF TRIANGULAR DIAGRAMS																														
Fe	54.3	70.1	52.0	48.1	45.8	43.8	50.1	46.0	45.0	34.8	44.5	43.3	45.7	32.3	19.1	38.2	28.2	27.3	30.8	29.4	31.0	38.5	42.9	26.6	21.7	10.7	14.0	14.1	12.5	15.9
Alk	20.9	12.9	17.5	24.8	24.6	28.8	20.8	24.7	25.6	40.3	30.2	37.6	40.2	60.2	75.9	49.7	63.7	64.4	59.5	61.7	63.2	47.1	41.7	67.6	72.0	68.8	84.5	83.2	84.6	83.4
Mg	24.8	17.0	30.4	27.1	29.6	27.4	29.1	29.3	29.4	24.9	25.3	19.1	14.1	7.5	5.0	12.1	8.1	8.3	9.7	8.8	5.8	14.4	15.3	5.8	6.2	0.4	1.5	2.7	2.9	0.7
Ca	70.4	72.9	76.4	63.3	65.7	59.6	64.1	65.1	64.1	42.2	56.0	49.3	55.6	30.1	14.2	41.5	27.0	31.1	30.6	31.3	24.4	45.7	47.8	27.0	23.3	3.6	7.0	12.6	12.5	1.2
Na	17.0	18.5	19.3	23.5	28.6	24.5	24.4	25.7	26.8	33.0	22.4	25.7	28.8	38.7	47.7	33.3	39.0	36.2	37.6	38.8	52.8	27.9	35.2	51.3	59.8	43.8	38.4	41.2	37.1	47.5
K	12.6	8.6	4.2	13.2	5.7	16.0	11.5	9.2	9.2	24.8	21.6	25.0	15.5	31.2	38.1	25.2	34.1	32.7	31.8	29.8	22.8	26.4	16.9	21.7	16.9	52.6	54.6	46.3	50.3	51.3
Q†	*	*	*	*	*	*	*	*	*	*	*	*	*	*	*	*	*	*	*	*	33.6	*	*	37.5	33.4	26.9	31.1	29.5	31.5	32.3
Ab	*	*	*	*	*	*	*	*	*	*	*	*	*	*	*	*	*	*	*	*	55.6	*	*	52.4	60.1	43.0	38.2	44.2	38.7	38.7
Or	*	*	*	*	*	*	*	*	*	*	*	*	*	*	*	*	*	*	*	*	10.7	*	*	10.1	6.6	30.1	30.6	36.4	29.8	29.0
†Or	*	*	*	*	*	*	*	*	*	*	*	*	*	*	*	*	*	*	*	*	13.6	*	*	13.2	8.4	40.3	42.5	34.1	39.9	42.8
Ab	*	*	*	*	*	*	*	*	*	*	*	*	*	*	*	*	*	*	*	*	70.6	*	*	68.4	76.6	57.4	53.1	57.3	51.7	57.2
An	*	*	*	*	*	*	*	*	*	*	*	*	*	*	*	*	*	*	*	*	15.8	*	*	18.4	15.0	2.3	4.5	8.6	8.4	–

* Not determined.
† Mesonorms have been used for these coordinates.

1. E.3269.1 Gabbro; south of Engel Peaks.
2. E.3293.1 Gabbro; north-west ridge of Mount Sullivan.
3. KG.1207.4 Norite; south-west of Mount Edgell.
4. E.4238.1 Diorite; head of Fleming Glacier.
5. KG.1201.1 Tonalite; mainland east of the Rhyolite Islands.
6. KG.1206.7 Tonalite; south-western side of Mount Edgell.
7. KG.1222.2 Tonalite; Mount Guernsey.
8. KG.1219.4 Tonalite; Mica Islands.
9. E.3241.1 Tonalite; south of Relay Hills.
10. E.3241.3 Tonalite; south of Relay Hills.
11. E.3299.1 Tonalite; north-eastern side of Mount Hope.
12. E.3248.2 Pre-volcanic granodiorite; head of Fleming Glacier.
13. E.3278.2 Granodiorite; west of Engel Peaks.
14. E.3260.3 Granodiorite; north-eastern ridge of Mount Charity.
15. E.3246.1 Granodiorite; Crescent Scarp.
16. KG.1200.6 Granodiorite; south of Mount Edgell.
17. KG.1221.1 Granodiorite; north-western ridge of Mount Edgell.
18. KG.1207.3 Granodiorite; xenolith in adamellite (E.1207.2).
19. E.3245.3 Porphyritic granodiorite; south-east of Garcie Peaks.
20. KG.1203.1 Porphyritic granodiorite; south-west of Mount Edgell.
21. KG.1220.1 Porphyritic granodiorite; Brindle Cliffs.
22. KG.1205.1 Xenolithic granodiorite; south-west of Mount Edgell.
23. KG.1201.3 Xenolithic granodiorite; mainland east of the Rhyolite Islands.
24. KG.1210.1 Xenolithic granodiorite; west of Mount Edgell.
25. KG.1210.2 Xenolithic granodiorite; west of Mount Edgell.
26. E.3618.2 Pre-volcanic adamellite; north-eastern ridge of Mount Charity.
27. E.3622.2 Pre-volcanic adamellite; north of Mount Charity.
28. E.3247.1 Adamellite; head of Fleming Glacier.
29. KG.1207.2 Adamellite; west of Mount Edgell.
30. E.3247.2 Granite; head of Fleming Glacier.

TABLE II

CHEMICAL ANALYSES OF ROCKS FROM THE METAMORPHIC COMPLEX TO THE EAST OF THE ETERNITY RANGE

	1	2	3	4	5	6	7	8	9	10	11	12	13	14	15	16	17	18	19	20	21	22	23	24	25	26
SiO_2	60.43	65.29	66.04	67.47	67.95	65.19	67.51	69.11	69.46	70.68	71.20	73.11	48.97	56.12	60.56	66.97	65.47	69.04	69.27	69.86	74.45	71.15	75.27	74.13	46.61	46.98
TiO_2	1.07	0.62	0.53	0.57	0.74	0.58	0.57	0.43	0.50	0.38	0.41	0.24	0.25	1.45	0.78	0.74	0.49	0.25	0.30	0.47	0.06	0.22	0.09	0.44	1.00	1.34
Al_2O_3	14.54	15.97	16.49	16.21	13.64	17.16	16.05	14.55	16.40	14.33	13.91	13.92	14.10	13.66	12.02	13.58	17.65	18.02	16.57	14.86	15.32	16.56	13.69	12.82	12.50	12.97
Fe_2O_3	2.76	1.63	1.83	2.64	1.80	0.83	1.41	1.55	1.25	1.58	1.12	0.84	3.46	2.32	2.26	2.38	2.75	0.33	1.79	1.79	0.03	0.25	0.62	2.51	3.57	6.36
FeO	5.41	2.40	1.54	1.07	2.81	2.50	1.63	1.73	1.45	1.34	1.96	1.17	4.09	7.71	5.72	3.12	1.23	1.17	0.63	1.64	0.41	1.87	0.68	0.30	10.00	8.43
MnO	0.12	0.06	0.03	0.03	0.09	0.04	0.03	0.13	0.03	0.07	0.05	0.03	0.18	0.21	0.14	0.12	0.07	0.03	0.06	0.05	0.01	0.05	0.04	0.03	0.23	0.29
MgO	3.34	2.74	2.39	2.77	3.10	1.27	1.09	0.45	0.99	0.61	0.60	0.31	12.82	1.90	4.64	2.06	1.45	0.68	0.88	0.61	0.11	0.28	0.07	0.07	8.00	9.48
CaO	5.56	3.45	2.45	3.02	1.52	2.87	2.10	1.55	2.15	1.25	1.74	1.09	13.98	6.79	5.56	2.85	3.14	1.91	2.10	1.81	1.05	1.21	0.74	0.55	12.25	7.77
Na_2O	2.72	3.22	2.99	3.10	2.04	3.10	2.67	2.82	2.86	3.82	2.84	3.00	0.79	2.90	2.36	2.61	3.76	3.43	1.98	3.36	2.49	3.45	3.76	3.51	1.31	1.89
K_2O	2.51	3.00	5.31	3.33	5.04	4.87	5.23	6.22	4.87	4.97	4.92	6.04	1.01	1.81	3.01	4.45	4.10	6.14	7.78	4.90	6.81	5.82	5.25	6.28	0.92	1.45
P_2O_5	0.29	0.25	0.26	0.07	0.05	0.29	0.17	0.08	0.14	0.08	0.10	0.03	0.03	0.62	0.21	0.20	0.25	0.27	0.15	0.09	0.03	0.07	0.01	0.07	0.19	0.16
H_2O+	0.34	0.16	0.38	0.13	0.42	0.34	0.28	0.04	0.23	0.26	0.32	0.14	1.16	1.16	0.63	0.43	0.18	0.30	0.45	0.18	0.04	0.07	0.22	0.20	1.17	2.30
H_2O-	0.22	0.16	0.12	0.36	0.20	0.14	0.22	0.25	0.16	0.20	0.14	0.14	0.16	0.12	0.20	0.18	0.24	0.10	0.14	0.28	0.22	0.36	0.14	0.12	0.18	0.24
TOTAL	99.31	98.95	100.36	100.77	99.30	99.18	98.96	98.91	100.49	99.57	99.48	100.06	101.00	96.77	98.09	99.69	100.78	101.67	102.10	99.90	101.03	101.36	100.52	101.02	98.00	99.66
ELEMENT PERCENTAGES LESS TOTAL WATER																										
Si^{4+}	28.61	30.95	30.92	31.45	32.16	30.88	32.05	32.76	32.44	33.34	33.67	34.25	22.97	27.48	29.11	31.60	30.50	31.87	31.90	32.84	34.54	32.96	35.11	34.41	22.56	22.61
Ti^{4+}	0.65	0.38	0.32	0.34	0.45	0.35	0.35	0.26	0.30	0.23	0.25	0.14	0.15	0.91	0.48	0.45	0.29	0.15	0.18	0.28	0.04	0.13	0.05	0.26	0.62	0.83
Al^{3+}	7.79	8.57	8.74	8.55	7.31	9.20	8.63	7.81	8.67	7.65	7.45	7.38	7.49	7.57	6.54	7.25	9.31	9.42	8.64	7.91	8.05	8.68	7.23	6.74	6.85	7.07
Fe^{3+}	1.95	1.16	1.28	1.84	1.27	0.59	1.00	1.10	0.87	1.11	0.79	0.59	2.43	1.70	1.63	1.68	1.92	0.23	1.23	1.26	0.02	0.17	0.43	1.74	2.59	4.58
Fe^{2+}	4.26	1.89	1.20	0.83	2.21	1.97	1.29	1.36	1.13	1.05	1.54	0.91	3.19	6.28	4.57	2.45	0.95	0.90	0.48	1.28	0.32	1.44	0.53	0.23	8.05	6.75
Mn^{2+}	0.09	0.05	0.02	0.02	0.07	0.03	0.02	0.10	0.02	0.05	0.04	0.02	0.14	0.17	0.11	0.09	0.05	0.02	0.05	0.04	0.01	0.04	0.03	0.02	0.18	0.23
Mg^{2+}	2.04	1.67	1.44	1.67	1.89	0.78	0.67	0.28	0.60	0.37	0.37	0.19	7.76	1.20	2.88	1.25	0.87	0.41	0.52	0.37	0.07	0.17	0.04	0.04	5.00	5.89
Ca^{2+}	4.02	2.50	1.75	2.15	1.10	2.08	1.52	1.12	1.54	0.90	1.26	0.78	10.02	5.08	4.09	2.06	2.24	1.35	1.48	1.30	0.74	0.86	0.53	0.39	9.07	5.72
Na^{+}	2.04	2.42	2.22	2.29	1.53	2.33	2.01	2.12	2.12	2.86	2.13	2.23	0.59	2.25	1.80	1.95	2.78	2.51	1.45	2.51	1.83	2.54	2.78	2.59	1.01	1.44
K^{+}	2.11	2.53	4.41	2.76	4.24	4.10	4.41	5.24	4.04	4.16	4.13	5.02	0.84	1.57	2.57	3.73	3.39	5.03	6.36	4.09	5.61	4.79	4.35	5.18	0.79	1.24
P^{5+}	0.13	0.11	0.11	0.03	0.02	0.13	0.08	0.04	0.06	0.04	0.04	0.01	0.01	0.28	0.09	0.09	0.11	0.12	0.06	0.04	0.01	0.03	–	0.03	0.09	0.07
O^{2-}	46.30	47.78	47.58	48.06	47.75	47.57	47.97	47.81	48.22	48.23	48.33	48.46	44.42	45.51	46.13	47.70	47.59	48.00	47.65	48.08	48.77	48.20	48.91	48.37	43.21	43.57
MESONORMS																										
Q	22.83	27.26	22.53	28.68	32.61	22.29	26.99	24.87	28.38	25.67	31.15	28.62	–	18.15	19.54	28.35	20.61	20.52	22.27	26.66	29.51	24.51	29.63	27.05	–	2.79
or	3.28	9.39	25.00	13.34	20.49	23.46	27.77	35.13	25.53	27.47	26.44	34.36	3.22	2.31	9.73	19.26	20.78	32.87	43.75	26.84	29.52	31.23	30.42	37.19	1.41	–
ab	25.18	29.47	26.95	27.93	18.83	28.34	24.61	26.01	25.91	34.84	26.21	27.30	1.47	28.04	22.13	24.08	33.73	30.37	17.71	30.68	22.40	30.82	33.93	31.71	9.17	17.71
an	20.69	13.57	8.64	12.58	4.77	10.50	7.51	5.82	8.08	4.42	6.73	4.43	31.69	20.38	12.92	10.53	12.22	6.74	8.36	6.87	4.81	4.75	3.31	0.70	26.95	23.63
bi	19.21	13.88	10.38	10.23	16.16	9.31	6.29	4.17	5.59	3.75	5.47	2.88	4.32	14.72	14.13	12.39	5.46	4.61	3.22	4.14	1.25	4.74	1.18	0.20	6.93	14.30
act	2.92	–	–	–	–	–	–	–	–	–	–	–	37.34	9.12	15.92	–	–	–	–	–	–	–	–	0.07	38.59	15.96
hy	–	–	–	–	–	–	–	–	–	–	–	–	–	–	–	–	–	–	–	–	–	–	–	–	–	15.42
ed	–	–	–	–	–	–	–	–	–	–	–	–	17.79	–	–	–	–	–	–	–	–	–	–	–	10.39	–
mt	2.97	1.74	1.92	2.56	1.93	0.88	1.51	1.66	1.32	1.68	1.20	0.89	3.59	2.61	2.47	2.56	2.87	0.34	1.60	1.90	0.03	0.26	0.65	0.77	3.94	6.94
hm	–	–	–	0.14	–	–	–	–	–	–	–	–	–	–	–	–	–	–	0.18	–	–	–	–	1.24	–	–
tn	2.30	1.32	1.11	1.19	1.59	1.23	1.22	0.92	1.05	0.81	0.88	0.51	0.52	3.26	1.70	1.59	1.02	0.51	0.62	1.00	0.13	0.46	0.19	0.92	2.20	2.92
ap	0.63	0.53	0.55	0.15	0.11	0.62	0.37	0.17	0.30	0.17	0.22	0.06	0.06	1.40	0.46	0.43	0.52	0.56	0.31	0.19	0.06	0.15	0.02	0.15	0.42	0.35
C	–	2.84	2.93	3.20	3.52	3.35	3.72	1.24	3.85	1.19	1.70	0.94	–	–	–	0.81	2.78	3.48	1.98	1.73	2.30	3.09	0.68	–	–	–
TRACE ELEMENTS (ppm)																										
Cr	9	25	22	72	53	9	32	–	25	8	3	–	715	5	14	15	9	8	4	7	–	3	–	–	140	447
Ni	4	17	20	41	43	9	15	2	14	6	5	5	196	–	8	–	8	10	8	7	3	4	3	5	108	256
Ga	23	27	27	25	18	23	22	16	22	18	19	15	11	23	20	20	27	23	25	16	13	22	17	10	17	22
Rb	77	141	226	180	185	175	235	185	208	211	270	263	68	75	150	253	176	204	310	226	204	451	386	242	54	72
Sr	357	480	403	513	407	438	364	108	352	145	139	46	149	310	322	299	845	375	506	162	298	137	7	28	167	365
Y	25	17	14	4	38	13	12	34	9	32	27	35	6	49	27	26	19	27	14	30	–	24	39	53	21	35
Zr	352	260	245	141	491	320	227	348	188	240	236	191	9	307	181	290	190	157	123	263	67	161	123	426	63	69
Nb	11	18	11	15	15	18	23	18	19	14	17	18	1	22	12	19	17	10	23	15	4	25	30	23	2	5
Ba	2 163	585	705	653	1 028	1 030	756	1 026	691	788	557	533	58	740	598	1 233	869	728	886	901	1 252	377	122	859	99	288
La	36	55	44	30	34	88	79	73	48	44	53	73	17	50	36	44	48	41	41	48	31	65	43	64	16	18
Ce	43	89	66	48	46	133	116	123	69	75	84	115	7	87	59	72	72	32	65	74	20	109	73	95	15	16
Pb	18	24	56	51	78	40	59	39	57	39	46	36	10	25	31	55	24	82	83	57	50	71	56	70	8	14
Th	5	48	15	16	16	51	57	20	29	21	30	34	–	13	18	12	23	5	28	22	4	70	56	30	1	–
ELEMENT RATIOS																										
K/Rb	274	160	195	153	229	234	188	185	194	197	153	191	122	209	171	147	193	247	205	181	275	106	113	214	146	172
Ba/Rb	28.1	4.1	3.1	3.6	5.6	5.9	3.2	5.5	3.3	3.7	2.1	2.0	0.9	9.9	4.0	4.9	4.9	3.6	2.9	3.9	6.1	0.8	0.3	3.5	1.8	4.0
K/Sr	58	52	109	54	103	92	119	478	115	285	294	1 090	56	48	78	124	40	136	128	251	190	353	6 226	1 862	46	33
K/Ba	9.8	43.2	62.6	42.3	41.2	39.8	58.3	51.0	58.5	52.8	74.1	94.2	144.8	21.2	43.0	30.3	39.0	69.1	71.8	45.4	44.8	127.1	356.6	60.3	79.8	43.1
Rb/Sr	0.22	0.29	0.44	0.35	0.45	0.40	0.65	1.71	0.59	1.46	1.94	5.71	2.19	0.24	0.47	0.85	0.21	0.54	0.61	1.39	0.68	3.29	55.14	8.64	0.32	0.20
Ca/Sr	112.6	52.1	43.4	41.9	27.0	47.5	41.8	103.7	43.8	62.1	90.6	169.6	672.5	163.9	127.0	68.9	26.5	36.0	29.2	80.2	24.8	62.8	757.1	139.2	543.1	156.7
Ba/Sr	6.06	1.22	1.75	1.27	2.53	2.35	2.08	9.5	1.96	5.43	4.01	11.59	0.39	2.39	1.86	4.12	1.03	1.94	1.75	5.56	4.20	2.75	17.4	30.7	0.59	0.79
COORDINATES OF TRIANGULAR DIAGRAMS																										
Fe	50.1	31.5	23.5	28.5	31.3	26.2	24.4	24.4	22.8	22.7	26.0	16.8	37.9	61.3	46.1	37.3	28.9	12.4	17.1	26.7	4.3	17.7	11.8	20.2	61.0	56.9
Mg	16.4	17.3	13.7	17.8	17.0	8.0	7.1	2.7	6.8	3.9	4.1	2.1	52.4	9.2	21.4	11.3	8.8	4.5	5.2	3.9	0.8	1.8	0.5	0.4	28.7	29.6
Alk	33.5	51.2	62.8	53.8	51.7	65.8	68.5	72.9	70.3	73.5	69.9	81.1	9.7	29.4	32.5	51.4	62.3	83.1	77.7	69.4	94.9	80.4	87.7	79.4	10.3	13.5
Ca	49.2	33.6	20.9	29.9	16.0	24.4	19.2	13.2	20.0	11.4	16.7	9.7	87.5	57.0	48.3	26.6	26.6	15.2	15.9	16.5	9.1	10.5	6.9	4.8	83.5	68.1
Na	25.0	32.5	26.5	31.8	22.3	27.4	25.3	25.0	27.6	36.1	28.3	27.8	5.1	25.3	21.3	25.3	33.1	28.3	15.6	31.7	22.4	31.0	36.3	31.7	9.3	17.2
K	25.8	33.9	52.6	38.3	61.7	48.2	55.5	61.7	52.5	52.5	54.9	62.5	7.3	17.7	30.4	48.2	40.3	56.6	68.5	51.8	68.5	58.5	56.8	63.5	7.3	14.8
Q	*	*	*	*	*	*	34.0	28.9	35.6	29.2	37.2	31.7	*	*	*	*	*	24.5	26.6	31.7	32.3	28.3	31.5	28.2	*	*
Or	*	*	*	*	*	*	35.0	40.8	32.0	31.2	31.6	38.1	*	*	*	*	*	39.2	52.3	31.9	43.2	36.1	32.4	38.8	*	*
Ab	*	*	*	*	*	*	31.0	30.2	32.5	39.6	31.3	30.2	*	*	*	*	*	36.3	21.2	36.4	24.5	35.6	36.1	33.0	*	*
An	*	*	*	*	*	*	12.3	8.9	13.7	6.6	11.1	6.7	*	*	*	*	*	9.8	12.1	10.7	7.2	6.2	4.8	1.1	*	*
Ab	*	*	*	*	*	*	41.1	38.8	43.5	52.2	44.0	41.3	*	*	*	*	*	43.1	25.4	47.5	33.7	47.2	50.2	45.9	*	*
Or	*	*	*	*	*	*	46.6	52.3	42.8	41.2	44.9	52.0	*	*	*	*	*	47.1	62.5	41.8	59.1	46.6	45.0	53.0	*	*

* Not determined.

1. E.3287.1 Biotite-gneiss.
2. E.3612.1 Biotite-gneiss.
3. E.3612.2 Biotite-gneiss.
4. E.3606.1 Biotite-gneiss.
5. E.3607.1 Biotite-gneiss.
6. E.3286.2 Augen-gneiss.
7. E.3608.1 Augen-gneiss.
8. E.3295.1 Augen-gneiss.
9. E.3614.1 Augen-gneiss.
10. E.3296.1 Augen-gneiss.
11. E.3611.1 Augen-gneiss.
12. E.3603.1 Augen-gneiss.
13. E.3282.3 Amphibolite.
14. E.3294.1 Amphibolite.
15. E.3291.12 Amphibolite.
16. E.3291.11 Amphibolite.
17. E.3279.6 Acid gneiss.
18. E.3613.1 Acid gneiss.
19. E.3285.1 Acid gneiss.
20. E.3609.1 Acid gneiss.
21. E.3286.4 Acid gneiss.
22. E.3291.10 Acid gneiss.
23. E.3290.1 Acid gneiss.
24. E.3271.1 Engel Peaks granite
25. E.3291.6 Greenschist dyke.
26. E.3296.2 Greenschist dyke.

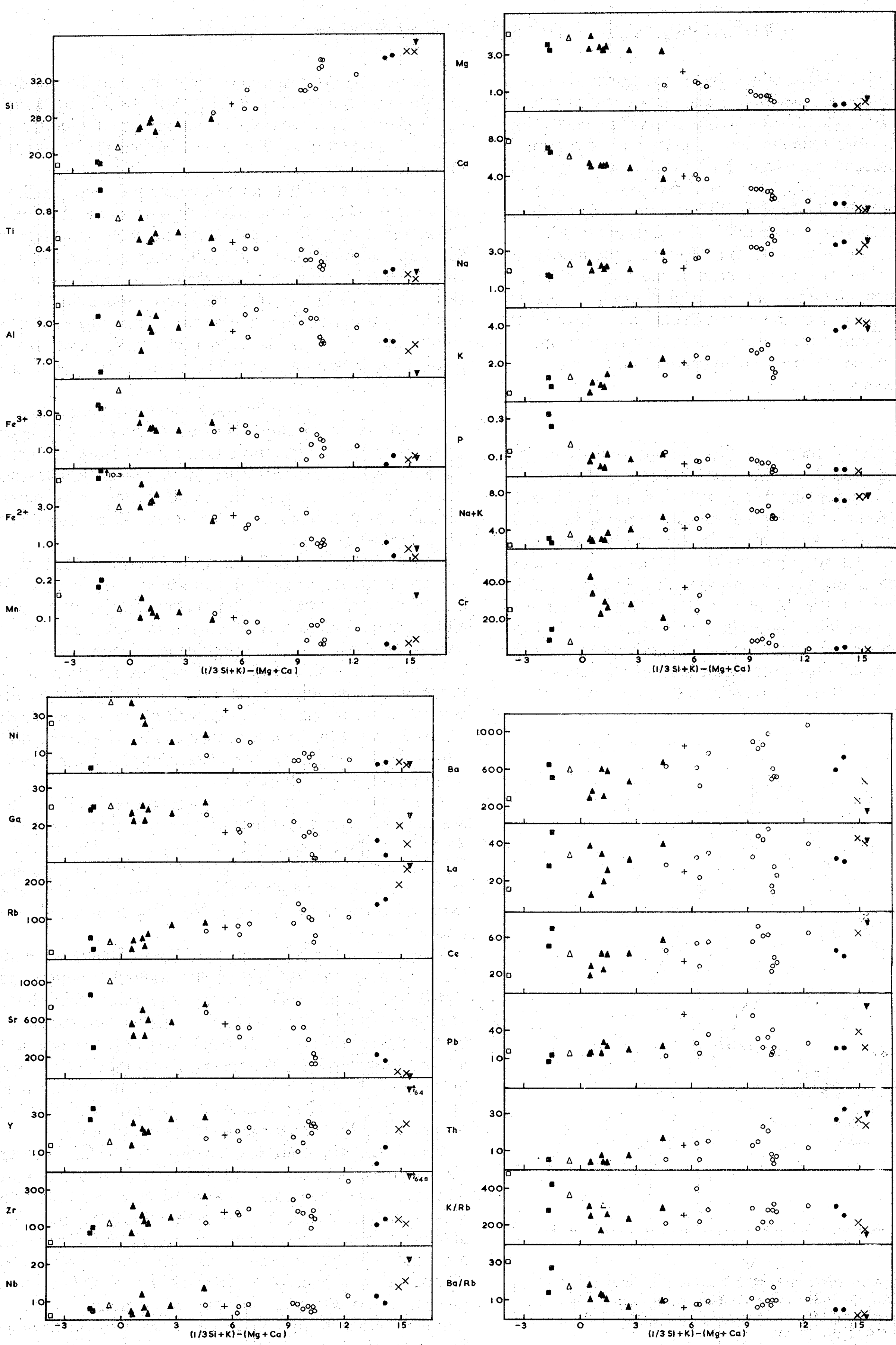

FIGURE 29
Variation diagram for the plutonic rocks showing major and trace elements, and element ratios, plotted against ($\frac{1}{3}$ Si+K)-(Ca+Mg).
The symbols are the same as in Fig. 27.

The two types of tonalite, which were distinguished petrographically, do not possess distinctive chemical characteristics. However, specimen E.3241.3 has higher potassium and silica contents than the other tonalites and it plots with the granodiorites on the variation diagrams. This tonalite was found in close proximity to specimen E.3241.1 and may possibly be part of the same intrusion. Its K/Rb ratio is considerably higher than that of specimen E.3241.1 and therefore it is unlikely that it is a differentiate of the more basic tonalite. However, the increased potash content in this rock can be seen in the thin section as microperthite, which corrodes earlier formed crystals and is intergrown with quartz, and these constituents may have been introduced by metasomatism; textures resembling graphic intergrowths may have been formed by hydrothermal solutions or metasomatism (Marmo, 1971, p. 166).

3. *Granodiorites*

These are the most abundant of the plutonic rocks and the most heterogeneous, both in the thin sections and in their chemistry. It has been pointed out that on the K–Na–Ca diagram (Fig. 28) some of the granodiorites plot away from the main trend, towards the sodium apex. On the plot of potassium against the modified Larsen factor (Fig. 29), these three rocks are joined by another porphyritic granodiorite. These deviates from the main trend can best be seen on the variation diagrams of silica, sodium, potassium, barium and strontium (Fig. 29), in which they plot above the main trend in the silica and sodium diagrams, but below it in the potassium, barium and strontium diagrams. Three of these granodiorites have over 80% normative Q+Ab+An and they have been plotted on a Q–Ab–Or variation diagram (Fig. 30). As the points fall close to the Q–Ab sideline, outside the field of normal granites and away from the minimum of Tuttle and Bowen (1958), they are not magmatic rocks.

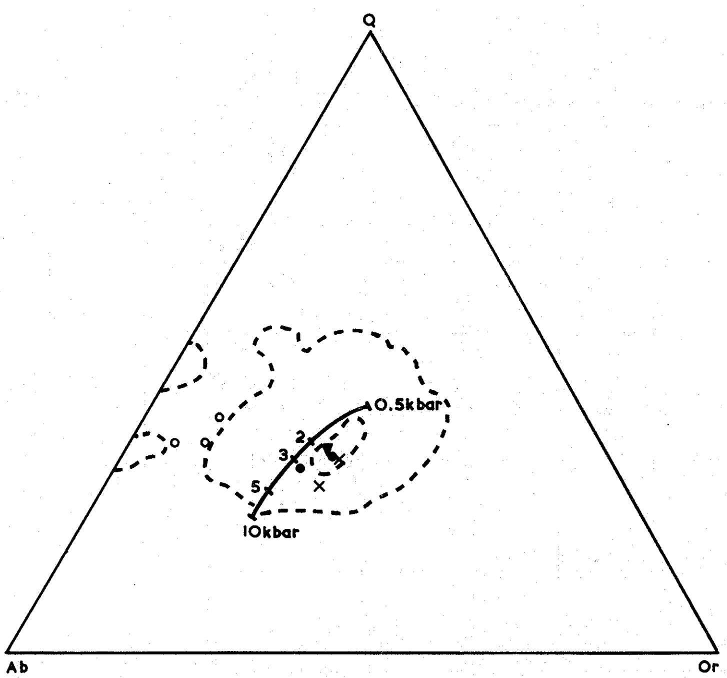

FIGURE 30

A plot of normative quartz, albite and orthoclase for the plutonic rocks containing normative Q+Ab+Or ⩾ 80%. The symbols are the same as in Fig. 27. The inner dashed line encloses 14% and the outer line 86% of all the granites considered by Winkler (1974, fig. 18-11).
The solid line indicates the trend of the ternary minima and eutectics at water pressures of between 0.5 and 10 kbar (Tuttle and Bowen, 1958; Luth and others, 1964).

At station KG.1201, an adamellite intrudes tonalite and the former has been contaminated to give a hybrid granodiorite. These rocks have been plotted on the variation diagrams (Fig. 29) and, although this hybrid granodiorite has a lower modified Larsen factor than the anomalous granodiorites discussed above, this rock plots appreciably above the main trend for silica and below for potassium and barium. This suggests that the contamination of an acid magma by more basic rocks could produce the anomalous chemical features of some of the granodiorites.

However, the process forming these anomalous granodiorites is selective because only a few of the hybrid granodiorites are included and two of the porphyritic granodiorites. Furthermore, these two groups are very different in microscopic texture and in the outcrop, the porphyritic granodiorites being more homogeneous. Metasomatism is the most likely process to have caused these features.

From Anvers Island, Hooper (1962) described a metasomatic trondhjemitic porphyry, which consists of large quartz and albite porphyroblasts in a matrix of interlocking quartz and albite grains with traces of potash feldspar, and which has a similar chemistry to the porphyritic granodiorites and hybrid granodiorites discussed above. However, the phenocrysts of the porphyritic granodiorite seem to be primary and the metasomatism has albitized the plagioclase and altered the matrix of the rock. As in the process envisaged by Hooper (1962) for the trondhjemitic porphyry, the metasomatism mainly involved an introduction of silica and sodium.

The textures of the hybrid granodiorites, KG.1210.1 and 2, are very different from those of the porphyritic granodiorites but their chemical compositions are similar. In these rocks, quartz forms graphic intergrowths with patch microperthite and albite, and experimental evidence (Marmo, 1971, p. 166) has shown that such textures can be produced by hydrothermal solutions or metasomatism.

There are a few large bodies of homogeneous granodiorite in the area mapped and, although tonalites are numerous, their K/Rb and Ba/Rb ratios are mostly lower than those of the granodiorites (Fig. 29), making it unlikely that the latter formed by the differentiation of a tonalitic magma. However, in the area around Mount Edgell, the basic granodiorite (KG.1200.6) has a higher K/Rb and Ba/Rb ratio than the more acid types (KG.1207.3 and 1221.1) and therefore differentiation may have occurred within these homogeneous granodiorites.

Within the granodiorites, specimen E.3248.2 belongs to the pre-volcanic rocks but specimen KG.1200.6 is post-volcanic. It is evident from columns 12 and 16 in Table X that they are similar in their chemistry, the main differences being the lower alumina and soda, and the higher magnesium, chromium, nickel and lead contents of the pre-volcanic granodiorites. The other homogeneous granodiorites (KG.1221.1, E.3278.2 and 3620.3) are more closely allied to the post-volcanic rocks in these elements. As with the adamellites, much radiometric dating will be necessary to supplement the meagre field relations, in order to establish whether such chemical criteria can be used to distinguish the plutonic rocks of different ages.

4. *Adamellites*

Two pre-volcanic adamellites (E.3618.2 and 3622.4) and two adamellites (E.3247.1 and KG.1207.2), whose relationship to the volcanic rocks is not known, have been analysed. Dykes of micro-adamellite cut the Upper Jurassic volcanic rocks, indicating the presence of a post-volcanic acid magma. West (1974, p. 48) recorded many chemical differences between the pre-volcanic granitic rocks and the post-volcanic granophyres of the Danco Coast. The earlier granitic rocks are more acidic and have lower barium and higher rubidium contents, lower K/Rb and Ba/Rb ratios, and are impoverished in zinc, zirconium, cerium, copper, yttrium, lanthanum and lead. In Palmer Land, while the pre-volcanic adamellites have lower barium, higher rubidium and lower K/Rb and Ba/Rb ratios than the other two adamellites, they are enriched in cerium, lanthanum and yttrium.

It is evident that the geochemical data are not adequate to discriminate between the acid plutonic rocks of different ages in northern Palmer Land. Many more field relations and radiometric dates are required before any satisfactory conclusions can be reached. It may be found that it is impossible to distinguish between the plutonic rocks of different ages by geochemical methods. Based on the available radiometric evidence, Marsh (1968, p. 196) described Jurassic plutonic rocks from the east coast of Graham Land which he could not distinguish on the basis of the major elements from the younger Andean plutonic rocks.

The geochemical differences between the adamellites and the acid igneous rocks of the metamorphic complex are, however, more obvious. From the K–Na–Ca diagram (Fig. 28), it is clear that the acid metamorphic complex rocks are richer in potash. They are also richer in iron, magnesium and calcium, and the associated trace elements (Tables III and X).

It is unlikely that the adamellites formed by the differentiation of a more basic magma. While the Ba/Rb ratios of the adamellites are slightly lower than those of the more basic rocks, their K/Rb ratios are higher than those of many of the granodiorites and tonalites (Fig. 29). The granodiorites are such a mixed group of rocks, many of which have a hybrid or metasomatic origin, that they could not have a parental relationship to an adamellite magma. On the contrary, an adamellite magma may have formed many of the hybrid granodiorites.

The adamellites have normative Q+Ab+An>80% and they have been plotted on Q–Ab–Or and Or–Ab–An diagrams (Figs 30 and 31). In the former, the adamellites plot in the normal field of granitic rocks but one of the pre-volcanic adamellites and one of the others plot closer to the albite apex of the triangle, which probably indicates that they were formed under higher water pressures than the other adamellites. Both of the pre-volcanic adamellites are slightly enriched in orthoclase, suggesting that, as in the acid gneisses and feldspar-gneisses, a metasomatic replacement of plagioclase by potash feldspar has taken place; this is also evident in the thin sections. On the Or–Ab–An diagram (Fig. 31) the pre-volcanic adamellites plot in the low-temperature trough (Kleeman, 1965) but the other two lie at the boundary of the trough. The variations between the two groups of adamellites may be due to different source rocks being melted. Kleeman (1965, fig. 8) has shown the trends of melts initiated by the intrusion of basaltic magmas and these are reproduced in Fig. 31 together with an outline of the field of the acid gneisses and augen-gneisses. The palingenetic veins derived from granites have produced a liquid richer in albite than the parental rock

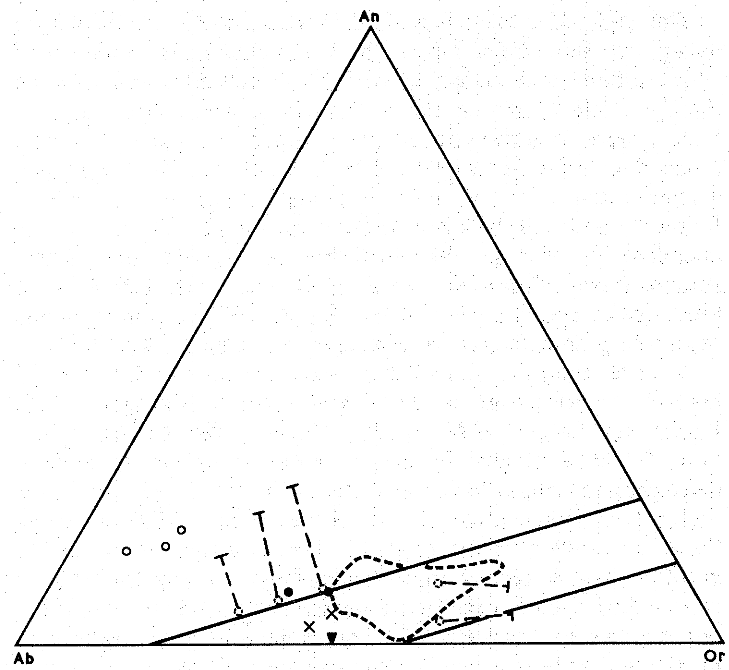

FIGURE 31

A plot of normative anorthite, albite and orthoclase for the plutonic rocks containing normative Q+Ab+Or ⩾ 80%. The symbols are the same as in Fig. 27. The parallel lines enclose the outer limits of compositions indicative of crystallization of liquids in the thermal trough of this system, allowing for analytical error (Kleeman, 1965, fig. 4A). The area enclosed by the dashed line indicates the main concentration of acid rocks from the metamorphic complex. The dashed symbols indicate the trend of melts, after Kleeman (1965, fig. 8).

and so it is possible that the pre-volcanic adamellites formed by partial melting of the potash-rich acid rocks of the metamorphic complex, and that the other adamellites formed by fusion of more basic rocks.

C. CONCLUSIONS

It is evident that the processes of metasomatism, contamination, anatexis and possibly differentiation were involved in the formation of these plutonic rocks. However, the relative significance of these processes is uncertain and it is not clear whether some of these processes could give rise to the large volumes of relatively homogeneous tonalite and granodiorite present in this area.

The trends on the variation diagrams (Figs 27, 28 and 29) are similar to those obtained for rocks from other parts of the Antarctic Peninsula (Adie, 1955; Marsh, 1968) and for other calc-alkaline suites (Nockolds and Allen, 1953), and these smooth trends were thought to indicate differentiation. The small volume of basic rocks compared with the intermediate rocks, plus the lack of iron enrichment compared with known differentiated rocks, have been strong arguments against the application of this process to calc-alkaline rocks. Furthermore, while Osborn (1969) has proved experimentally that differentiation can give a calc-alkaline trend by the fractionation of magnetite, trace-element studies by Taylor (1969) suggested that this process has not taken place in the formation of andesites and associated calc-alkaline rocks. It is therefore probable that differentiation was not a major process in the formation of the plutonic rocks in northern Palmer Land.

The acid and intermediate plutonic rocks of Anvers Island are thought to have been formed by the metasomatic addition of silica, sodium and potassium to primary tonalites and gabbros (Hooper, 1962), and on the K–Na–Ca diagram (Fig. 28) they have a more sodium-enriched trend compared to that of normal Andean intrusive rocks (Adie, 1955). Apart from the anomalous granodiorites, most of the intermediate rocks from northern Palmer Land fall between these two trends. There is little chemical or petrographic evidence to suggest that metasomatism was of more than local significance in the formation of these rocks and this view is in keeping with current opinions regarding granitization (Carmichael and others, 1974, p. 593).

A contamination model has been commonly invoked to explain the formation of calc-alkaline rocks (Baragar, 1966; Pitcher and Berger, 1972, p. 120). This involves the contamination of a basic magma by acid material or vice versa. Several petrographic criteria have been used to infer a hybrid origin for Antarctic plutonic rocks (Curtis, 1966; West, 1974) but when these are applied to the relatively homogeneous granodiorites and tonalites the results are not conclusive; some of the features can be attributed to other mechanisms and, unless several of the criteria can be recognized in the same rock, it is unwise to postulate a hybrid origin on this evidence alone. Furthermore, while West's (1974) hybrid rocks show non-curvilinear trends with considerable scatter on the linear variation diagrams, especially on the plots of phosphorus, titania and manganese, these features are not found in the tonalites and granodiorites of northern Palmer Land (Fig. 29).

Although it seems that the contamination of an acid magma by norite or tonalite has taken place to form the heterogeneous xenolithic granodiorites, in the same area a large body of adamellite containing granodiorite xenoliths intrudes the norite, and all the contacts are sharp with no visible contamination. Comparable variations in contact phenomena have been noted by Pitcher and Berger (1972, p. 351), who concluded that "the character of a granitic pluton, and of its relationship with its present envelope, need bear little relation to position in the crust."

The lack of evidence for hybridization in the relatively homogeneous tonalites and granodiorites, together with their large volume and the presence of sharp contacts between some of the intrusive rocks, suggest that these are primary rocks which originated independently and were intruded as several discrete pulses. A similar origin has been postulated for the rocks of the Sierra Nevada batholith (Bateman and Eaton, 1967). The ultimate origin of these rocks may be due to melting of the sialic crust, the variation in rock types being due to the heterogeneous nature of the crust (Carmichael and others, 1974, p. 582) or differing water pressures at the times of generation (Pitcher and Berger, 1972, p. 347), or they may have been derived from the mantle by a two-stage process as envisaged by Green and Ringwood (1968) and Taylor (1969).

IX. ALKALI-GRANITE

1. *Field relations*

Alkali-granite has only been recorded in a group of nunataks at the head of Fleming Glacier (E.3247). It is a red granite with quartz-filled vugs. The granite is intruded by basic dykes.

2. *Petrography*

This coarse-grained granite is composed mainly of microperthite, quartz, pleochroic yellow-green aegerine ($\alpha{:}c = 10°$) and dark blue pleochroic riebeckite (large $2V\alpha$; $\alpha{:}c = 20°$); the latter two minerals form broken laths. The microperthite crystals are coarse patch types and the plagioclase : potash feldspar ratio varies a great deal from one crystal to another, antiperthites, mesoperthites and perthites being represented. Intergranular albite is common between the microperthite crystals.

3. *Geochemistry*

The alkali-granite pluton is exposed extensively at the head of Fleming Glacier. Its high alkali-feldspar content and the presence of riebeckite and aegerine indicate its alkaline affinities and this is verified by its low alumina content, high alkalis and the occurrence of acmite and sodium silicate in the norm. Although the granite plots close to some of the adamellites in the Q–Ab–Or diagram (Fig. 30), implying a magmatic origin, it differs substantially from the adamellites in its chemistry. The most striking differences are the lower alumina, the higher manganese and higher zirconium of the granite, but yttrium, gallium, niobium and lead are significantly higher in the granite and it is depleted in strontium and barium, features which are typical of alkali-granites (Bowden and Turner, 1974, p. 337; Gerasimovsky, 1974, p. 402). The significant differences between the granite and adamellite suggest that they are not genetically related.

Although alkali-granites are relatively rare in the Antarctic Peninsula, they have been recorded at a few localities. Marsh (1968, p. 180) described an alkali-granite containing ferrohastingsite from the Foyn Coast; this he suggested had formed by fractionation from alkali-gabbro which is present in the area. Goldring (1962) also described an alkali-granite containing aegerine-augite and riebeckite which was thought to have formed by the differentiation of a granodiorite magma. Intrusions of alkali-granite have also been recorded from the Fallières Coast (personal communication from R. B. Wyeth).

The lack of intermediate and basic rocks having alkaline affinities makes it unlikely that the granite has formed by fractional crystallization. Two theories have been put forward to explain the alkali-granites of Nigeria. Bailey and Schairer (1966) suggested that a peralkaline magma was generated within a basic lower crust or upper mantle and was contaminated during its ascent to yield the metaluminous and peraluminous rocks. Bowden (1970), however, suggested that the peralkaline magma formed in the upper crust from Precambrian basement rocks of "charnockitic" composition which on further progressive melting and cooling yielded metaluminous and peraluminous rocks. Brown and Bowden (1973) have shown experimentally that the metaluminous and peraluminous rocks can be formed by partial melting of such a crust and they suggested that, if volatile alkali-rich vapours from the lower crust or upper mantle initiated the partial melting, peralkaline liquids could be generated at low temperatures from a non-peralkaline charnockitic monzonite source.

Charnockitic rocks have not been recorded from the metamorphic complex of the Antarctic Peninsula and therefore the former theory is more applicable to northern Palmer Land. In addition, Bailey (1974, p. 441), in his investigations on anatectic alkaline magmas, concluded that alkaline felsic magmas are generated on a large scale by partial melting in the deeper crust, a release of pressure at depth leading to an influx of volatiles and mobile elements from the underlying mantle and giving the magma its alkaline character.

As alkaline rocks are found mainly in tectonically stable regions of the crust (Sørensen, 1974, p. 145), it is likely that this granite is the youngest plutonic rock in northern Palmer Land.

X. HYPABYSSAL ROCKS

ACID, intermediate and basic dykes are commonly observed in all the rock units. However, as the stratigraphy of the main rock units is uncertain, it is especially difficult to resolve the position of the various suites of dykes. Schistose dykes, intruding rocks of the metamorphic complex and described with the latter, occur alongside undeformed dykes at station E.3291. At station KG.1200, basic dykes are cut by apophyses from the Andean plutonic rocks and therefore some of the basic dykes are younger than the volcanic rocks but older than the Andean plutonic rocks.

Despite the above field evidence, no general criteria for distinguishing dykes of different ages have been recognized.

A. PETROGRAPHY

1. *Microgabbros*

Microgabbro dykes cut the pre-volcanic adamellite at Mount Charity and the Upper Jurassic volcanic rocks at stations KG.1200 and 1216; at station KG.1200, some of the basic dykes which intrude the volcanic rocks are cut by apophyses from the nearby Andean pluton. The microgabbros are porphyritic with large plagioclase laths (up to 1 cm long) which may be normally zoned (An_{69-34}) and altered to sericite or larger flakes of muscovite (Fig. 32). Colourless clinopyroxene ($\gamma{:}c = 41°$; large $2V\gamma$) forms a few large phenocrysts but it is usually found as smaller interstitial grains; it has been altered to one or more of the following: hornblende, tremolite-actinolite, chlorite or calcite. The matrices of these rocks are mostly of plagioclase microlites, associated with pyroxene, chlorite, calcite, ilmenite (altered to leucoxene) and sphene.

2. *Microdiorites*

Microdiorite dykes intrude acid gneisses at station E.3291, pre-volcanic adamellite at station E.3624, and the Mount Charity sedimentary rocks. In specimens E.3250.1 and 3624.4 the laths of andesine, which are sometimes normally zoned (An_{42-29}), are altered to sericite, chlorite and biotite. Small remnants of original clinopyroxene are in evidence amongst their alteration products, mainly tremolite-actinolite and pale green chlorite. Clots and streaks of brown biotite forming a decussate texture are present in specimen E.3250.1, indicating that contact metamorphism by later intrusions has been effective.

Specimen E.3291.1 is a porphyritic rock containing euhedral or subhedral prisms of hornblende and clinopyroxene ($\gamma{:}c = 46°$) in an altered microlitic and iron ore-rich groundmass. Specimen E.3623.1 is from an altered microdiorite containing quartz-filled vesicles which intrudes the Mount Charity sedimentary rocks and is probably a feeder for the overlying volcanic rocks.

3. *Hornblende-microdiorite*

This rock is almost wholly formed of euhedral or subhedral prisms of hornblende which is pleochroic from pale brown to green. Quartz, feldspar, iron ore, chlorite, epidote and calcite are the interstitial minerals; the last forms poikilitic crystals around the hornblende.

4. *Altered basic and intermediate dykes*

Most of these dykes (KG.1201.8, 1202.2, 1208.3, 1213.6 and 1216.4) intrude volcanic rocks but specimen KG.1219.1 is from a dyke intruding metamorphic rocks in the Mica Islands, and specimen KG.1220.3 is from a dyke intruding porphyritic granodiorite at Brindle Cliffs. All these altered rocks occur in the Mount Edgell area where most of the Upper Jurassic volcanic rocks are situated. Both porphyritic and equigranular rocks are represented and all are characterized by plagioclase which has been extremely altered to albite, sericite, epidote, chlorite or iron ore. Their matrices comprise similar minerals and quartz. Specimen KG.1213.6 has individual phenocrysts and glomeroporphyritic aggregates of pale green pleochroic tremolite-actinolite as well as plagioclase; the former are probably pseudomorphs after pyroxene.

5. *Microgranodiorites*

These are porphyritic rocks which intrude the gabbros, the diorite, the porphyritic granodiorite (E.4239) and volcanic tuffs (E.3243). The commonest phenocrysts are of acid plagioclase, which has been intensely altered to calcite, sericite or epidote. Embayed quartz, hornblende (partially altered to chlorite) and pseudomorphs of chlorite and iron ore replacing biotite are the other phenocrystic phases present. The groundmass of these dykes is composed mainly of fine-grained quartz and feldspar.

6. *Micro-adamellites*

The micro-adamellites are more equigranular and coarser-grained than the other acid dykes and their textures resemble more closely those of the plutonic rocks which they intrude. At stations KG.1206, 1222 and E.3241 they intrude tonalites but at station E.3278.1 a micro-adamellite dyke intrudes granodiorite. Microscopically, they consist of laths of acid plagioclase (albite-

FIGURE 32
Muscovite flakes in optical continuity replacing fractured plagioclase in a microgabbro dyke. (E.3618.3; X-nicols; × 140)

oligoclase), up to 4 mm in length, normally zoned and altered to sericite, calcite or epidote, and interstitial cloudy potash feldspar and quartz; the latter form graphic intergrowths in specimen KG.1222.1. Mafic phases include brown biotite, extensively altered to chlorite, and green hornblende crystals. Secondary clots of brown biotite similar to those described in microdiorite specimen E.3250.1, occur in specimen KG.1222.1.

The granulated quartz with an undulose extinction and the microcline of the groundmass of specimen E.3278.1 suggest that it was forcibly intruded into the undeformed host granodiorite.

7. *Microgranites*

Microgranite dykes intrude the Upper Jurassic volcanic rocks at stations E.3244 and 3248. Specimen E.3248.6 is a quartz-microperthite-plagioclase-porphyry, the phenocrysts of which are set in a devitrified flow-banded matrix. The plagioclase phenocrysts are albite-oligoclase and these are rare in comparison with the patch microperthite and embayed quartz. Specimen E.3244.3 is a more altered microperthite-plagioclase-porphyry which does not contain phenocrystic quartz.

B. GEOCHEMISTRY

As only a limited number of greenschist dykes, metavolcanic rocks and Upper Jurassic lavas have been analysed, their geochemistry will be discussed here.

Whilst most of the hypabyssal rocks (Table XI) plot in the same field as the plutonic rocks on the (Fe″+Fe‴)–Alk–Mg diagram (Fig. 33), many of the basic dykes are more iron- or magnesium-rich, the former type being mainly the greenschist dykes and the metavolcanic rocks. The unmetamorphosed dykes, therefore, show a weak iron-enrichment trend. On the (Fe″+Fe‴)–Alk–Mg diagram (Fig. 33) there is a gap between the acid rocks and the basic and intermediate types, and this bimodal distribution is emphasized on the plot of magnesium against nickel (Fig. 34), implying that the two groups are not genetically related. The two acid Upper Jurassic volcanic rocks

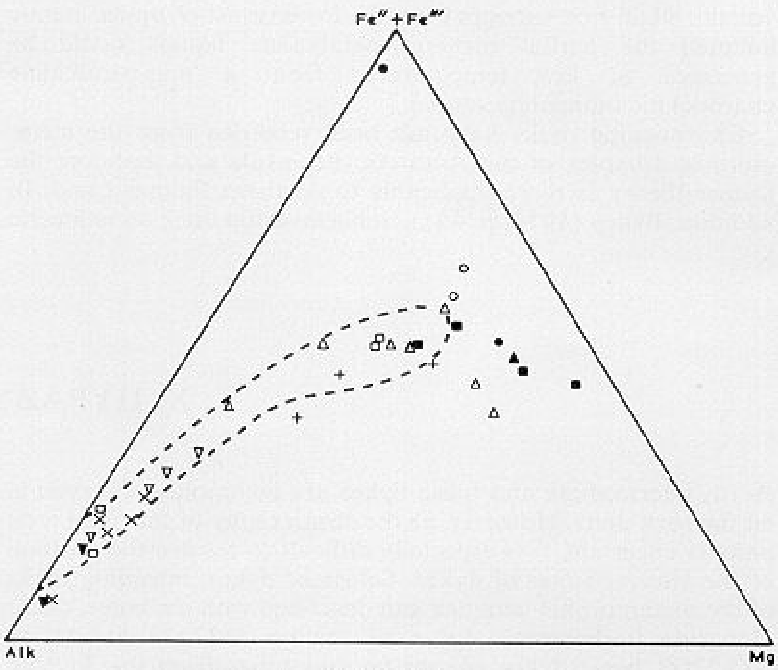

FIGURE 33
Triangular variation diagram plotted on the coordinates (Fe″+Fe‴)–Alk–Mg for hypabyssal rocks, Upper Jurassic lavas, greenschist dykes and metavolcanic rocks. The dashed line delineates the main concentration of plutonic rocks.

■ Microgabbro.
\+ Microdiorite.
▲ Hornblende-microdiorite.
△ Altered basic and intermediate hypabyssal rocks.
▽ Microgranodiorites.
X Micro-adamellites.
▼ Microgranites.
□ Upper Jurassic lavas.
● Metavolcanic rocks.
○ Greenschist dykes.

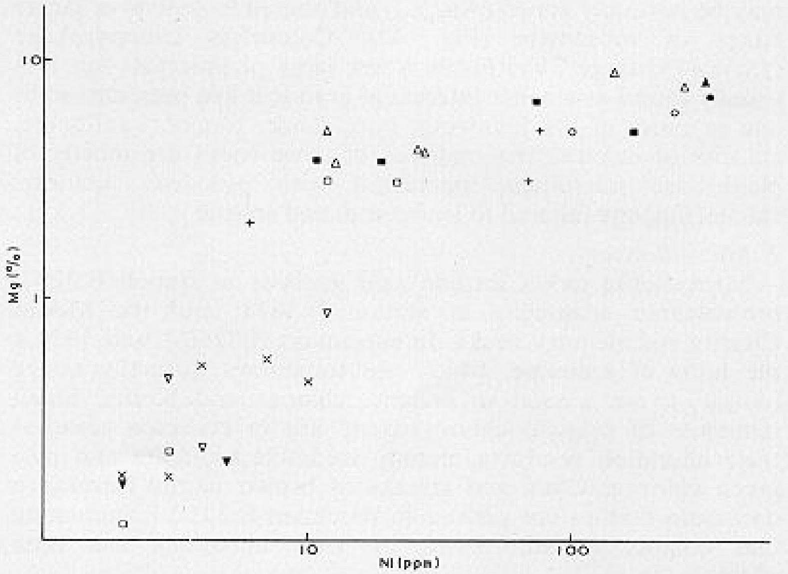

FIGURE 34
Mg–Ni variation diagram for hypabyssal rocks, Upper Jurassic lavas, greenschist dykes and metavolcanic rocks with over 1 ppm nickel.
The symbols are the same as in Fig. 33.

Table XI

CHEMICAL ANALYSES OF HYPABYSSAL ROCKS FROM NORTHERN PALMER LAND

	1	2	3	4	5	6	7	8	9	10	11	12	13	14	15	16	17	18	19	20	21	22	23	24	25	26
SiO_2	44.08	45.11	49.41	53.54	52.11	55.10	55.95	49.37	46.70	50.48	51.37	52.05	54.33	55.17	56.95	62.83	66.01	66.81	71.92	64.41	70.11	70.47	70.90	74.90	73.13	75.43
TiO_2	0.26	0.28	0.61	0.77	1.09	0.81	1.44	0.84	0.90	1.23	1.31	0.75	1.16	0.52	0.61	0.53	0.36	0.43	0.24	0.50	0.34	0.14	0.36	0.15	0.28	0.12
Al_2O_3	19.63	17.23	19.17	16.40	14.91	13.66	11.72	9.60	13.66	14.31	16.46	12.78	14.54	17.73	22.02	18.59	16.23	17.25	13.91	18.30	15.22	16.90	15.68	14.48	13.88	13.57
Fe_2O_3	3.24	3.87	4.69	3.69	4.82	3.69	4.85	5.42	5.66	4.20	4.25	4.51	3.01	3.25	1.93	2.50	1.89	0.96	0.20	1.43	1.23	0.61	1.64	0.26	1.36	0.45
FeO	3.62	5.67	3.11	4.46	4.38	4.00	4.90	6.14	6.41	7.58	5.02	4.13	6.94	4.54	3.09	1.38	1.88	1.91	1.64	1.01	1.02	1.53	1.07	0.23	0.40	0.26
MnO	0.10	0.19	0.13	0.16	0.20	0.18	0.19	0.24	0.28	0.24	0.30	0.23	0.16	0.21	0.21	0.18	0.08	0.16	0.05	0.04	0.07	0.02	0.04	0.01	0.07	0.11
MgO	10.29	11.96	5.86	5.91	8.15	4.21	3.15	13.10	14.05	8.01	6.66	12.45	6.71	3.32	1.52	1.25	1.43	0.75	0.40	0.75	0.87	0.30	0.92	0.30	0.35	0.28
CaO	10.66	10.15	9.73	7.86	7.79	6.52	6.07	11.12	4.40	6.26	7.37	7.70	4.93	5.09	5.63	2.86	3.23	2.57	1.60	2.50	2.28	2.18	2.53	1.23	0.76	0.61
Na_2O	0.67	0.85	2.03	2.58	2.42	3.65	2.95	1.97	1.61	2.66	3.17	2.74	3.71	4.56	3.33	5.72	4.18	3.30	3.74	4.63	3.72	5.15	3.98	4.14	5.22	1.93
K_2O	0.11	1.34	0.28	1.04	1.85	2.30	2.51	0.65	3.19	0.82	1.20	1.17	1.42	0.90	3.05	3.05	2.76	4.58	4.81	5.55	4.24	3.09	3.71	4.08	3.70	7.29
P_2O_5	0.03	0.03	0.20	0.18	0.33	0.19	0.30	0.22	0.13	0.24	0.34	0.18	0.25	0.42	0.20	0.27	0.12	0.11	0.03	0.09	0.06	0.04	0.06	0.03	0.05	0.01
H_2O+	2.24	2.32	1.05	1.53	0.51	0.96	1.11	1.08	2.10	1.72	0.96	1.96	0.71	1.29	0.98	0.51	1.21	0.50	0.15	0.21	0.07	0.16	0.21	0.12	0.08	0.15
H_2O-	0.44	0.40	0.38	0.46	0.56	0.28	0.24	0.22	0.22	0.60	0.36	0.48	0.30	0.60	0.28	0.28	0.14	0.48	0.40	0.30	0.26	0.16	0.14	0.28	0.32	0.22
Total	95.37	99.40	96.65	98.58	99.12	96.08	95.38	99.97	99.31	98.36	98.77	101.13	98.17	97.60	99.80	99.94	99.52	99.81	100.54	99.70	99.98	100.75	101.24	98.22	99.55	100.54
													Element percentages less total water													
Si^{4+}	22.23	21.81	24.26	25.91	24.85	27.16	29.28	23.39	22.51	24.58	24.65	24.66	26.14	26.95	27.02	29.62	31.43	31.60	34.12	30.35	33.08	32.80	32.85	35.08	34.46	35.24
Ti^{4+}	0.17	0.17	0.38	0.48	0.67	0.51	0.97	0.51	0.56	0.77	0.81	0.46	0.72	0.33	0.37	0.32	0.22	0.26	0.15	0.30	0.21	0.08	0.21	0.09	0.17	0.07
Al^{3+}	11.21	9.43	10.65	8.99	8.05	7.62	6.94	5.15	7.45	7.89	8.94	6.85	7.92	9.80	11.83	9.92	8.75	9.24	7.47	9.76	8.13	8.91	8.22	7.68	7.40	7.18
Fe^{3+}	2.44	2.80	3.44	2.67	3.44	2.72	3.80	3.84	4.08	3.06	3.05	3.20	2.17	2.37	1.37	1.76	1.35	0.68	0.14	1.01	0.87	0.42	1.14	0.18	0.96	0.31
Fe^{2+}	3.04	4.56	2.54	3.59	3.47	3.28	0.17	4.84	5.14	6.14	4.00	3.25	5.55	3.69	2.44	1.08	1.49	1.50	1.29	0.79	0.80	1.18	0.82	0.18	0.31	0.20
Mn^{2+}	0.08	0.15	0.11	0.13	0.16	0.15	0.16	0.19	0.22	0.19	0.24	0.18	0.13	0.17	0.17	0.14	0.06	0.13	0.04	0.03	0.05	0.02	0.03	0.01	0.05	0.09
Mg^{2+}	6.70	7.46	3.71	3.69	5.01	3.01	3.13	8.01	8.74	5.03	4.12	7.61	4.17	2.09	0.93	0.76	0.88	0.46	0.24	0.46	0.53	0.18	0.55	0.18	0.21	0.17
Ca^{2+}	8.22	7.50	7.30	5.82	5.68	4.91	4.86	8.05	3.24	4.66	5.41	5.58	3.63	3.80	4.08	2.06	2.35	1.86	1.16	1.80	1.59	1.55	1.79	0.88	0.55	0.44
Na^{+}	0.54	0.65	1.58	1.98	1.83	2.86	2.45	1.48	1.23	2.06	2.41	2.06	2.83	3.53	2.51	4.28	3.16	2.48	2.82	3.46	2.79	3.80	2.93	3.08	3.90	1.43
K^{+}	0.10	1.15	0.24	0.89	1.57	2.01	2.33	0.55	2.73	0.71	1.02	0.98	1.21	0.78	2.57	2.55	2.33	3.85	4.05	4.64	3.55	2.55	3.05	3.39	3.10	6.05
P^{5+}	0.01	0.01	0.09	0.08	0.15	0.09	0.15	0.10	0.06	0.11	0.15	0.08	0.11	0.19	0.09	0.12	0.05	0.05	0.01	0.04	0.03	0.02	0.03	0.01	0.02	–
O^{2-}	45.26	44.29	45.68	45.77	45.14	45.67	46.76	43.89	44.04	44.82	45.20	45.10	45.43	46.29	46.63	47.38	47.92	47.90	48.50	47.35	48.38	48.48	48.37	49.24	48.85	48.82
Position (1/3 Si+K) −(Ca+Mg)	−6.88	−6.34	−2.57	+0.01	−0.84	+2.96	+4.55	−7.63	−1.71	−0.77	−0.30	−3.94	+2.06	+3.69	+6.45	+9.51	+9.39	+11.91	+13.80	+12.39	+12.33	+11.79	+11.75	+13.98	+13.70	+17.18
													C.I.P.W. norms													
Q	0.51	–	8.32	9.42	4.46	7.00	17.75	–	–	4.32	3.26	–	4.48	8.38	10.59	10.48	21.92	22.80	27.12	9.86	26.31	22.40	26.51	32.16	26.69	34.40
C	–	–	–	–	–	–	–	–	–	–	–	–	–	0.93	3.44	1.15	0.62	2.36	–	0.21	0.58	1.04	0.57	1.02	–	1.35
Z	–	–	0.02	0.03	0.03	0.03	0.05	0.02	–	0.02	0.04	–	0.03	0.03	0.03	0.07	0.02	0.05	0.04	0.11	0.04	0.02	0.04	0.02	0.06	0.02
or	0.70	8.18	1.74	6.36	11.14	14.36	16.62	3.88	19.44	5.04	7.27	6.99	8.63	5.55	18.27	18.18	16.63	27.40	28.86	33.06	25.33	18.16	21.76	24.14	22.05	43.10
ab	6.11	7.43	18.02	22.58	20.86	32.51	27.91	16.85	14.03	23.42	27.49	23.44	32.28	40.27	28.57	48.72	35.98	28.22	32.09	39.42	31.74	43.34	33.35	35.07	44.48	16.31
an	54.17	40.55	44.44	31.13	24.81	14.82	12.65	15.60	21.22	25.69	27.81	19.33	19.36	23.83	27.25	13.00	15.95	12.46	7.04	12.25	10.80	10.95	12.24	6.11	3.52	3.11
di	2.24	9.09	4.11	6.63	10.07	14.61	11.85	30.82	0.45	4.20	6.19	14.46	3.47	–	–	–	–	–	0.89	–	–	–	–	–	0.12	–
hy	30.60	14.40	14.51	16.37	18.62	8.91	3.28	18.23	14.87	27.95	18.26	25.94	24.37	14.04	7.35	3.13	5.09	4.21	3.13	1.88	2.61	2.84	2.36	0.75	0.82	0.81
ol	–	13.87	–	–	–	–	–	4.29	19.38	–	–	1.21	–	–	–	–	–	–	–	–	–	–	–	–	–	–
mt	5.07	5.80	7.13	5.53	7.12	5.63	–	7.94	8.45	6.34	6.32	6.61	4.49	4.92	2.84	3.52	2.79	1.41	0.29	1.95	1.80	0.88	2.36	0.34	0.71	0.65
cm	–	0.04	–	–	–	0.05	–	0.23	0.08	–	–	0.11	0.02	–	–	–	–	–	–	–	–	–	–	–	–	–
il	0.53	0.55	1.22	1.51	2.11	1.62	0.90	1.61	1.76	2.43	2.55	1.44	2.27	1.03	1.17	1.01	0.70	0.83	0.46	0.96	0.65	0.26	0.68	0.29	0.54	0.23
hm	–	–	–	–	–	–	5.42	–	–	–	–	–	–	–	–	0.09	–	–	–	1.10	–	–	–	0.03	0.88	–
tn	–	–	–	–	–	–	2.78	–	–	–	–	–	–	–	–	–	–	–	–	–	–	–	–	–	–	–
ap	0.08	0.07	0.50	0.44	0.80	0.47	0.79	0.53	0.32	0.59	0.82	0.43	0.61	1.04	0.48	0.64	0.29	0.26	0.07	0.21	0.14	0.09	0.14	0.07	0.12	0.02
													Trace elements (ppm)													
Cr	10	184	8	22	40	195	31	991	352	47	15	473	94	–	–	–	20	5	3	1	5	3	5	3	2	–
Ni	72	172	11	19	77	70	5	318	147	12	27	286	18	1	1	–	12	3	4	10	8	3	7	2	5	2
Ga	16	18	25	23	24	24	24	19	21	21	18	22	21	21	22	22	23	16	16	21	15	23	15	10	18	13
Rb	5	82	7	22	72	152	93	7	103	21	29	29	49	18	68	98	108	141	130	165	183	81	145	91	106	228
Sr	541	285	965	630	876	648	463	497	282	471	809	667	318	519	344	658	697	348	157	433	223	665	201	175	83	203
Y	5	4	12	19	16	15	35	13	5	13	26	13	17	19	28	20	9	9	6	13	20	3	23	7	24	13
Zr	20	12	73	125	142	115	216	76	59	90	166	91	134	129	170	328	100	228	181	535	172	88	184	108	301	95
Nb	1	2	4	5	8	9	11	3	4	2	7	4	5	2	6	15	7	9	10	17	3	6	6	6	16	15
Ba	67	237	432	503	553	726	733	191	464	253	581	327	271	748	703	1 292	1 052	889	842	1 084	535	1 215	649	664	960	408
La	8	8	19	22	34	20	35	27	11	15	29	15	22	29	34	56	20	38	36	25	59	13	28	17	45	33
Ce	8	8	34	36	54	46	64	30	12	22	47	28	43	53	35	87	32	52	52	38	47	22	41	30	69	58
Pb	10	10	9	37	44	28	35	20	25	55	104	10	10	24	15	30	34	58	21	15	34	45	21	27	19	102
Th	–	–	2	6	5	4	3	8	1	–	2	2	1	3	–	15	11	15	22	24	37	4	23	15	11	34
													Element ratios													
K/Rb	200	140	343	405	218	132	251	786	265	338	352	338	247	433	378	260	216	273	312	281	194	315	377	373	292	265
Ba/Rb	13.4	2.9	61.7	22.9	7.7	4.8	7.9	27.3	4.5	12.0	20.0	11.3	5.5	41.6	10.3	13.2	9.7	6.3	6.5	6.6	2.9	15.0	4.5	7.3	9.1	1.8
													Coordinates of triangular diagrams													
Fe	42.8	44.3	51.9	48.8	45.1	43.2	36.4	46.4	42.1	54.1	48.3	37.7	48.5	48.6	38.8	27.3	30.8	24.3	16.8	17.4	19.5	19.7	23.1	5.2	15.0	6.3
Alk	5.0	10.8	15.8	22.4	22.2	35.1	44.0	10.8	18.1	16.3	23.5	17.8	25.4	34.6	51.7	65.5	59.7	70.6	80.3	78.2	74.2	78.0	70.4	92.3	82.5	91.6
Mg	52.3	44.9	32.2	28.8	32.7	21.7	19.6	42.8	39.9	29.6	28.2	44.5	26.1	16.8	9.5	7.3	9.5	5.1	2.9	4.4	6.2	2.2	6.5	2.6	2.5	2.1
Q†	*	*	*	*	*	*	*	*	*	*	*	*	*	*	*	*	*	*	31.0	12.9	31.7	26.5	32.5	33.4	27.2	35.3
Ab	*	*	*	*	*	*	*	*	*	*	*	*	*	*	*	*	*	*	29.7	36.9	27.4	18.8	23.7	25.6	22.6	45.8
Or	*	*	*	*	*	*	*	*	*	*	*	*	*	*	*	*	*	*	39.3	50.2	40.9	54.6	43.8	40.9	50.3	18.8

* Not determined.
† Calculated from mesonorms.

1. KG.1216.2 Microgabbro; west of Mount Edgell.
2. E.3618.3 Microgabbro; north-eastern side of Mount Charity.
3. KG.1200.3 Microgabbro; south of Mount Edgell.
4. KG.1216.6 Microgabbro; west of Mount Edgell.
5. E.3250.1 Microdiorite; head of Fleming Glacier.
6. E.3291.5 Microdiorite; south-west of Mount Sullivan.
7. E.3624.4 Microdiorite; south-western side of Mount Charity.
8. E.3280.1 Hornblende-microdiorite; west of Engel Peaks.
9. KG.1201.8 Altered basic dyke; mainland east of the Rhyolite Islands.
10. KG.1202.2 Altered basic dyke; Rhyolite Islands.
11. KG.1220.3 Altered basic dyke; Brindle Cliffs.
12. KG.1213.6 Altered intermediate dyke; south of the Relay Hills.
13. KG.1219.1 Altered intermediate dyke; Mica Islands.
14. KG.1208.3 Altered intermediate dyke; south-west of Mount Edgell.
15. KG.1216.4 Altered intermediate dyke; west of Mount Edgell.
16. E.3243.3 Microgranodiorite; Garcie Peaks.
17. E.3293.4 Microgranodiorite; north side of Mount Sullivan.
18. E.4239.3 Microgranodiorite; south-east of Garcie Peaks.
19. E.4238.2 Microgranodiorite; head of Fleming Glacier.
20. E.3241.2 Micro-adamellite; south of the Relay Hills.
21. KG.1206.6 Micro-adamellite; south-western side of Mount Edgell.
22. E.3278.1 Micro-adamellite; west of Engel Peaks.
23. KG.1222.1 Micro-adamellite; Mount Guernsey.
24. KG.1201.2 Micro-adamellite; mainland east of the Rhyolite Islands.
25. E.3244.3 Microgranite; Mount Leo.
26. E.3248.6 Microgranite; head of Fleming Glacier.

plot with the acid hypabyssal rocks, while the basalts are in the basic group.

The lack of stratigraphical guidelines in the Antarctic Peninsula, including the absence of radiometric dates, makes an analysis of the dykes difficult. The basic and intermediate dykes intrude all the other rock units but they seem to be most numerous in the Upper Jurassic volcanic rocks. On the other hand, the acid dykes seem to intrude mainly the plutonic rocks and the Upper Jurassic volcanic rocks, implying a genetic relationship with the acid plutonic rocks. These observations may, however, be affected by a bias in sampling. The basic and intermediate dykes commonly cut the acid plutonic rocks, suggesting that they are not related to the older basic plutonic rocks, but none of the dyke types is restricted to intruding only one rock unit, e.g. microdiorites intrude metamorphic rocks, a pre-volcanic pluton and the granite, which is probably the youngest plutonic rock.

The iron enrichment shown by the unmetamorphosed basic and intermediate dykes could be accounted for by differentiation and such a scatter of points at the basic end of a calc-alkaline trend could be attributed to cumulation (Nockolds and Allen, 1953; Adie, 1955). The hornblende-microdiorite is probably a cumulate but the other rocks do not have cumulative textures. The variation diagram of potassium plotted against rubidium (Fig. 35) does not show the rubidium enrichment, and the plots of the K/Rb and Ba/Rb ratios against the modified Larsen factor (Fig. 36) do not show the gradual decrease which would be expected if fractional crystallization was the main process in the formation of these rocks. In addition, there is a considerable scatter on plots of aluminium, iron, magnesium, manganese and titanium against the modified Larsen factor, and this suggests that the basic and intermediate dykes belong to several episodes of intrusion which are not linked by differentiation, although differentiation may have influenced the composition of the individual phases.

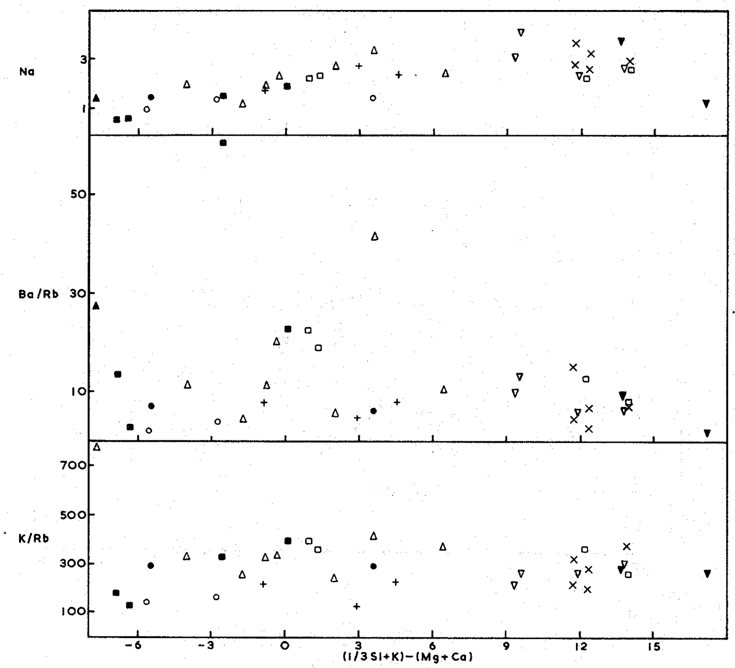

FIGURE 36
Variation diagrams for the hypabyssal rocks, Upper Jurassic lavas, greenschist dykes and metavolcanic rocks, showing Na, K/Rb and Ba/Rb plotted against ($\frac{1}{3}$ Si+K)–(Ca+Mg).
The symbols are the same as in Fig. 33.

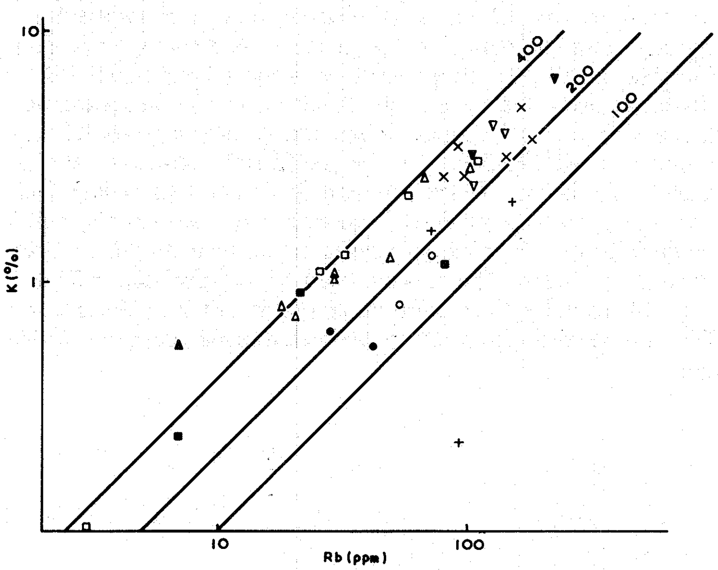

FIGURE 35
K–Rb variation diagram for hypabyssal rocks, Upper Jurassic lavas, greenschist dykes and metavolcanic rocks. The lines show K/Rb ratios of 100, 200 and 400.
The symbols are the same as in Fig. 33.

The altered nature of many of the basic and intermediate dykes, and the metamorphism which has affected the greenschist dykes and metavolcanic rocks, makes a comparison of the various rock types difficult. However, Pearce and Cann (1973) and Pearce (1975) have suggested that elements such as titanium, zirconium and yttrium, which are least susceptible to movement during alteration and metamorphism, can be used to detect the original tectonic setting of basic rocks. In accordance with Pearce and Cann's (1973) scheme, the basic hypabyssal and volcanic rocks and one gabbro (E.3293.1) have been plotted, first on a Ti/100–Zr–Y×3 discrimination diagram (Fig. 37a) and, secondly, on a Ti–Zr diagram (Fig. 37b). Bearing in mind the limited number of analyses and possible ambiguities due to the method, the Upper Jurassic volcanic rocks and two of the microgabbros are calc-alkaline, whereas the greenschist dykes, the gabbro (E.3293.1) and metavolcanic rocks are most like ocean-floor basalts, although one of the dykes and one of the lavas overlap the field of low-potassium tholeiites on the Ti–Zr diagram, and one of the altered basic dykes is calc-alkaline while the others are "within-plate" types. It is apparent from this study that there was a significant change in the type of magmatism between the emplacement of the metavolcanic rocks, the gabbro (E.3293.1) and the greenschist dykes, and the formation of the calc-alkaline lavas and dykes which are so common on the western side of Palmer Land.

In the acid hypabyssal rocks, the Ba/Rb ratio decreases slightly with increasing modified Larsen factor, despite a scatter of points, but the K/Rb ratio remains relatively constant (Fig. 36) and there is no rubidium enrichment relative to potassium (Fig. 35), as would be expected if the dykes were formed by differentiation. Therefore, it is probable that the acid dykes are associated with the various phases of acid plutonic activity.

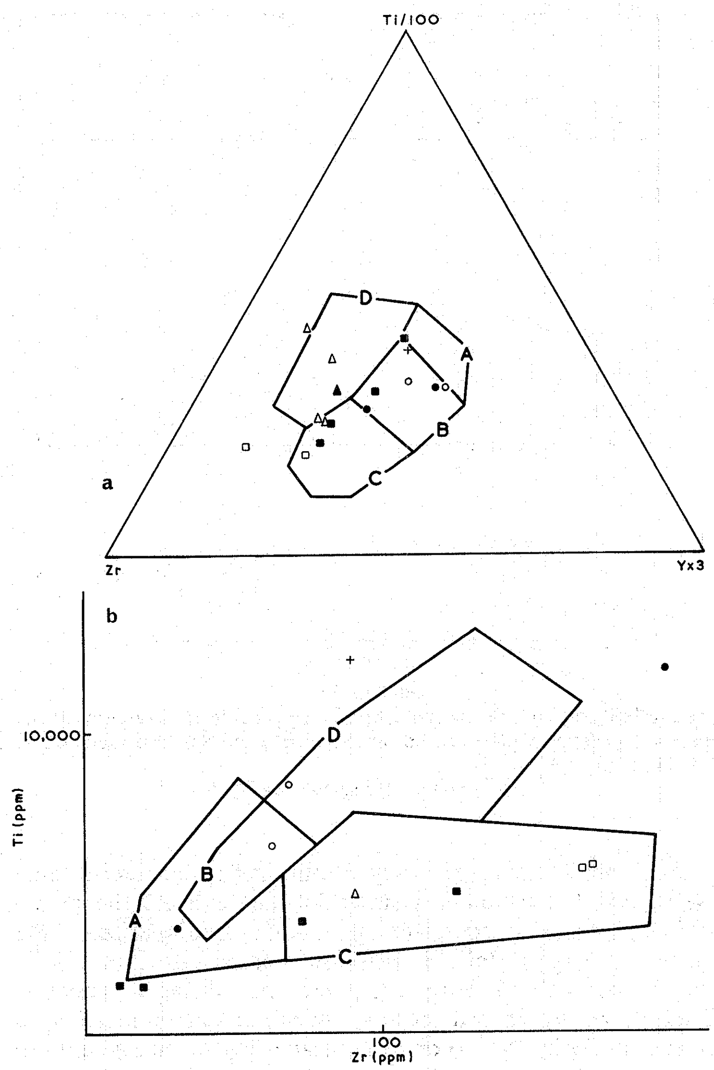

FIGURE 37

The tectonic setting of the basic igneous rocks from northern Palmer Land using the discrimination analysis method of Pearce and Cann (1973).

All the analyses have been plotted in Fig. 37a and those falling in fields A, B and C have been re-plotted in Fig. 37b. In Fig. 37a the following fields are represented: ocean-island or continental basalts (D), ocean-floor basalts (B), low-potassium tholeiites (A and B) and calc-alkali basalts (C and B); in Fig. 37b ocean-floor basalts plot in fields D and B, low-potassium tholeiites in fields A and B, and calc-alkali basalts in fields C and B.

Coordinates of triangular diagrams and symbols

		Ti/100	Zr	Y×3
■ Microgabbros	E.3618.3	15.5	19.1	65.5
	KG.1216.2	22.9	51.4	25.7
	KG.1216.6	17.9	54.8	27.4
	KG.1200.3	20.4	56.4	23.2
▲ Hornblende-microdiorite	E.3280.1	23.8	42.5	33.6
△ Altered basic dykes	KG.1201.8	25.9	31.6	42.5
	KG.1202.2	32.5	44.4	23.1
	KG.1220.3	21.7	51.5	26.8
	KG.1213.6	21.2	51.2	27.6
□ Upper Jurassic lavas	KG.1212.5	16.3	57.3	26.2
	KG.1212.9	18.0	63.4	18.6
● Basic metalavas	E.3268.1	26.1	26.9	47.0
	E.3276.1	25.4	41.2	33.4
○ Greenschist dykes	E.3291.6	26.7	29.3	44.0
	E.3296.1	26.0	25.1	48.9
+ Gabbro	E.3293.1	39.0	29.5	31.4

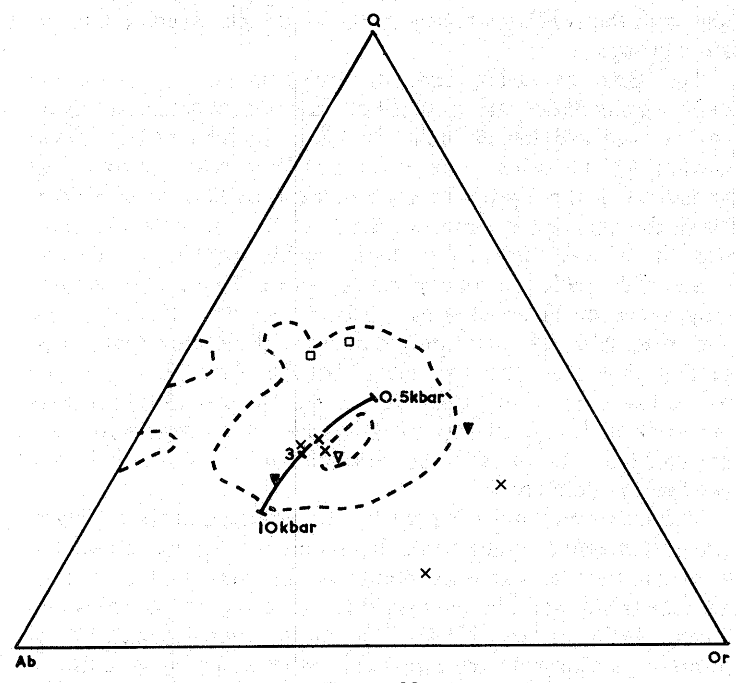

FIGURE 38

A plot of normative quartz, albite and orthoclase for the hypabyssal rocks and Upper Jurassic lavas which contain normative Q+Ab+Or > 80%.

The symbols are the same as in Fig. 33. The inner dashed line encloses 14% and the outer line 86%, of all the granites considered by Winkler (1974, fig. 18-11).

The solid line indicates the trend of the ternary minima and eutectics at water pressures of between 0.5 and 10 kbar (Tuttle and Bowen, 1958; Luth and others, 1964).

On the Q–Ab–Or diagram (Fig. 38) most of the acid dykes with Q+Ab+Or > 80% plot close together in the field of normal granites, one of the microgranites having been formed at considerably higher water pressures, but the other microgranite (E.3248.6) and two micro-adamellites (E.3241.2 and 3278.1) are enriched in orthoclase. This microgranite is a two-feldspar porphyry and it could be the product of differentiation of a tholeiitic magma or the product of fusion (Carmichael, 1963), the latter being the more likely in this case. The micro-adamellites are more equigranular rocks and specimen E.3241.2 was found in close proximity to the potash-rich tonalite of station E.3241. As in the tonalite, the adamellite contains potash feldspar in a corroding relationship to earlier formed crystals, which could indicate a late-stage metasomatism, or it may have been formed by fusion. The textural features of specimen E.3278.1 are obscured by the deformation but it probably formed by fusion of potash-rich rocks in the metamorphic complex of this area.

XI. STRUCTURE

THE scattered nature of the outcrops and the frost-shattered exposures limited the structural information which could be collected in this area. No major folding was observed in the metamorphic complex east of the Eternity Range but the foliation in the augen- and acid gneisses is consistent in its north-north-west to south-south-east trend; this compares with the fold trend in the metamorphic rocks of the Bowman and Wilkins Coasts (Fraser and Grimley, 1972). There is also a broad north–south regional trend in the metamorphic rocks on the western side of the Antarctic Peninsula—in the Mica Islands, on the mainland east of the Rhyolite Islands and farther south (Rowe, 1973; Skinner, 1973).

In the few localities where the bedding is visible in the metamorphic and metasedimentary rocks, it is steeply dipping to the west and the cleavage in these rocks has a relatively consistent north-north-west to south-south-east trend, which is the same as the foliation in the metamorphic rocks. This structural trend differs from that farther north in the Bowman and Wilkins Coasts, where the second generation of folding affecting all the rocks is west-north-west to east-south-east (Fraser and Grimley, 1972).

The Upper Jurassic volcanic rocks are relatively undeformed and no folding was observed. However, in Alexander Island, rocks of a similar age and the overlying Cretaceous sediments have suffered two phases of gentle folding, possibly during the early Tertiary (Bell, 1974*a*), and these events are probably also represented in Palmer Land. This relatively gentle folding in western Palmer Land contrasts markedly with the severe folding in the Upper Jurassic volcanic and sedimentary rocks of the Lassiter Coast, on the eastern side of the Antarctic Peninsula (Williams and others, 1971).

The presence of faults is difficult to prove in the Antarctic Peninsula, because glaciers erode along and cover fault lines, and because of the lack of stratigraphical indicators. The most conspicuous feature probably due to faulting is George VI Sound; this has been considered by some authors to be a rift valley (Adie, 1964; King, 1964; Bell, 1974*a*) but Horne (1967) has suggested that the western side was formed by west-to-east thrusting.

The relationship between the metavolcanic and metasedimentary rocks and the main outcrop of the metamorphic complex was not observed, but the consistent westerly dip of the metavolcanic rocks towards the metamorphic complex suggests that a faulted boundary is present. Such a fault could be responsible for the cataclasis in the metavolcanic and metasedimentary rocks, as in Alexander Island, where Bell (1974*b*) suggested that a major north–south-trending strike-slip fault zone at least 50 km wide caused extreme cataclasis in the (?) Carboniferous rocks.

Extensive block faulting during the Tertiary is thought to have been responsible for the present physiography of the Antarctic Peninsula (Linton, 1964).

XII. CONCLUSIONS AND REGIONAL CORRELATIONS

AN attempt will be made here to summarize and expand on the conclusions and regional correlations given previously.

In the western part of this area the metamorphic complex is represented by relatively small exposures of quartz-mica-feldspar-garnet-gneisses and schists but east of the Eternity Range there is a more extensive north–south-trending belt of metamorphic rocks cropping out between the younger plutonic rocks and the small exposures of the metavolcanic and metasedimentary rocks.

Here, the sequence, from oldest to youngest, appears to be biotite-gneisses, augen-gneisses, amphibolites, acid gneisses, and schists and greenschist dykes. The schists, which were probably originally quartz-plagioclase-porphyries, and the greenschist dykes were probably associated with the period of volcanicity of the metavolcanic and metasedimentary rocks. The Engel Peaks granite crops out some distance east of the main metamorphic complex and this is overlain by the basal breccia beneath the metavolcanic and metasedimentary rocks.

From the petrography and geochemistry of the metamorphic rocks, it is suggested that the biotite-gneisses are *para*gneisses and that the augen-gneisses, acid gneisses (both *ortho*gneisses) and the Engel Peaks granite are the products of partial melting at different water pressures, their potash-rich nature being due to a metasomatic replacement of plagioclase by microcline.

Metasomatism may have occurred during three distinct episodes to allow the growth of potash-feldspar porphyroblasts in the biotite-gneisses, amphibolites and schists. Furthermore, assuming that the schists belong to the same period of volcanicity as the metavolcanic and metasedimentary rocks, some of the acid gneisses may be younger than them. It is suggested that three periods of metamorphism have affected these rocks, the first and highest belonging to the almandine-amphibolite facies.

Although it is impossible to correlate the metamorphic rocks occurring in the various parts of the Antarctic Peninsula, certain similarities and contrasts are significant. The metamorphic rocks mapped in southern Graham Land and Palmer Land are mainly *ortho*gneisses (Hoskins, 1963; Rowe, 1973; Skinner, 1973) and, although metamorphic indicators are rare, there is general agreement that the rocks have been metamorphosed to at least the almandine-amphibolite facies. In addition, Fraser and Grimley (1972) recorded a regional alkali metasomatism in the metamorphic rocks of the Bowman and Wilkins Coasts.

In the northern part of the Antarctic Peninsula, a metamorphic belt comprising mainly *para*schists extends from Elephant Island to Livingston Island (Adie, 1964; Dalziel and Elliot, 1973) and on the eastern side of Graham Land, Stubbs (1968) described a metamorphic complex of *ortho*gneisses and *para*gneisses. Smellie and Clarkson (1975) have suggested that these two areas of metamorphic rocks form a paired metamorphic belt, the western member having suffered high-pressure–low-temperature metamorphism and the eastern one having been formed under high-temperature–low-pressure conditions; the formation of this belt has been ascribed to west-to-east subduction under an island arc or a continental margin, probably before the Jurassic.

The metavolcanic and metasedimentary rocks occur in small scattered exposures bordering the metamorphic complex east of the Eternity Range. The base of the sequence is a breccia overlying the Engel Peaks granite and above this are metabasalts, sheared andesites, dacites, quartz-keratophyres, metasedimentary rocks and greenstones. These rocks have retained their original character but they have been extensively sheared and metamorphosed to the greenschist facies.

On the basis of the evidence given previously, the metavolcanic and metasedimentary rocks have been correlated with the keratophyres of the Wilkins and Bowman Coasts (Fraser and Grimley, 1972) and the Trinity Peninsula Series rather than with the late Jurassic deformed sedimentary and volcanic rocks of the Lassiter Coast.

The Trinity Peninsula Series in the northern part of the Antarctic Peninsula has been well documented (Adie, 1957; Elliot, 1965, 1966) but farther south, where typical exposures are absent, it has been suggested that it is represented by quartzo-feldspathic schists (Elliot, 1966) and biotite-gneisses (Stubbs, 1968). However, in the former case, Grikurov (1971) considered that these rocks belonged to the "Precambrian Complex". In the Bowman and Wilkins Coasts, Fraser and Grimley (1972) explained the higher metamorphic grade in the rocks, comparable in age to that of the Trinity Peninsula Series, to the deeper structural level exposed on the upthrow side of the major fault system in Mobiloil Inlet.

In contrast, the metavolcanic and metasedimentary rocks east of the Eternity Range are distinct in appearance from the metamorphic complex rocks, and the fact that they are petrographically and chemically similar to the greenschist dykes indicates that they are younger than most of the rocks in the metamorphic sequence. The limited geochemical data available for these rocks suggest that the metabasalts and the greenschist dykes, from the metamorphic complex, are not calc-alkaline like the Upper Jurassic lavas but resemble ocean-floor basalts, and this could indicate the presence of an ancient marginal basin.

There is considerably more information available on the Upper Jurassic volcanic rocks compared with the rock groups previously considered. In northern Palmer Land, this unit comprises volcanic breccias and tuffs with subsidiary basalt, rhyolite and dacite lavas, and sedimentary rocks. Although there is no direct evidence of their age in this area, similar rocks on Adelaide Island (Thomson, 1972) and at Carse Point on the eastern side of George VI Sound (Thomson, 1975*a*) contain fossils of an Upper Jurassic age but the period of volcanicity is believed to have spanned a longer time interval than the Upper Jurassic (Taylor and others, 1979).

The geochemistry of the lavas indicates that they are calc-alkaline rocks and that the basalts resemble island-arc types (Jakes and White, 1972). The dacite and andesite lavas analysed were not derived by the differentiation of a basic magma but were formed by fusion of pre-existing rocks or by the mixing of magmas and/or assimilation.

The Upper Jurassic volcanic rocks are associated with marine sediments on Adelaide Island (Thomson, 1972) and at Carse Point (Thomson, 1975*a*) but in northern Palmer Land it is not certain whether the rare sedimentary horizons at the base of, and intercalated with the volcanic rocks, are marine. Clearly, most of the volcanic rocks were extruded subaerially on to an eroded surface of metamorphic and plutonic rocks.

There is some difference of opinion regarding the tectonic setting of the Antarctic Peninsula during the Mesozoic. Katz (1973) believed that the orogenic belts of South America and the Antarctic Peninsula are not related, the latter being an intra-continental feature containing localized partly fault-bounded basins which became filled with molasse-type terrestrial and shallow-water marine sediments. The Fossil Bluff Formation of Alexander Island is thought to have been deposited under such conditions.

On the other hand, Suárez (1976) considered that the Antarctic Peninsula was probably an island arc and he has correlated the tectono-stratigraphic units recognized in Palmer Land and Alexander Island with similar units in South America. These units are: an ensialic arc (Upper Jurassic Volcanic Group), fore-arc or intra-arc marine deposits (Fossil Bluff Formation of Alexander Island), a back-arc marine basin (Crabeater Point sediments and Latady Formation of the Lassiter Coast) and a possible trench assemblage (the deformed (?) Carboniferous sediments of Alexander Island).

The limited geochemical evidence suggests that the latter interpretation is the correct one. However, both theories invoke a subduction zone to account for the Upper Jurassic volcanic rocks but there is insufficient geochemical information available for Palmer Land to test whether the potash content of the volcanic rocks increases across the arc, and so to detect the position and orientation of subduction at that time (Dickinson, 1970). Field work in progress in Alexander Island may confirm the suggestion that the (?) Carboniferous rocks are in fact trench deposits.

In common with Upper Jurassic–Lower Cretaceous sequences in other parts of Palmer Land (Rowe, 1973) and Alexander Island (Elliott, 1974), these volcanic rocks have suffered low-grade regional metamorphism to the prehnite–pumpellyite facies.

Basic plutonic rocks are by far subordinate to the tonalites, granodiorites, adamellites and alkali-granite in northern Palmer Land, and it is suggested, on the basis of the field evidence, petrography and geochemistry, that the main rock types formed independently and were intruded as several discrete phases. The processes of metasomatism, hybridization and differentiation, though probably active in the formation of these rocks, are considered to have played a subsidiary role. It has not been possible to recognize plutonic rocks of different ages on the basis of geochemistry, and the chemical criteria West (1974) used to differentiate between the post- and pre-volcanic plutonic rocks in the Danco Coast are not valid in this area.

It is difficult to be sure of the plutonic history of the Antarctic Peninsula, because very few radiometric dates are available and geochemical information is of a limited extent. Since the Antarctic Peninsula is part of the circum-Pacific orogenic belt, it is reasonable to draw analogies with the Pacific margins of both North and South America. Dickinson (1970) has maintained that in North America the intrusive episodes were broadly contemporaneous throughout large segments of the orogenic belt and that each episode was confined to a rather narrow curvilinear belt, but Lanphere and Reed (1973) did not agree that the time intervals between the intrusive episodes and their duration were as established as this.

The information for South America is also contradictory. Farrar and others (1970) considered that the foci of granitic intrusion have migrated eastward in northern Chile, from the present coastal region in the Lower Jurassic to 120 km inland in the Upper Eocene. Stewart and others (1974), in their study of the batholiths of the Western Cordillera of Peru, found a continuous spectrum of ages from 100 to 10 Ma with no gaps longer than 10 Ma but they have suggested the possibility of a north-eastward migration of magmatic foci across the Coastal Batholith. However, no such migration was recorded by Halpern (1973) in southern Chile.

In North America, mineralogical and compositional changes have been recognized across several batholiths. Moore (1959) drew a quartz-diorite line separating quartz-dioritic rocks in the west from quartz-monzonitic types farther east; this mineralogical variation is mainly due to an eastward increase in potash content (Dickinson, 1970). Furthermore, the compositional variation in the plutonic rocks, like that in the andesitic volcanic rocks, is thought to be related to a palaeoseismic zone, although the exact method of their formation is uncertain (Dickinson, 1970). In addition, it has been suggested by Hamilton (1969) that the Cordillera batholiths of Peru are closely related to the andesitic volcanoes.

Up to the present time the geological work carried out in the Antarctic Peninsula has been systematic and, consequently, to obtain a regional picture and to test such suggestions as the existence of a quartz-diorite line (Williams and others, 1971), the hypothesis that the (?) Palaeozoic plutonic rocks of Marguerite Bay were the roots of the Mesozoic volcanoes (Dalziel and others, 1975) and the nature of subduction in the Mesozoic (Katz, 1973; Suárez, 1976), the quantity of geochemical information will have to be considerably increased and related to a comprehensive radiometric dating survey.

Several types of acid to basic hypabyssal rocks have been recorded but it has not been possible to separate the phases of different ages. Many of the dykes intrude and are associated with the Upper Jurassic volcanic rocks but some of them must be much younger as many of the acid plutons contain basic dykes. It is suggested that the acid dykes were formed independently of the basic types and many are probably apophyses of the numerous acid plutonic rocks.

XIII. ACKNOWLEDGEMENTS

I SHOULD like to thank Professor A. Williams for making available the facilities of the Department of Geological Sciences, University of Birmingham, and Dr R. J. Adie for helpful criticism of the manuscript.

I am grateful to all my colleagues at the British Antarctic Survey scientific station at Stonington Island, especially my field companions R. C. Pashley and J. Woodhouse. R. C. Pashley compiled plane-table maps, and specimens collected by K. D. Holmes, A. C. Skinner and R. B. Wyeth have been used in this report.

I am indebted to Drs D. Millward, J. Tarney and G. L. Hendry, and other members of the Department of Geological Sciences, for advice and help with the chemical methods, and especially to Dr Millward for unstinting assistance with the computer techniques. Thanks are also due to my colleagues in the British Antarctic Survey and the Department of Geological Sciences for much helpful discussion.

XIV. REFERENCES

ADIE, R. J. 1954. The petrology of Graham Land: I. The Basement Complex; early Palaeozoic plutonic and volcanic rocks. *Falkland Islands Dependencies Survey Scientific Reports*, No. 11, 22 pp.

——. 1955. The petrology of Graham Land: II. The Andean Granite–Gabbro Intrusive Suite. *Falkland Islands Dependencies Survey Scientific Reports*, No. 12, 39 pp.

——. 1957. The petrology of Graham Land: III. Metamorphic rocks of the Trinity Peninsula Series. *Falkland Islands Dependencies Survey Scientific Reports*, No. 20, 26 pp.

——. 1964. Geological history. (*In* PRIESTLEY, R. E., ADIE, R. J. *and* G. DE Q. ROBIN, *ed. Antarctic research*. London, Butterworth and Co. (Publishers) Ltd., 118–62.)

——. 1971*a*. Recent advances in the geology of the Antarctic Peninsula. (*In* ADIE, R. J., *ed. Antarctic geology and geophysics*, Oslo, Universitetsforlaget, 121–24.)

——. 1971*b*. Evolution of volcanism in the Antarctic Peninsula. (*In* ADIE, R. J., *ed. Antarctic geology and geophysics*. Oslo, Universitetsforlaget, 137–41.)

BAILEY, D. K. 1974. Melting in the deep crust. (*In* SØRENSEN, H., *ed. The alkaline rocks*. London, New York, Sydney, Toronto, John Wiley and Sons, 436–42.)

——. *and* J. F. SCHAIRER. 1966. The system Na_2O–Al_2O_3–Fe_2O_3–SiO_2 at 1 atmosphere and the petrogenesis of alkaline rocks. *J. Petrology*, **7**, Pt. 1, 114–70.

BARAGAR, W. R. A. 1966. Geochemistry of the Yellowknife volcanic rocks. *Can.. J. Earth Sci.*, **3**, No. 1, 9–30.

BATEMAN, P. C. *and* J. P. EATON. 1967 Sierra Nevada batholith. *Science, N.Y.*, **158**, No. 3807, 1407–17.

BATTEY, M. H. 1955. Alkali metasomatism and the petrology of some keratophyres. *Geol. Mag.*, **92**, No. 2, 104–26.

BELL, C. M. 1973. The geology of southern Alexander Island. *British Antarctic Survey Bulletin*, Nos. 33 and 34, 1–16.

——. 1974*a*. *The geology of parts of Alexander Island*. Ph.D. thesis, University of Birmingham, 125 pp. [Unpublished.]

——. 1974*b*. Geological observations in northern Alexander Island. *British Antarctic Survey Bulletin*, No. 39, 35–44.

BISHOP, D. G. 1972. Progressive metamorphism from prehnite–pumpellyite to greenschist facies in the Dansey Pass area, Otago, New Zealand. *Geol. Soc. Am. Bull.*, **83**, No. 11, 3177–98.

BLACK, R. B. 1945. Geographical operations from East Base, United States Antarctic Service Expedition, 1939–1941. *Proc. Am. phil. Soc.*, **89**, No. 1, 4–12.

BOWDEN, P. 1970. Origin of the younger granites of northern Nigeria. *Contr. Miner. Petrol. (Beitr. Miner. Petrogr.)*, **25**, No. 2, 153–62.

——. *and* D. C. TURNER. 1974. Peralkaline and associated ring-complexes in the Nigeria–Niger Province, West Africa. (*In* SØRENSEN, H., *ed. The alkaline rocks*. London, New York, Sydney, Toronto, John Wiley and Sons, 330–51.)

BOWES, D. R. 1967. The petrochemistry of some Lewisian granitic rocks. *Mineralog. Mag.*, **36**, No. 279, 342–63.

BROWN, G. C. *and* P. BOWDEN. 1973. Experimental studies concerning the genesis of the Nigerian Younger Granites. *Contr. Miner. Petrol. (Beitr. Miner. Petrogr.)*, **40**, No. 2, 131–39.

CARMICHAEL, I. S. E. 1963. The crystallization of feldspar in volcanic acid liquids. *Q. Jl geol. Soc. Lond.*, **119**, Pt. 1, No. 473, 95–131.

——., TURNER, F. J. *and* J. VERHOOGEN. 1974. *Igneous petrology*. New York, etc., McGraw-Hill Book Company.

COOMBS, D. S. 1960. Lower grade mineral facies in New Zealand. *21st Int. geol. Congr., Norden, 1960*, Pt. 13, 339–51.

——. 1971. Present status of the zeolite facies. *Adv. Chem. Ser.*, No. 101, 317–27.

——., HORODYSKI, R. J. *and* R. S. NAYLOR. 1970. Occurrence of prehnite-pumpellyite facies metamorphism in northern Maine. *Am. J. Sci.*, **268**, No. 2, 142–56.

——., ELLIS, A. J., FYFE, W. S. *and* A. M. TAYLOR. 1959. The zeolite facies, with comments on the interpretation of hydrothermal syntheses. *Geochim. cosmochim. Acta*, **17**, Nos. 1/2, 53–107.

CURTIS, R. 1966. The petrology of the Graham Coast, Graham Land. *British Antarctic Survey Scientific Reports*, No. 50, 51 pp.

DALZIEL, I. W. D. *and* D. H. ELLIOT. 1973. The Scotia arc and Antarctic margin. (*In* STEHLI, F. G. *and* A. E. M. NAIRN, *ed. The ocean basins and their margins. I. The South Atlantic*. New York, Plenum Publishing Corporation, 171–246.)

——., DE WIT, M. J. *and* C. R. STERN. 1975. Structural and petrologic studies in the Scotia arc. *Antarct. Jnl U.S.*, **10**, No. 4, 180–82.

DAVIES, T. G. 1975. The physiography of part of northern Palmer Land. *British Antarctic Survey Bulletin*, Nos. 41 and 42, 99–111.

DEWAR, G. J. 1970. The geology of Adelaide Island. *British Antarctic Survey Scientific Reports*, No. 57, 66 pp.

DICKINSON, W. R. 1970. Relations of andesites, granites and derivative sandstones to arc-trench tectonics. *Rev. Geophys.*, **8**, No. 4, 813–60.

ELLIOT, D. H. 1965. Geology of north-west Trinity Peninsula, Graham Land. *British Antarctic Survey Bulletin*, No. 7, 1–24.

——. 1966. Geology of the Nordenskjöld Coast and a comparison with north-west Trinity Peninsula, Graham Land. *British Antarctic Survey Bulletin*, No. 10, 1–43.

ELLIOTT, M. H. 1974. Stratigraphy and sedimentary petrology of the Ablation Point area, Alexander Island. *British Antarctic Survey Bulletin*, No. 39, 87–113.

FARRAR, E., CLARK, A. H., HAYNES, S. J., QUIRT, G. S., CONN, H. *and* M. ZENTILLI. 1970. K-Ar evidence for the post-Paleozoic migration of granitic intrusion foci in the Andes of northern Chile. *Earth planet. Sci. Lett.*, **10**, No. 1, 60–66.

FLEMING, W. L. S. 1938. Geology and glaciology. (*In* FLEMING, W. L. S., STEPHENSON, A., ROBERTS, B. B. *and* G. C. L. BERTRAM. Notes on the scientific work of the British Graham Land Expedition, 1934–37. *Geogrl J.*, **91**, No. 6, 508–12.)

FRASER, A. G. 1965. The petrology of Stonington and Trepassey Islands, Marguerite Bay. *British Antarctic Survey Scientific Reports*, No. 52, 51 pp.

——. *and* P. H. GRIMLEY. 1972. The geology of parts of the Bowman and Wilkins Coasts, Antarctic Peninsula. *British Antarctic Survey Scientific Reports*, No. 67, 59 pp.

GERASIMOVSKY, V. I. 1974. Trace elements in selected groups of alkaline rocks. (*In* SØRENSEN, H., *ed. The alkaline rocks*. London, New York, Sydney, Toronto, John Wiley and Sons, 402–12.)

GIBBS, R. J. 1967. The geochemistry of the Amazon river system. Part I. The factors that control the salinity and composition and concentration of the suspended solids. *Geol. Soc. Am. Bull.*, **78**, No. 10, 1203–32.

GOLDRING, D. C. 1962. The geology of the Loubet Coast, Graham Land. *British Antarctic Survey Scientific Reports*, No. 36, 50 pp.

GREEN, T. H. *and* A. E. RINGWOOD. 1968. Genesis of the calc-alkaline suite. *Contr. Miner. Petrol. (Beitr. Miner. Petrogr.)*, **18**, No. 8, 105–62.

GRIKUROV, G. E. 1971. Tectonics of the Antarctandes. (*In* ADIE, R. J., *ed. Antarctic geology and geophysics*. Oslo, Universitetsforlaget, 163–67.)

——., KRYLOV, A. YA. *and* YU. I. SILIN. 1966. Absolyutnyy vozrast nekotorykh porod iz rayona zaliva Margerit, Antarkticheskiy poluostrov [Absolute age of certain rocks in the Marguerite Bay region of the Antarctic Peninsula]. *Dokl. Akad. Nauk SSSR, Geology*, **171**, No. 6, 1399–401. [English translation: *Dokl. (Proc.) Acad. Sci. U.S.S.R.*, Geological sciences sect., **171**, 127–30.]

HALPERN, M. 1971. Rb-Sr total-rock and mineral ages from the Marguerite Bay area, Kohler Range and Fosdick Mountains. (*In* ADIE, R. J., *ed. Antarctic geology and geophysics*. Oslo, Universitetsforlaget, 197–204.)

——. 1973. Regional geochronology of Chile south of 50° latitude. *Geol. Soc. Am. Bull.*, **84**, No. 7, 2407–22.

HAMILTON, W. 1969. The volcanic central Andes—a modern model for the Cretaceous batholiths and tectonics of western North America. (*In* MCBIRNEY, A. R., *ed.* Proceedings of the andesite conference. *Bull. Ore. St. Dep. Geol. miner. Ind.*, No. 65, 165–84.) [International Upper Mantle Project, Scientific Report 16.]

HARKER, A. 1950. *Metamorphism: a study of the transformations of rock-masses*. 3rd edition. London, Methuen and Co. Ltd.

HASHIMOTO, M. 1966. On the prehnite-pumpellyite metagreywacke facies. *J. geol. Soc. Japan*, **72**, No. 5, 253–65.

HAYAMA, Y. 1959. Some considerations on the color of biotite and its relation to metamorphism. *J. geol. Soc. Japan*, **65**, No. 1, 21–30.

HOOPER, P. R. 1962. The petrology of Anvers Island and adjacent islands. *Falkland Islands Dependencies Survey Scientific Reports*, No. 34, 69 pp.

HORNE, R. R. 1967. Structural geology of part of south-eastern Alexander Island. *British Antarctic Survey Bulletin*, No. 11, 1–22.

——. 1968. Petrology and provenance of the Cretaceous sediments of south-eastern Alexander Island. *British Antarctic Survey Bulletin*, No. 17, 73–82.

HOSKINS, A. K. 1963. The Basement Complex of Neny Fjord, Graham Land. *British Antarctic Survey Scientific Reports*, No. 43, 49 pp.

IRVINE, T. N. *and* W. R. A. BARAGAR. 1971. A guide to the chemical classification of the common volcanic rocks. *Can. J. Earth Sci.*, **8**, No. 5, 523–48.

JAKES, P. *and* A. J. R. WHITE. 1972. Major and trace element abundances in volcanic rocks of orogenic areas. *Geol. Soc. Am. Bull*, **83**, No. 1, 29–39.

JOERG, W. L. G. 1936. The topographical results of Ellsworth's trans-Antarctic flight of 1935. *Geogrl Rev.*, **26**, No. 3, 454–62.

KAMENEV, E. N. 1973. Geological investigations at McMurdo station, 1972–1973. *Antarct. Jnl U.S.*, **8**, No. 6, 338–39.

KATZ, H. R. 1973. Contrasts in tectonic evolution of orogenic belts in the south-east Pacific. *J. R. Soc. N.Z.*, **3**, No. 3, 333–61.

KING, L. 1964. Pre-glacial geomorphology of Alexander Island. (*In* ADIE, R. J., *ed. Antarctic geology*. Amsterdam, North-Holland Publishing Company, 53–64.)

KLEEMAN, A. W. 1965. The origin of granitic magmas. *J. geol. Soc. Aust.*, **12,** Pt. 1, 35–52.

KNOWLES, P. H. 1945. Geology of southern Palmer Peninsula, Antarctica. *Proc. Am. phil. Soc.*, **89,** No. 1, 132–45.

KRYNINE, P. D. 1935. Arkose deposits in the humid tropics. A study of sedimentation in southern Mexico. *Am. J. Sci.*, **29,** No. 172, 353–63.

LANPHERE, M. A. *and* B. L. REED. 1973. Timing of Mesozoic and Cenozoic plutonic events in circum-Pacific North America. *Geol. Soc. Am. Bull.*, **84,** No. 12, 3773–82.

LEMASURIER, W. E. 1971. Volcanic record of Cenozoic glacial history of Marie Byrd Land. (*In* ADIE, R. J., *ed. Antarctic geology and geophysics*. Oslo, Universitetsforlaget, 251–59.)

LINTON, D. L. 1964. Landscape evolution. (*In* PRIESTLEY, R. E., ADIE, R. J. *and* G. DE Q. ROBIN, *ed. Antarctic research*. London, Butterworth and Co. (Publishers) Ltd., 85–99.)

LIOU, J. G. 1971. Synthesis and stability relations of prehnite, $Ca_2Al_2Si_3O_{10}(OH)_2$. *Am. Miner.*, **56,** Nos. 3 and 4, 507–31.

LUTH, W. C., JAHNS, R. H. *and* O. F. TUTTLE. 1964. The granite system at pressures of 4 to 10 kilobars. *J. geophys. Res.*, **69,** No. 4, 759–73.

MARMO, V. 1971. *Developments in petrology. Vol. 2. Granite petrology and the granite problem*. Amsterdam, London, New York, Elsevier Publishing Company.

MARSH A. F. 1968. *Geology of parts of the Oscar II and Foyn Coasts, Graham Land.* Ph.D. thesis, University of Birmingham, 291 pp. [Unpublished.]

MILLER, J. A. 1960. Potassium-argon ages of some rocks from the South Atlantic. *Nature, Lond.*, **187,** No. 4742, 1019–20.

MOORE, J. G. 1959. The quartz diorite boundary line in the western United States. *J. Geol.*, **67,** No. 2, 198–210.

NITSCH, K. H. 1971. Stabilitätsbeziehungen von Prehnit- und Pumpellyit-hältigen Paragenesen. *Contr. Mineral. Petrol. (Beitr. Miner. Petrogr.)*, **30,** No. 3, 240–60.

NOCKOLDS, S. R. *and* R. ALLEN. 1953. The geochemistry of some igneous rock series. *Geochim. Cosmochim. Acta*, **4,** No. 3, 105–42.

OSBORN, E. F. 1969. Experimental aspects of calc-alkaline differentiation. (*In* MCBIRNEY, A. R., *ed.* Proceedings of the andesite conference. *Bull. Ore. St. Dep. Geol. miner. Ind.*, No. 65, 33–42.) [International Upper Mantle Project, Scientific Report 16.]

PACKHAM, G. H. *and* K. A. W. CROOK. 1960. The principle of diagenetic facies and some of its implications. *J. Geol.*, **68,** No. 4, 392–407.

PEARCE, J. A. 1975. Basalt geochemistry used to investigate post-tectonic environments on Cyprus. *Tectonophysics*, **25,** No. 1, 41–68.

——. *and* J. R. CANN. 1973. Tectonic setting of basic volcanic rocks determined using trace element analyses. *Earth planet Sci. Lett.*, **19,** No. 4, 290–300.

PETTIJOHN, F. J. 1957. *Sedimentary rocks*. 2nd edition. New York, Evanston and London, Harper and Brothers.

——., POTTER, P. E. *and* R. SIEVER. 1972. *Sand and sandstone*. New York, Springer-Verlag.

PHILLIPS, E. R. 1974. Myrmekite—one hundred years later. *Lithos*, **7,** No. 3, 181–94.

PITCHER, W. S. *and* A. R. BERGER, 1972. *The geology of Donegal: a study of granite emplacement and unroofing*. New York, London, Sydney, Toronto, Wiley-Interscience.

RAJU, R. D. *and* J. S. R. K. RAO. 1972. Chemical distinction between replacement and magmatic rocks. *Contr. Miner. Petrol. (Beitr. Miner. Petrogr.)*, **35,** No. 2, 169–72.

REX, D. C. 1971. K-Ar age determinations on volcanic and associated rocks from the Antarctic Peninsula and Dronning Maud Land. (*In* ADIE, R. J., *ed. Antarctic geology and geophysics*. Oslo, Universitetsforlaget, 133–36.)

RONNE, F. 1948. Ronne Antarctic Research Expedition, 1946–48. *Geogrl Rev.*, **38,** No. 3, 355–91.

ROWE, P. J. 1973. The geology of the area between Riley and Bertram Glaciers, Palmer Land. *British Antarctic Survey Bulletin*, No. 35, 51–72.

ROWLEY, P. D. 1973. Geologic observations on the northern Lassiter Coast and southern Black Coast. *Antarct. Jnl U.S.*, **8,** No. 4, 154–55.

RYMILL, J. R. 1938. *Southern lights. The official account of the British Graham Land Expedition, 1934–1937*. London, Chatto and Windus.

SEKI, Y. 1966. Pumpellyite-bearing mineral assemblages and type of metamorphism. *J. Jap. Ass. Miner. Petrol. econ. Geol.*, **55,** No. 3, 104–12.

SKINNER, A. C. 1973. Geology of north-western Palmer Land between Eureka and Meiklejohn Glaciers. *British Antarctic Survey Bulletin*, No. 35, 1–22.

SMELLIE, J. L. *and* P. D. CLARKSON. 1975. Evidence for pre-Jurassic subduction in western Antarctica. *Nature, Lond.*, **258,** No. 5537, 701–02.

SØRENSEN, H. 1974. Regional distribution and tectonic relations: introduction. (*In* SØRENSEN, H., *ed. The alkaline rocks*, London, New York, Sydney, Toronto, John Wiley and Sons, 436–42.)

SPRY, A. 1969. *Metamorphic textures*. Oxford, London, Edinburgh, etc., Pergamon Press.

STEPHENSON, A. 1940. Graham Land and the problem of Stefansson Strait. *Geogrl J.*, **96,** No. 3, 167–74.

STEWART, J. W., EVERNDEN, J. F. *and* N. J. SNELLING. 1974. Age determinations from Andean Peru: a reconnaissance survey. *Geol. Soc. Am. Bull.*, **85,** No. 7, 1107–16.

STRAKHOV, N. M. 1969. *Principles of lithogenesis. Vol. 2.* New York, Consultants Bureau; Edinburgh, Oliver & Boyd. [Translated by J. P. Fitzsimmons; edited by S. I. Tomkeieff and J. E. Hemmingway.]

STUBBS, G. M. 1968. *Geology of parts of the Foyn and Bowman Coasts, Graham Land.* Ph.D. thesis, University of Birmingham, 244 pp. [Unpublished.]

SUÁREZ, M. 1976. Plate-tectonic model for southern Antarctic Peninsula and its relation to southern Andes. *Geology*, **4,** No. 4, 211–14.

TAYLOR, B. J., THOMSON, M. R. A. *and* L. E. WILLEY. 1979. The geology of the Ablation Point–Keystone Cliffs area, Alexander Island. *British Antarctic Survey Scientific Reports*, No. 82, 65 pp.

TAYLOR, S. R. 1965. The application of trace element data to problems in petrology. (*In* AHRENS, L. H., PRESS, F., RUNCORN, S. K. *and* H. C. UREY, *ed. Physics and chemistry of the Earth*, **6,** Oxford, London, Edinburgh, New York, Paris, Frankfurt, Pergamon Press, 133–213.)

——. 1969. Trace element chemistry of andesites and associated calc-alkaline rocks. (*In* MCBIRNEY, A. R., *ed.* Proceedings of the andesite conference. *Bull. Ore. St. Dep. Geol. miner. Ind.*, No. 65, 43–63.) [International Upper Mantle Project, Scientific Report 16.]

THOMSON, M. R. A. 1967. A probable Cretaceous invertebrate fauna from Crabeater Point, Bowman Coast, Graham Land. *British Antarctic Survey Bulletin*, No. 14, 1–14.

——. 1972. New discoveries of fossils in the Upper Jurassic Volcanic Group of Adelaide Island. *British Antarctic Survey Bulletin*, No. 30, 95–101.

——. 1975*a*. Upper Jurassic Mollusca from Carse Point, Palmer Land. *British Antarctic Survey Bulletin*, Nos. 41 and 42, 31–42.

——. 1975*b*. First marine Triassic fauna from the Antarctic Peninsula. *Nature, Lond.*, **257,** No. 5527, 577–78.

——. 1975*c*. New palaeontological and lithological observations on the Legoupil Formation, north-west Antarctic Peninsula. *British Antarctic Survey Bulletin*, Nos. 41 and 42, 169–85.

TUREKIAN, K. K. *and* K. H. WEDEPOHL. 1961. Distribution of the elements in some major units of the Earth's crust. *Geol. Soc. Am. Bull.*, **72,** No. 2, 175–91.

TURNER, F. J. *and* J. VERHOOGEN. 1960. *Igneous and metamorphic petrology*. 2nd edition. New York, Toronto and London, McGraw-Hill Book Company, Inc.

TUTTLE, O. F. *and* N. L. BOWEN. 1958. Origin of granite in the light of experimental studies in the system $NaAlSi_3O_8$–$KAlSi_3O_8$–SiO_2–H_2O. *Mem. geol. Soc. Am.*, No. 74, 153 pp.

VANCE, J. A. 1965. Zoning in igneous plagioclase: patchy zoning. *J. Geol.*, **73,** No. 4, 636–51.

WASHINGTON, H. S. 1917. Chemical analyses of igneous rocks published from 1884 to 1913 inclusive. *Prof. Pap. U.S. geol. Surv.*, No. 99, 1201 pp.

WEST, S. M. 1974. The geology of the Danco Coast, Graham Land. *British Antarctic Survey Scientific Reports*, No. 84, 58 pp.

WILKINS, H. 1929. The Wilkins–Hearst Antarctic Expedition, 1928–29. *Geogrl Rev.*, **19,** No. 3, 353–76.

WILLIAMS, P. L. 1970. Geology of the Lassiter Coast. *Antarct. Jnl U.S.*, **5,** No. 4, 98–99.

——. *and* P. D. ROWLEY. 1972. Composition of Jurassic sandstones, Lassiter Coast. *Antarct. Jnl U.S.*, **7,** No. 5, 145–46.

——., SCHMIDT, D. L., PLUMMER, C. C. *and* L. E. BROWN. 1971. Geology of the Lassiter Coast area, Antarctic Peninsula: preliminary report. (*In* ADIE, R. J., *ed. Antarctic geology and geophysics*. Oslo, Universitetsforlaget, 143–48.)

WINKLER, H. G. F. 1974. *Petrogenesis of metamorphic rocks*. 3rd edition. Berlin, Heidelberg, New York, Springer-Verlag.

ZEN, E-AN. 1961. The zeolite facies; an interpretation. *Am. J. Sci.*, **259,** No. 6, 401–09.

——. 1974. Burial metamorphism. *Can. Mineralogist*, **12,** Pt. 7, 445–55.